GMD 4th year, 2014-2015

An Introduction To ElastoHydrodynamic Lubrication

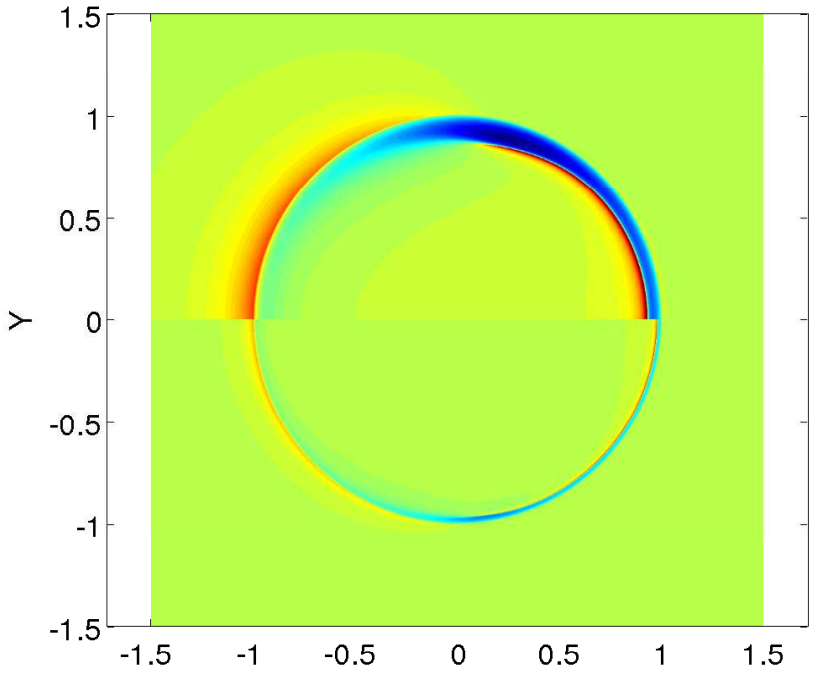

A.A. Lubrecht

Laboratoire de Mécanique des Contacts et des Structures
UMR CNRS 5259, INSA de Lyon, France.

Title page picture shows pressure difference ΔP for $M = 100$ (top) and $M = 1000$ (bottom) and $L = 10$, indicating radial symmetry aswell as size of boundary layer.

Contents

Notation

A_d	dimensionless deformed amplitude $A_d = [\max_T H_c(T) - \min_T H_c(T)]/2$
A_i	dimensionless initial amplitude $A_i = a_i R/b^2$
a	radius of Hertzian contact $[m]$ $a = \sqrt[3]{(3wR_x)/(2E')}$
b	half width of Hertzian line contact $[m]$ $b = \sqrt{(8w_1R)/(\pi E')}$
E'	reduced modulus of elasticity $[Pa]$ $2/E' = (1-\nu_1^2)/E_1 + (1-\nu_2^2)/E_2$
G	dimensionless materials parameter $G = \alpha\ E'$
h	film thickness $[m]$
H	dimensionless film thickness $H = hR/b^2$ (1d), $H = hR_x/a^2$ (2d)
H^D	dimensionless film thickness (Dowson) $H^D = h/R$ (1d), $H^D = h/R_x$ (2d)
H^M	dimensionless film thickness (Moes) $H^M = h/(R\sqrt{U})$ (1d), $H^M = h/(R_x\sqrt{U})$ (2d)
H^*	dimensionless Ertel Grubin film thickness $H^* = h^*/R$ (1d)
$\bar{H}$	dimensionless boundary layer parameter
L	dimensionless material parameter (Moes) $L = G(U)^{0.25}$
L_{10}	number of million stress cycles 90% of a population will surpass
M_1	1d dimensionless load parameter (Moes) $M_1 = W_1(U)^{-0.5}$

M_2	2d dimensionless load parameter (Moes) $M_2 = W(U)^{-0.75}$
n_t	number of time steps
n_x	number of (grid)points in x direction
p	pressure $[Pa]$
p_h	Hertzian pressure $[Pa]$ $p_h = \sqrt{(w_1 E')/(2\pi R)}$ (1d) $p_h = \frac{1}{\pi}\sqrt[3]{(3wE'^2)/(2R_x^2)}$ (2d)
P	dimensionless pressure $P = p/p_h$
$\overline{\Delta}P$	dimensionless boundary layer parameter
q	reduced pressure $[Pa]$, $q = (1 - e^{-\alpha p})/\alpha$
R	reduced radius of curvature (1d) $[m]$ $1/R = 1/R_1 + 1/R_2$
$\bar{R}$	reduced radius of curvature in elliptical contacts (2d) $[m]$ $1/\bar{R} = 1/R_x + 1/R_y$
R_x	reduced radius of curvature in x direction (2d) $[m]$ $1/R_x = 1/R_{1x} + 1/R_{2x}$
R_y	reduced radius of curvature in y direction (2d) $[m]$ $1/R_y = 1/R_{1y} + 1/R_{2y}$
$\mathcal{S}$	slide to roll ratio $\mathcal{S} = u_2/u_m = 2u_2/(u_1 + u_2)$
t	time $[s]$
T	dimensionless time $T = tu_m/b$ (1d), $T = tu_m/a$ (2d)
u_1	velocity of lower (smooth) surface $[m/s]$
u_2	velocity of upper surface $[m/s]$
u_m	mean velocity $u_m = (u_1 + u_2)/2$ $[m/s]$
U	dimensionless speed parameter $U = \eta_0(u_1 + u_2)/(E'R)$
x, y, z	coordinates $[m]$
X, Y, Z	dimensionless coordinates with respect to b (1d) or a (2d)
$\bar{X}$	dimensionless boundary layer coordinate
z	Roelands parameter $[-]$
w_1	1d load per unit length $[N/m]$
w	2d load $[N]$
W_1	1d dimensionless load parameter (Dowson) $W_1 = w_1/(E'R)$
W_2	2d dimensionless load parameter (Dowson) $W_2 = w/(E'R_x^2)$

α	pressure viscosity index $[Pa^{-1}]$
δ	approach/deformation [m]
δ_T	maximum approach/deformation [m]
Δ_T	dimensionless time step
Δ_X	dimensionless mesh size
η	viscosity $[Pa\ s]$
η_0	viscosity at ambient pressure $[Pa\ s]$
$\bar{\eta}$	dimensionless viscosity $\bar{\eta} = \eta/\eta_0$
∇_1	dimensionless wavelength parameter (1d) $\nabla_1 = (\lambda/b)(M_1^{3/4}/L^{1/2})$
∇_2	dimensionless wavelength parameter (2d) $\nabla_2 = (\lambda/a)(M_2^{1/2}/L^{1/6})$
ν	Poisson ratio $[-]$
θ	ratio of oil film and gap height: filling rate
λ	waviness wavelength $[m]$
ρ	density $[kg/m^3]$
ρ_0	density at atmospheric pressure $[kg/m^3]$
$\bar{\rho}$	dimensionless density $\bar{\rho} = \rho/\rho_0$
σ	shear stress $[Pa]$
σ_u	fatigue limit $[Pa]$
$\mathcal{E}, \mathcal{F}$	elliptical integrals

Foreword

In ElastoHydrodynamic Lubrication as in many other disciplines, one starts by studying idealized situations, in which many realistic phenomena are neglected. Some of these realistic conditions are treated in more advanced courses, as outlined in chapter 4. However, in any industrial problem, many of those phenomena occur simultaneously. This is especially problematic when contact performance is less than expected, based on an idealized calculation. It is then up to the engineer to decide which is the most likely candidate responsible for the deterioration of the performance, and to eliminate that one. Occasionally a second cause will emerge, limiting the performance increase achieved by the removal of the first one, and the 'search-and-destroy' process starts anew. These causes limiting contact performance can be very different from one case to the other, however, with a thorough understanding of the basics of lubrication as described in chapters 2 and 3, an engineer will find it possible to come up with the right answers. This is because he* understands the fundamental mechanisms of lubrication, and can therefore deduce which one is not properly working, and then examine why. A current trend is complicating this process, since lubricated contacts are pushed to the limits of their performance, and 'advanced tricks' are used to keep them operating reliably.

The interested reader will find more material in the literature list, if he* wants to study a certain topic in detail.

* please read 'she' instead of 'he' 50% of the time.

These lecture notes are organised in the following way:

The first chapter introduces the topic of film thickness prediction under EHL conditions and gives a short overview of past advances in its understanding, and a brief outlook of future directions.

The second chapter introduces the different equations describing the isothermal EHL problem: Reynolds, elastic deformation and force balance. Furthermore, due to the extremely high pressures generated in such a contact, the variation in density and viscosity have to be added.

This system of three coupled equations, is very difficult to solve, so the third chapter starts with some simplified solutions, working towards the complete solution of the two dimensional EHL problem. An other advantage of this gradual approach is that the reader discovers the global trends before being exposed to the full complexity of the problem. This chapter also introduces the different dimensionless groups that describe EHL operating conditions.

The fourth chapter deals with a variety of 'advanced' topics and each section can be used as the basis of a two hour lecture.

The fifth chapter describes a number of techniques that were specifically developed for EHL. They include specific measurement techniques as well as numerical techniques.

Acknowledgment

1998-1999 edition The author is indebted to Prof. B.O. Jacobson, Dr. P.M.E. Cann and Dr. P. Sainsot for proofreading the 1997-1998 edition of these course-notes. The discussions have resulted in a number of corrections, clarifications and extensions. Furthermore, a number of exercises has been added.

1999-2000 edition Includes a few corrections compared to the previous version pointed out by Mr. J. Molimard, Dr. D. Mazuyer and Prof. L. Flamand. Furthermore, a few exercises have been added.

2000-2001 edition Includes additional exercises and corrections pointed out by Dr. F. Colin and Dr. D. Nelias. Furthermore, the notation of the different dimensionless film thicknesses has been improved. Two sections on the dimensionless parameters describing the impact problem, an appendix and an index have been added.

2001-2002 edition Includes additional corrections, a few small extensions and the most important phrases and equations are highlighted. Furthermore, the Hertzian impact section was extended with the help of Mr. M. Gagachian.

2002-2003 edition Includes some corrections pointed out by Mr. B. Damiens, Dr. S. Coulon.

2003-2004 edition Includes some corrections pointed out by Ms. P. Cavin and an addition to section 4.14 pointed out by Mr. A. Chapkov.

2004-2005 edition Includes some additions and corrections pointed out by Ms. E. Querlioz.

2005-2006 edition Includes a section on adhesive contacts and some minor corrections.

2006-2007 edition Includes some minor modifications and corrections pointed out by Mr. N. Biboulet, Mr. J. Meunier, Mr. D. NGuyen and Mr. A. Guillier de Chalvron.

2007-2008 edition Includes some minor modifications and corrections pointed out by Mr. N. Biboulet, Mr. J. Loncle and Ms. S. Yarhfouri.

2008-2009 edition Includes some minor modifications and corrections.

2010-2011 edition Includes some minor modifications and corrections pointed out by Mr. R. Marchand.

2011-2012 edition Includes some minor modifications and corrections pointed out by Mr. F. v. Drigalski.

2012-2013 edition Includes some minor additions concerning the appendix A.

2013-2014 edition Includes some minor corrections of appendix A and a number of corrections pointed out by Mr. A. Brady.

2014-2015 edition Includes a section on boundary layers, some minor corrections and appendix C on a different dimensionless elasticity equation co-written by Mr. B. Zhang.

Lyon, September 2014

Ton Lubrecht

Chapter 1

Introduction

This course on ElastoHydrodynamic Lubrication (EHL) is intended as a short introductory course to complement an introduction to Hydrodynamic Lubrication (HL). For a first introduction, the sections marked with an asterisk $*$ can be skipped. These parts can be used as part of a more extensive and advanced course. In some countries EHL is part of a course on 'machine elements', since EHL conditions are commonly encountered in rolling element bearings, gears, cam-tappets etc.

We start the introduction by giving the basic definition

ElastoHydrodynamic Lubrication (EHL) is a thin film lubrication mode where two phenomena play an *essential role*:
•**large elastic deformations** (generally larger to much larger than the lubricant film thickness).
•**important piezo-viscous effects** (the lubricant viscosity in the film is (much) larger than the atmospheric viscosity).

We will encounter the central role of these two mechanisms throughout this study:
In the second chapter, each of these two mechanisms takes its part in the central equation: the Reynolds equation.
Towards the end of the third chapter, we study the type of lubrication when only one of the two mechanisms is dominant.
Throughout chapter four, these two characteristics enable major simplifications of the Reynolds equations, allowing a profound physical understanding of the phenomena observed.

1.1 Performance

When designing an EHL contact, the designer has to assure the performance of the future contact. In order to do so, three basic requirements have to be fulfilled in the order given below. Once these three points are satisfied, the designer will wish to optimize the contact performance with respect to one or several criteria. Once again the three following points have to be addressed:

1 Will it work or how to avoid immediate failure.
2 What does it require to work or how to reduce energy dissipation.
3 Will it last or how to ensure the required operating life.

The answer to these three questions will deal with a number of very different aspects of EHL contacts, as we will see below.

ad 1: Obviously, the first requirement is that the stresses resulting from the contact do not exceed the limits of the materials in use. This requirement is similar to dry contacts and can be addressed using Hertz theory. Secondly, ever since EHL (but also HL) has been applied, conventional wisdom is to keep the two surfaces completely separated by an oil film. In other words, the oil film generated should be sufficiently thick to prevent interaction of the surface asperities. Whenever this condition is satisfied, a big step towards fulfilling the second and third condition is also made: lubricated friction is generally (much) lower than dry friction and the complete separation of the asperities will lead to very little or no wear at all.

ad 2: After complete separation of the two surfaces has been achieved, by choosing an appropriate (high viscosity) lubricant, the power losses associated with the friction in and around the contact are examined. Generally one wishes to reduce this friction, and thus to use a lower viscosity oil. However, the choice of a low viscosity oil might conflict with the first point and a compromise has to be found.

ad 3: Finally, when the first two points have been settled, the designer may wish to study the life of the contact, or its durability: how long will it function, given a certain set of criteria to be satisfied, with respect to precision, wear, vibration, noise, friction torque, temperature, etc. This operational life will ultimately be limited by high cycle fatigue. If the predicted life is regarded as insufficient, the designer can choose lower loads, or larger contact areas through larger components, components of higher quality, other materials etc etc.

The first aspect remains the principal one, whenever it is satisfied, it is likely that the two others will be close to what is desired. Consequently points two and three may need only some fine tuning, but the major concern is the first point. As a result, the majority of the work on EHL has been devoted to the study and the prediction of the lubricant film thickness. Hence the study of the film thickness is the major topic of this course and it is outlined in the next chapters. In some final

sections the other two points concerning friction and life will be discussed briefly.

In reality a number of additional conditions are likely to be imposed: the lubricating fluid is prescribed, the outer dimensions of the contact are given, the surface roughness is imposed etc etc. In such cases a number of subsequent loops through the three points will be necessary to satisfy all requirements, starting with the most severe demand, and adding the others one by one. Such design loops are normally accompanied by tests on prototypes, to check if the contact performs as predicted.

1.2 Past

This section presents a short, and far from complete, review of the major events in the development of EHL theory. A much more complete overview in given by Dowson [10]

1881 Publication of the study of the contact between two spherical bodies by H. Hertz.
1886 Publication of the equation describing the slow fluid flow in narrow gaps, that now carries his name, by O. Reynolds.
1893 Publication of the exponential viscosity-pressure relation by C. Barus.
1920 Work by Martin and Gümbel on Hydrodynamic Lubrication (HL), failure to explain the lubrication of gear teeth.
1939/49 Work by Ertel and Grubin: calculation of the film thickness using the Hertzian deformation and a piezo-viscous inlet analysis.
1951 Petrusevich obtains the first 'numerical' solution of the EHL pressure distribution including the pressure spike.
1959/1966 Dowson and Higginson compute many line contact EHL film thicknesses numerically and give equations for minimum film thickness based on the dimensionless parameters W_1, U and G.
1970s Development of optical interferometry, experimental verification of theoretical film thickness predictions.
1976 Hamrock and Dowson compute many EHL point contact film thicknesses numerically and give equations for minimum film thickness based on the dimensionless parameters W_2, U and G.
1980s Improvement of experimental (interferometry $h \downarrow 10$ nm) and numerical (multigrid $n \uparrow 10^6$ points) techniques and study of non-newtonian properties (friction).
1990s Transient studies (experimental + numerical), refinements (indents, roughness, debris, grease) and films becoming so thin that they approach molecular levels.

1.3 Present

EHL plays a silent but important role in everyday life. It occurs where components contact with large relative velocities, large forces are transmitted and minimal wear and minimal power loss are required. The most common elements are rolling element bearings and gears, but also cam and tappets, constant velocity joints, big-end and small-end bearings etc. If one extends the strict definition to include also the iso-viscous/elastic lubrication, contacts like the head-magnetic tape contact in a VCR, seals and the human joints fall into this category.
The main denominator of all these contacts is that they combine high power throughput with low friction, low wear, long life, and generally small and light envelopes.

1.4 Future

A number of technical but also economical and ecological developments are taking place these days which require that the EHL components continue to evolve. The main reasons are a requirement for improved fuel efficiency and stricter pollution laws. This leads to higher temperatures, smaller contacts and higher loads, and thus to thinner films. Furthermore, the contacting surfaces should be manufactured at an ever decreasing cost and operate with an ever increasing reliability. Finally, these contacts will have to be more and more often lubricated with liquids that are environmentally friendly.
All these requirements are contradictory and the only possible way to reconcile these conflicting demands is through an increased understanding of EHL.
A second development is the prediction and optimization of contact performance under realistic conditions, accounting for the influence of surface roughness, indentations, machining marks, polluted oils, transient loads, varying speeds etc.
A third and very important development is the reduction of the lubricant film thickness to molecularly small levels. The behaviour of the fluid film can no longer be extrapolated from the bulk (macroscopic) behaviour of the lubricant: the laws of physics and those of chemistry have to be added to the mechanical laws, in order to be able to predict contact performance under these conditions.

Exercise What are the two essential phenomena in ElastoHydrodynamic Lubrication?

Exercise How to ensure the performance of an EHL contact?

Exercise If EHL contacts work reliably today, why is it necessary to continue the research to ensure reliable operation of tomorrows EHL contacts?

Chapter 2

Basic Equations

In this chapter the basic equations describing the ElastoHydrodynamic Lubrication are outlined. They include the Reynolds equation describing slow viscous flow in narrow gaps, the elastic deformation equation, describing the linear elastic deformation of a semi-infinite body subjected to a pressure distribution at the surface. Furthermore, the material properties such as viscosity and density are not constant and viscosity pressure and density pressure relations are needed to describe the correct behaviour. Finally, the Reynolds equation allows negative pressures which are non-physical: it should be complemented by a cavitation condition, and in order to have a force equilibrium, a force balance equation is added.

2.1 Equivalent Geometry

In general the geometry of the two bodies in contact is rather complicated: think of the ball-raceway contact in a bearing, or the contact between two gear teeth. Furthermore, the geometry tends to change with time: think again of the ball-raceway contact. We will first try to simplify the time dependent geometry, by choosing a coordinate system which moves with respect to world coordinates, and which is **stationary** with respect to the **contact**. This transformation leads in many cases to such a stationary geometry. We will see in the next section that the equations describing the fluid flow, allow such a transformation.
Now we will attempt to simplify the geometry. Because the contact area is very small compared to the overall dimensions of the bodies, it is possible to approximate the geometry close to the contact zone by a much simpler one, without introducing important errors. The geometry is reduced to that of two parabolical bodies, introducing an error that is normally negligible. Body 1 is approximated by a radius of

curvature R_{1x} in x-direction and a radius of curvature R_{1y} in y-direction. Similarly body 2 is approximated by the radii of curvature R_{2x} and R_{2y}.

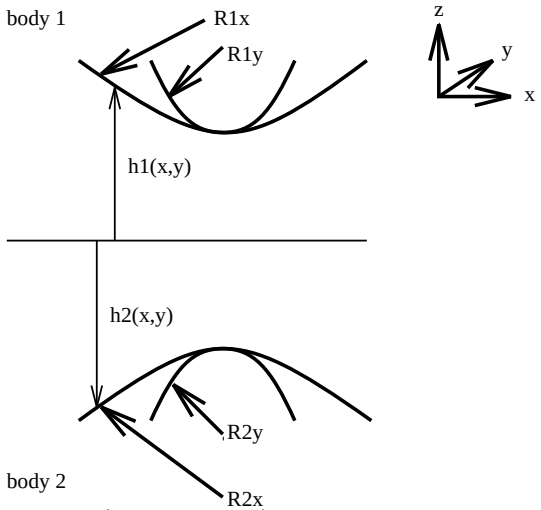

Figure 2.1 *Second order (parabolical) approximation of the geometry around the contact area.*

The coordinate system $Oxyz$ is chosen such that the origin lies on the line connecting the centers of the 2 bodies. The total gap (in the z-direction) between the two bodies $h(x, y)$ can now be described up to second order accuracy by:

$$h(x,y) = h_1(x,y) + h_2(x,y) = h_{10} + \frac{x^2}{2R_{1x}} + \frac{y^2}{2R_{1y}} + h_{20} + \frac{x^2}{2R_{2x}} + \frac{y^2}{2R_{2y}}$$

Because the acceleration forces in the fluid can be neglected with respect to the viscous forces, the pressure distribution $p(x, y)$ generated in the gap, depends only on the gap height $h(x, y)$, and not on its precise geometry. This is the basic hypothesis of the Reynolds equation: the thin film approximation (see the next section). Thus one can introduce the reduced radii of curvature R_x and R_y, such that:

$$\frac{1}{R_x} = \frac{1}{R_{1x}} + \frac{1}{R_{2x}}$$

and

$$\frac{1}{R_y} = \frac{1}{R_{1y}} + \frac{1}{R_{2y}}$$

introducing $h_0 = h_{10} + h_{20}$, the total gap height at $x = y = 0$, the gap height $h(x, y)$ can be written as:

$$h(x, y) = h_0 + \frac{x^2}{2R_x} + \frac{y^2}{2R_y}$$

Figure 2.2 gives the equivalent contact geometry, notice that the second body is represented by a plane.

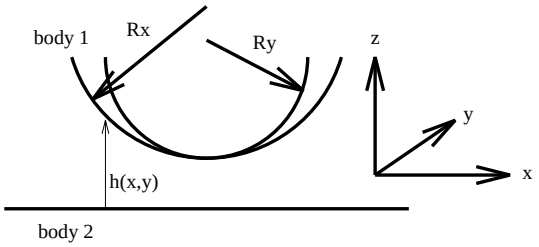

Figure 2.2 *Equivalent geometry.*

In general two types of contact are distinguished: conforming contacts and non-conforming contacts. In a conforming contact, Figure 2.3, the centres of the two bodies lie on the same side of the contact plane $z = 0$: R_{1x} and R_{2x} have opposite signs. An example of a conforming contact, is the contact in a journal bearing, between the shaft and the journal. Typical pressures for these contacts are in the 10 MPa range.

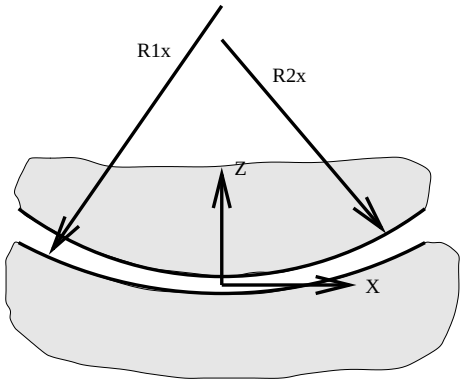

Figure 2.3 *Conforming contact.*

In a non-conforming contact, Figure 2.4, the centres of the two bodies lie on opposite sides of the contact plane $z = 0$: R_{1x} and R_{2x} have the same sign.
Generally the contact area in a non-conforming contact is much smaller than in a conforming one. Therefore, for a given load, non-conforming contacts will be

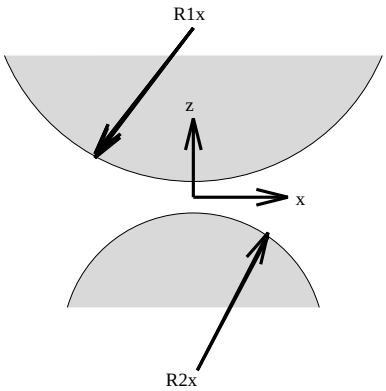

Figure 2.4 *Non-conforming contact.*

exposed to much higher pressures (load=pressure×area) in the GPa range. Consequently, they will generally deform elastically and fall into the ElastoHydrodynamic Lubrication regime. Conformal contacts generally fall into the category of Hydrodynamic Lubrication. A typical example of a non-conforming contact, is that of the ball-on-raceway contact in a ball bearing.

Note that the fact that acceleration terms have been neglected, allows the use of a moving coordinate system, which is stationary with respect to the contact. Obviously the surface velocities have to be recalculated with respect to this coordinate system.

Exercise In a cylindrical roller bearing, is the contact between outer ring and roller conforming or non-conforming? And the contact between inner ring and roller? What can one conclude concerning the contact pressures?

Exercise Compute the reduced radii of contact for the Figures 2.3 and 2.4, if $R_{1x} = 0.1$ m and $R_{2x} = 0.09$ m. Draw the two reduced geometries to scale.

Exercise Show that the gap between two non-conforming cylinders of radii R_{1x} and R_{2x} can be described up to second order accuracy by the equation $h(x) = h_0 + x^2/(2R_x)$, using a Taylor series development, with $h_0 = h(x = 0)$ and $1/R_x = 1/R_{1x} + 1/R_{2x}$.

Exercise What are the reduced radii of contact R_x and R_y in a non-conforming contact between a sphere of radius R and a cylinder of radius R, where the cylinder axis is aligned with the x-axis.

Exercise What are the surface velocities with respect to the contact point in the case of a cylinder rolling on a flat plane with velocity u? And what are these

velocities if the cylinder slides without rotation on the plane, with the same velocity u?

2.2 Reynolds Equation

The Reynolds equation [35] is derived from the Navier-Stokes equation for a slow viscous flow. This means that both inertia forces and external forces are neglected with respect to viscous forces. The second simplification is due to the narrow gap: the dimensions in the z direction are much smaller than those in both x and y direction. Using the condition of no-slip at the wall boundary, one obtains the velocity profile as a function of z. Remember that z is the direction of the height of the gap h.

$$u(z) = \frac{1}{2\eta}\frac{\partial p}{\partial x} z(z-h) + u_h \frac{z}{h} + u_0(1 - \frac{z}{h})$$

$$v(z) = \frac{1}{2\eta}\frac{\partial p}{\partial y} z(z-h) + v_h \frac{z}{h} + v_0(1 - \frac{z}{h})$$

where u and v are the velocity components in x and y direction, whereas u_h and u_0 are the x velocity components for $z = h$ and $z = 0$ respectively. Because of the no-slip boundary condition, these two velocities are equal to the velocities of the solid bodies u_2 and u_1 respectively. The same holds for the y direction with the velocity component v. Using the continuity equation over a cell of height equal to the gap height h:

$$\frac{d}{dt}\int_V \rho \, dV + \int_S \rho \left(u \, n_x + v \, n_y\right) dS = 0$$

where n_x and n_y are the x and y components of the normal of the surface element dS, and choosing the y axis to coincide with the direction where $v_1 + v_2 = 0$, one finds the Reynolds equation:

$$\underbrace{\frac{\partial}{\partial x}(\frac{\rho h^3}{12\eta}\frac{\partial p}{\partial x}) + \frac{\partial}{\partial y}(\frac{\rho h^3}{12\eta}\frac{\partial p}{\partial y})}_{poiseuille} - \underbrace{\frac{\partial(u_m \rho h)}{\partial x}}_{couette} - \underbrace{\frac{\partial(\rho h)}{\partial t}}_{transient} = 0$$

where $u_m = (u_1 + u_2)/2$ and the third term can be split into two terms to reveal three different pressure generating mechanisms:

$$\underbrace{\frac{\partial}{\partial x}(\frac{\rho h^3}{12\eta}\frac{\partial p}{\partial x}) + \frac{\partial}{\partial y}(\frac{\rho h^3}{12\eta}\frac{\partial p}{\partial y})}_{poiseuille} - \underbrace{u_m\frac{\partial(\rho h)}{\partial x}}_{wedge} - \underbrace{\rho h\frac{\partial(u_m)}{\partial x}}_{stretch} - \underbrace{\frac{\partial(\rho h)}{\partial t}}_{transient} = 0$$

the third term describes the classical wedge effect (converging gap) the fourth term describes the stretch effect (sheet rolling), while the fifth term describes the transient (buffer) terms. The stretch effect will normally be absent, except in sheet rolling and wire drawing. The first two terms describe the pressure generated by the last three terms.
The equation can further be simplified to a stationary equation when:

$$\frac{\partial(\rho h)}{\partial t} << u_m\frac{\partial(\rho h)}{\partial x}$$

Finally we will often use the stationary one dimensional or line contact equation. In this stationary one dimensional case the Reynolds equation simplifies to:

$$\frac{\partial}{\partial x}(\frac{\rho h^3}{12\eta}\frac{\partial p}{\partial x}) - u_m\frac{\partial(\rho h)}{\partial x} = 0$$

this equation can be integrated once, introducing the constant h^* to give:

$$\frac{\rho h^3}{12\eta}\frac{\partial p}{\partial x} = u_m(\rho h - \rho^* h^*)$$

where the term h^* represents the film thickness at the position where the pressure gradient is zero $\partial p/\partial x = 0$: $h^* = h(\partial p/\partial x = 0)$, and ρ^* represents the density where the pressure gradient is zero $\rho^* = \rho(\partial p/\partial x = 0)$. Rearranging the terms, and neglecting compressibility effects gives:

$$\frac{\partial p}{\partial x} = 12\eta u_m\frac{h - h^*}{h^3}$$

Exercise Give an example in which each of the three pressure generating terms is important, and describe the details of this mechanism. What happens if all three pressure generating terms are zero?

Exercise What is the Reynolds equation describing a non-rotating cylinder of radius R falling onto a stationary plane with velocity w_0. Is it possible to instantaneously generate the same pressure profile $p(x)$ using the above stationary Reynolds equation? If so what is the relation between $u_m(x)$ and w_0 at the moment the cylinder touches the plane? Assume ρ and η to be constant.

Exercise Assuming very slow transient behaviour of period τ, for which values of τ can the transient terms in the Reynolds equation be neglected. Assume that a is a typical contact dimension. Explain how in this case the transient problem can be solved as a succession of stationary problems.

2.2.1 Cavitation

The pressures obtained by the Reynolds equation in the previous section are generally positive, however, nothing prevents the pressure from taking on negative values. An example from Hydrodynamic Lubrication is the Sommerfeld solution, which predicts positive pressures in the converging gap $\partial h/\partial x < 0$ and negative pressures in the diverging gap $\partial h/\partial x > 0$. Such negative pressures are not physically relevant, since a fluid can not sustain significant negative pressures (tension). In such cases, the fluid will evaporate (boil) and the pressure is limited by the vapor pressure of the fluid. This process is called cavitation. The vapor pressure is generally small compared to the pressure generated in an EHL contact. As such, the vapor pressure can be neglected, and the pressure is limited to zero or positive values. The combination of the Reynolds equation with the cavitation condition changes the problem to a complementarity problem: the complete domain Δ is divided into two distinct domains Δ_1 and Δ_2. The Reynolds equation with $p > 0$ is valid in part of the calculational domain called Δ_1, and the cavitation condition is valid in the rest of the domain Δ_2.

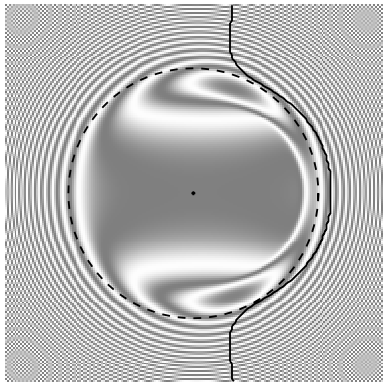

Figure 2.5 *Cavitation boundary in a circular EHL contact, Δ_1 on the left, Δ_2 (cavitated) on the right.*

The division of the domain Δ into the two sub domains is not known in advance, the division has to be computed during the calculational process. The problem has become a complementarity problem with a free boundary (the boundary between Δ_1

and Δ_2). In the line contact this boundary is a single point. In the circular contact problem, it is represented by a line: the exit meniscus represented in Figure 2.5 by a solid line. This is a film thickness graph in which the gap height is represented by grey tones, in a way comparable to the experimental interference technique. The inlet of the contact is situated on the left, the circle represents the Hertzian contact circle.

2.3 Elastic Deformation Equations

As stated in the introduction, elastic deformation of the two contacting bodies plays an important role in EHL. The deformations are close to the ones of the dry contact problem pioneered by Hertz [18]. In this course we will use two hypotheses to approximate the deformations of the real bodies:
• the deformation is linear elastic, and the two contacting bodies have uniform and isotropic properties.
• the contact dimensions a are small compared to the size of the bodies ($a << R_x$), allowing the approximation of the bodies by two semi-infinite half spaces.
Both hypotheses are generally valid, and the approximations obtained agree very well with experimental results. In that case the film thickness equation is given by:

$$h(x,y) = h_0 + \frac{x^2}{2R_x} + \frac{y^2}{2R_y} + \frac{2}{\pi E'} \int_{-\infty}^{+\infty} \int_{-\infty}^{+\infty} \frac{p(x',y')\,dx'\,dy'}{\sqrt{(x-x')^2 + (y-y')^2}}$$

where

$$\frac{2}{E'} = \frac{1-\nu_1^2}{E_1} + \frac{1-\nu_2^2}{E_2}$$

and ν is the Poisson ratio, and E the elastic modulus of the two bodies 1 and 2 respectively. E' is called the reduced elastic modulus.

In a line contact, p is constant in the y direction and the above equation simplifies to:

$$h(x) = h_0 + \frac{x^2}{2R} - \frac{2}{\pi E'} \int_{-\infty}^{+\infty} p(x') \ln \left(\frac{x-x'}{x_0} \right)^2 dx'$$

where x_0 is a reference distance where the deformation is taken to be zero.

When the contact dimensions are no longer small compared to the dimensions of the two bodies, or when the elastic properties of the bodies are not uniform etc etc, the deformations have to be calculated using Finite Element Methods.

Exercise Compute the elastic deformation in a line contact loaded by a parabolical pressure distribution between $-b < x < b$: $p(x) = p_0(1 - x^2/b^2)$, $-b < x < b$, $p(x) = 0$, otherwise. Take $x_0 = b$.

2.3.1 *Line contact problems

The elastic deformation in an infinitely long line contact causes two different problems, which are due to the assumption that the pressure in the y direction is constant over an infinitely long line. Consequently, the applied load $\int\int p(x,y)\,dx\,dy = \infty$. Let us study the constant x_0 first. Its first task is to make sure that the term $(x - x')/x_0$ is dimensionless, in order to assure a physically relevant logarithm. Rewriting the deformation term as

$$\delta(x) = -\frac{2}{\pi E'}\int_{-\infty}^{+\infty} p(x')\ln\left(x - x'\right)^2\,dx' + \frac{2}{\pi E'}\int_{-\infty}^{+\infty} p(x')\ln\left(x_0\right)^2\,dx'$$

one sees that for values of x_0 large compared to the contact area, the deformation in (and around) the point $x = x_0$ will be very small: since both terms cancel: x_0 is the point where the deformation is arbitrarily "set to zero". "Arbitrary" because there is no objective reference length for the line contact. The second problem becomes apparent for $x >> x_0$ when one computes the deformation, one finds that for large values of x, that is for large distances from the contact region, the deformation does not go to zero. Far from the contact the deformation can be approximated by bringing $p(x')$ outside the integral: using $\int_{-\infty}^{+\infty} p(x')\,dx' = w_1$, where w_1 is the load per unit width. Thus:

$$\delta(x) \simeq -\frac{2w_1}{\pi E'}\ln\left(\frac{x}{x_0}\right)^2$$

This equation indicates that for large values of x, the deformation integral tends logarithmically to minus infinity. This is obviously not physical, but is caused by the infinite applied load, as described above. Neither of the two problems causes a real difficulty, since they only influence the equation up to a constant. This constant is easily absorbed in the constant h_{00}, the solid body approach.

2.4 Viscosity/Density-Pressure Relations

For pressure variations of the order of one atmosphere (10^5 Pa), one can regard fluids as being incompressible, and having a constant viscosity. In ElastoHydrodynamically Lubricated contacts, the pressures can reach values of several GPa (1GPa

= 1 gigapascal = 10^9 Pa). Under such extreme pressure conditions, the molecules of a liquid will be packed closer together, thus changing its density. This reduction in mean distance does induce an increased interaction between the molecules, resulting in an increase in viscosity. It is thus necessary to describe both density and viscosity as a function of pressure.

2.4.1 Density-pressure

The simplest density pressure relation is given by the Dowson and Higginson relation (1966) [9]. It reads:

$$\rho(p) = \rho_0 \frac{5.9\,10^8 + 1.34\,p}{5.9\,10^8 + p}$$

where ρ_0 is the atmospheric density and p is given in Pa. Please note the two asymptotes: for small p ($p \to 0$), $\rho = \rho_0$, for very large p ($p \to \infty$), $\rho = 1.34\,\rho_0$.

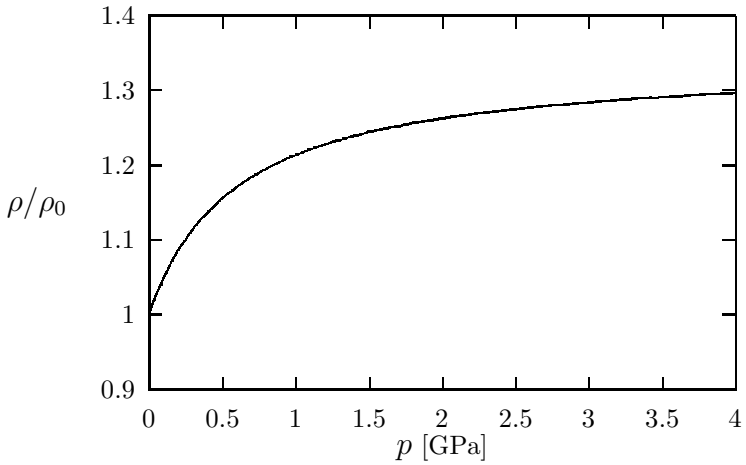

Figure 2.5 *Relative density ρ/ρ_0 as a function of p.*

Exercise Check the two asymptotes of the density pressure relation.

2.4.2 Barus viscosity-pressure

The simplest viscosity pressure relationship is an exponential relation, according to Barus [2]. It reads

$$\eta(p) = \eta_0 \exp(\alpha\, p)$$

where η_0 is the atmospheric viscosity and α is called the pressure viscosity coefficient. For mineral oils this coefficient varies between $1{\cdot}10^{-8}$ and $2{\cdot}10^{-8}$ Pa^{-1}. For pressures of 1 GPa an average viscosity increase of $\exp(15) \approx 3 \cdot 10^6$ is predicted, which is enormous.

Exercise Assuming that $\alpha = 2 \cdot 10^{-8}$ Pa^{-1}, compute the pressure for which the viscosity is twice its atmospheric value, according to Barus. Then calculate the pressure for which the viscosity increases by a factor of 1000, then by a factor of 10^6.

2.4.3 Roelands viscosity-pressure

A slightly more accurate, and also slightly more complicated viscosity pressure relation is the expression derived by Roelands in 1966 [36]:

$$\eta(p) = \eta_0 \exp[(\ln(\eta_0) + 9.67)(-1 + (1 + \frac{p}{p_0})^z)]$$

where z is the pressure viscosity index, typically $z = 0.6$, and $p_0 = 1.98\,10^8$ is a constant.

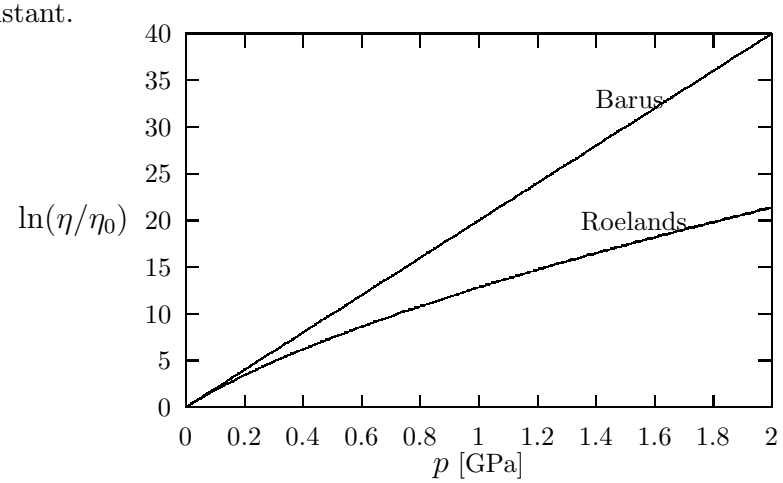

Figure 2.6 *Relative viscosity η/η_0 as a function of p.*

Even though the Roelands equation is more complete and complex than the Barus equation, it does not completely describe the high pressure behaviour of oil, see Bair [1].

2.4.4 *Comparison

If one defines the pressure viscosity coefficient α at atmospheric pressure, one can establish a relation between the Barus equation and the Roelands equation.

$$\alpha = \left[\frac{1}{\eta}\left(\frac{\partial \eta}{\partial p}\right)\right]_{p=0}$$

one can redefine the Roelands equation:

$$\eta(p) = \eta_0 \exp[\frac{\alpha p_0}{z}\left(-1 + (1 + \frac{p}{p_0})^z\right)]$$

From this one finds that the variables α, p_0, η_0 and z are dependent:

$$\frac{\alpha p_0}{z} = \ln(\eta_0) + 9.67$$

Exercise Show that using the definition of α as the slope at zero (ambient) pressure for both viscosity pressure equations, one obtains indeed that $\alpha p_0/z = \ln(\eta_0) + 9.67$.

2.4.5 *High pressure Reynolds equation

The Reynolds equation shows two very different types of behaviour over the contact domain. These will have important consequences for the physical behaviour, which are reflected in the numerical behaviour of the equation. This change is triggered by the piezo-viscosity of the lubricant. In order to understand this change let us study the transient line contact equation:

$$\frac{\partial}{\partial x}(\frac{\rho h^3}{12\eta}\frac{\partial p}{\partial x}) - u_m\frac{\partial(\rho h)}{\partial x} - \frac{\partial(\rho h)}{\partial t} = 0$$

In the inlet the pressure is low, and the viscosity will be close to the ambient value. The character of the equation is elliptical, dominated by the first term with its second order derivatives. In the central zone, the pressure can be very high, up to several GPa's. Due to the piezoviscous effect, the viscosity becomes enormous, and the Poiseuille term tends to zero. Because of this the Reynolds equation reduces to:

$$-u_m\frac{\partial(\rho h)}{\partial x} - \frac{\partial(\rho h)}{\partial t} = 0$$

or in dimensionless terms:

$$\frac{\partial(\bar{\rho} H)}{\partial X} + \frac{\partial(\bar{\rho} H)}{\partial T} = 0$$

When neglecting the variations in $\bar{\rho}$, the equation simplifies even more and becomes

$$\frac{\partial H}{\partial X} + \frac{\partial H}{\partial T} = 0$$

which is a hyperbolical first order differential equation, describing a propagating wave. The solution is $H(X-T)$ is constant, or in dimensional terms: $h(x-u_m t)$ is constant. The physical explanation is that in the high pressure zone, the viscosity increases so much that it inhibits the Poiseuille term: no pressure induced flow is possible. Thus in the high pressure zone only the Couette term persists. For a stationary solution this reduction gives:

$$\frac{\partial(\rho h)}{\partial x} = 0$$

Once again neglecting the compressibility, it says that $dh/dx = 0$, or $h(x)$ is constant. This can be observed from the numerical solutions given in the next chapter.

In case of a non-smooth surface combined with sliding, a number of surprising phenomena can be observed, which find their origin in this wave propagation character of the high pressure zone [14, 30].

Exercise Using the figures 3.9 - 3.14 show that $\partial(\rho h)/\partial x = 0$ is indeed found in the high pressure zone. Comment on the film thickness evolution from 3.9 - 3.14. Relate this evolution to the evolution in the pressure distribution.

Exercise Show that $H(X-T) = X^2 - 2XT + T^2$ is indeed a solution of the reduced Reynolds equation for high pressures: $\partial H/\partial X + \partial H/\partial T = 0$.

2.5 Force Balance

The integral of the pressure distribution obtained from the Reynolds equation should balance the externally applied load, in order to have an equilibrium of forces. For the two dimensional problem this condition reads:

$$w = \int_{-\infty}^{+\infty} \int_{-\infty}^{+\infty} p(x', y')\, dx'\, dy'$$

where w is the applied load in the two dimensional case.
For the line contact case, the force balance equation reads:

$$w_1 = \int_{-\infty}^{+\infty} p(x')\, dx'$$

where w_1 is the applied load per unit length in the one dimensional case.

2.5.1 *Transient case

When the load w is no longer constant with time, the entire solution becomes a transient solution: $p(x, y, t)$ and $h(x, y, t)$. However, when the acceleration terms of the bodies remain small, one can neglect them, and the previous point contact force balance equation is trivially extended to:

$$w(t) = \int_{-\infty}^{+\infty} \int_{-\infty}^{+\infty} p(x', y', t)\, dx'\, dy'$$

On the other hand, when the acceleration increases, a second term including the mass of the accelerating body (say body 2 with mass m_2) has to be incorporated in this equation:

$$w(t) + m_2 \ddot{h}_0 = \int_{-\infty}^{+\infty} \int_{-\infty}^{+\infty} p(x', y', t)\, dx'\, dy'$$

Suppose that $p = 0$, it means that $w(t) + m_2 \ddot{h}_0 = 0$, or the complete force is used to accelerate body 2, but in general both terms play a role.
For the line contact case similar extensions are valid, introducing m_2/l, the mass of body two per unit length.

2.6 *Dimensionless Equations

Since the highly loaded EHL pressure distribution and elastic deformation are very close to the Hertzian dry contact solution, it seems reasonable to introduce dimensionless parameters based on this asymptotic dry contact solution.
Its application has two different advantages, first of all it allows the introduction of two parameters that determine the contact operating conditions. The second advantage is that the pressure and film thickness values vary around 1.0, giving a maximum precision for the numerical calculations.
We will study the dimensionless two dimensional Reynolds equation, based on the circular Hertzian solution with a the radius of the contact circle and p_h the maximum Hertzian contact pressure. The relations between p_h and a and the contact geometry, operating conditions and materials parameters, are outlined in the next chapter. In general capitals are used for dimensionless parameters, with the exception of R. Dimensionless Greek characters are indicated by a bar over the original symbol.

Thus we introduce $P = p/p_h$, $X = x/a$, $Y = y/a$ and $H = hR_x/a^2$, based on Hertz and $T = u_m\, t/a$, $\bar{\eta} = \eta/\eta_0$ and $\bar{\rho} = \rho/\rho_0$.

Using these parameters the dimensionless Reynolds equation reads:

$$\frac{\partial}{\partial X}\left(\frac{a^3 p_h}{12\eta_0 R_x^2}\frac{\bar{\rho}H^3}{\bar{\eta}}\frac{\partial P}{\partial X}\right) + \frac{\partial}{\partial Y}\left(\frac{a^3 p_h}{12\eta_0 R_x^2}\frac{\bar{\rho}H^3}{\bar{\eta}}\frac{\partial P}{\partial Y}\right)$$
$$-u_m\frac{\partial(\bar{\rho}H)}{\partial X} - \bar{\rho}H\frac{\partial(u_m)}{\partial X} - u_m\frac{\partial(\bar{\rho}H)}{\partial T} = 0$$

Introducing $\epsilon = (\bar{\rho}H^3)/(\bar{\eta}\lambda)$, and $\lambda = (12\eta_0 u_m R_x^2)/(a^3 p_h)$, and assuming u_m is constant, we can simplify this equation

$$\frac{\partial}{\partial X}\left(\epsilon\frac{\partial P}{\partial X}\right) + \frac{\partial}{\partial Y}\left(\epsilon\frac{\partial P}{\partial Y}\right) - \frac{\partial(\bar{\rho}H)}{\partial X} - \frac{\partial(\bar{\rho}H)}{\partial T} = 0$$

each individual term is now dimensionless and ϵ can be regarded as a coefficient which varies over the domain.
The dimensionless film thickness equation including the elastic deformation equation becomes with these parameters:

$$H(X,Y) = H_0 + \frac{X^2}{2} + \frac{Y^2}{2} + \frac{2R_x p_h}{\pi a E'}\int_{-\infty}^{+\infty}\int_{-\infty}^{+\infty}\frac{P(X',Y')\,dX'\,dY'}{\sqrt{(X-X')^2+(Y-Y')^2}}$$

As can be found from the equations in the section on the Hertzian contact, $p_h/a = E'/(\pi R_x)$, thus:

$$H(X,Y) = H_0 + \frac{X^2}{2} + \frac{Y^2}{2} + \frac{2}{\pi^2}\int_{-\infty}^{+\infty}\int_{-\infty}^{+\infty}\frac{P(X',Y')\,dX'\,dY'}{\sqrt{(X-X')^2+(Y-Y')^2}}$$

Finally the dimensionless force balance equation becomes:

$$\frac{w}{p_h a^2} = \int_{-\infty}^{+\infty}\int_{-\infty}^{+\infty} P(X',Y')\,dX'\,dY'$$

Using the fact that the Hertzian pressure distribution is a semi-ellipsoid, and that the lubricated load and the dry contact load are the same, we find with:

$$w = \frac{2\pi p_h a^2}{3}$$

that:

$$\int_{-\infty}^{+\infty}\int_{-\infty}^{+\infty} P(X',Y')\,dX'\,dY' = \frac{2\pi}{3}$$

Exercise Check the derivation of the three dimensionless equations.

2.7 *Discrete HL Problem

In order to derive an efficient discretisation of the EHL problem, it is useful to study the discretisation of the Reynolds equation alone in a first step. The discrete grid used will be equidistant in both the X and Y direction. This equation is studied in its stationary form: $\partial H/\partial T = 0$.

$$\frac{\partial}{\partial X}(\epsilon\frac{\partial P}{\partial X}) + \frac{\partial}{\partial Y}(\epsilon\frac{\partial P}{\partial Y}) - \frac{\partial(\bar{\rho}H)}{\partial X} = 0$$

where the coefficient ϵ varies over the domain, but does not depend on the pressure: the iso-viscous rigid assumption. The most compact discretisation is obtained by first discretising the outer differential $\partial/\partial X$ using a short central discretisation:

$$\left(\frac{\partial}{\partial X}(\epsilon\frac{\partial P}{\partial X})\right)_{i,j} \doteq \frac{(\epsilon\frac{\partial P}{\partial X})_{i+1/2,j} - (\epsilon\frac{\partial P}{\partial X})_{i-1/2,j}}{\Delta X}$$

where i represents the grid index in the X direction and j the grid index in the Y direction. In other words: $X = X_0 + i\Delta X$ and $Y = Y_0 + j\Delta Y$.

In a second step the inner derivative is developed, using a short central discretisation:

$$\left(\epsilon\frac{\partial P}{\partial X}\right)_{i+1/2,j} \doteq \frac{\epsilon_{i+1/2,j}(P_{i+1,j} - P_{i,j})}{\Delta X}$$

A combination of these two steps gives:

$$\left(\frac{\partial}{\partial X}(\epsilon\frac{\partial P}{\partial X})\right)_{i,j} \doteq \frac{\epsilon_{i+1/2,j}P_{i+1,j} - (\epsilon_{i+1/2,j} + \epsilon_{i-1/2,j})P_{i,j} + \epsilon_{i-1/2,j}P_{i-1,j}}{\Delta X^2}$$

the same discretisation is applied in the Y direction:

$$\left(\frac{\partial}{\partial Y}(\epsilon\frac{\partial P}{\partial Y})\right)_{i,j} \doteq \frac{\epsilon_{i,j+1/2}P_{i,j+1} - (\epsilon_{i,j+1/2} + \epsilon_{i,j-1/2})P_{i,j} + \epsilon_{i,j-1/2}P_{i,j-1}}{\Delta Y^2}$$

taking ΔX and ΔY to be identical, and using the short central discretisation for the $\partial(\bar{\rho}H)/\partial X$ term as well, one obtains a second order accurate, short central discretisation of the Reynolds equation:

$$\frac{\epsilon_{i+1/2,j}P_{i+1,j} + \epsilon_{i,j+1/2}P_{i,j+1}}{\Delta X^2} - \frac{(\epsilon_{i+1/2,j} + \epsilon_{i-1/2,j} + \epsilon_{i,j+1/2} + \epsilon_{i,j-1/2})P_{i,j}}{\Delta X^2}$$

$$\frac{\epsilon_{i-1/2,j}P_{i-1,j} + \epsilon_{i,j-1/2}P_{i,j-1}}{\Delta X^2} - \frac{\bar{\rho}_{i+1/2,j}H_{i+1/2,j} - \bar{\rho}_{i-1/2,j}H_{i-1/2,j}}{\Delta X} = 0$$

Exercise What are the advantages of using intermediate points such as $\epsilon_{i+1/2,j}$ and what are the disadvantages?

2.8 *Discrete EHL Problem

In the EHL problem, the fluid flow is governed by the discrete Reynolds equation outlined in the previous section. However, the parameter ϵ depends on the pressure p. As a result, the coefficients in the intermediate points $i+1/2, j$ etc. cannot be computed easily, since they depend on the elastic deformation integrals. Consequently, they are approximated in the following way:

$$\epsilon_{i+1/2,j} = \frac{\epsilon_{i+1,j} + \epsilon_{i,j}}{2}$$

For stability reasons the central derivative of $\bar{\rho}H$ is often replaced by a first order backwards (upstream) derivative:

$$\left(\frac{\partial \bar{\rho}H}{\partial X}\right)_{i,j} \doteq \frac{\bar{\rho}_{i,j}H_{i,j} - \bar{\rho}_{i-1j}}{\Delta X}$$

Or by a second order backwards derivative, if one does not want to diminish the order of approximation:

$$\left(\frac{\partial \bar{\rho}H}{\partial X}\right)_{i,j} \doteq \frac{3\bar{\rho}_{i,j}H_{i,j} - 4\bar{\rho}_{i-1,j}H_{i-1,j} + \bar{\rho}_{i-2,j}H_{i-2,j}}{2\Delta X}$$

The elastic deformation equation is discretized as:

$$\delta_{i,j} = \sum_k \sum_l K_{i,k,j,l}\, P_{k,l}$$

where the kernel of the elastic deformations $K_{i,k,j,l}$ is given by:

$$K_{i,k,j,l} = \frac{2}{\pi^2}[|X_p| \ln(Y_p/X_p + \sqrt{1 + Y_p^2/X_p^2}) - |X_p| \ln(Y_m/X_p + \sqrt{1 + Y_m^2/X_p^2})$$

$$+|X_m| \ln(Y_m/X_m + \sqrt{1 + Y_m^2/X_m^2}) - |X_m| \ln(Y_p/X_m + \sqrt{1 + Y_p^2/X_m^2})$$

$$+|Y_p| \ln(X_p/Y_p + \sqrt{1 + X_p^2/Y_p^2}) - |Y_p| \ln(X_m/Y_p + \sqrt{1 + X_m^2/Y_p^2})$$

$$+|Y_m| \ln(X_m/Y_m + \sqrt{1 + X_m^2/Y_m^2}) - |Y_m| \ln(X_p/Y_m + \sqrt{1 + X_p^2/Y_m^2})]$$

where: $X_p = X_i - X_k + \Delta X/2$, $X_m = X_i - X_k - \Delta X/2$, $Y_p = Y_j - Y_l + \Delta Y/2$, and $Y_m = Y_j - Y_l - \Delta Y/2$.
the force balance equation becomes:

$$\sum_i \sum_j P_{i,j} \Delta X^2 - \frac{2\pi}{3} = 0$$

The line contact problem is discretized in exactly the same manner.

2.9 *Starved Formulation

In previous sections the Reynolds equation has been described for the situation where the gap between the two bodies is completely filled with oil, and thus pressure generation takes place from the inlet of the contact onwards. A more general description of the lubrication problem accounts for gaps which are only partially filled with lubricant. This is the most common situation, in which insufficient oil is available, and the pressure build up is delayed, until the oil film does completely fill the gap. This representation is also more physical since it allows a description accounting for the amount of oil available on the two surfaces, in front of the contact. In order to describe this situation correctly an additional parameter θ representing the degree at which the gap is filled with oil is introduced. This parameter is defined as $\theta(x, y)$ is the ratio of the oil film thickness $h_{oil}(x, y)$ and the gap height $h(x, y)$. Notice that in the previous sections the two parameters were identical, and that for a completely filled gap $\theta = 1$. For the when case the gap is completely empty (no oil), $\theta = 0$.

The new Reynolds equation incorporating the θ parameter becomes a complementarity equation: either $\theta < 1$ and $P = 0$, or $\theta = 1$ and $P > 0$. The boundary between these two zones is a free boundary and is not known in advance. It has to be established while calculating the solution.

Note that the cavitation boundary treated in an earlier section, is straightforwardly translated in terms of θ, for the cavitation zone $\theta < 1$ and $P = 0$ applies. This extended stationary Reynolds equation reads:

$$\frac{\partial}{\partial X}(\epsilon\frac{\partial P}{\partial X}) + \frac{\partial}{\partial Y}(\epsilon\frac{\partial P}{\partial Y}) - \frac{\partial(\bar{\rho}\theta H)}{\partial X} = 0$$

In this complementarity representation of the Reynolds equation, it is important to identify the physical meaning of these three terms. The Reynolds equation remains a flow continuity equation. The first two terms including the derivatives of the pressure describe the pressure induced Poiseuille flow. In the zone where the film is incomplete $\theta < 1$, this term is absent, since the pressure P is zero. In the complete film zone, the Poiseuille term is the same as before. The term including the derivative of the film thickness, is identical to the term in the previous sections in the zone of complete film, since $\theta = 1$. However, in the zone with a partial film, the mass flow continuity equation, now includes the derivative with respect to θ. In this zone, the Couette term is thus modified and accounts for partially filled gaps. Thus the mass flow continuity is satisfied in both zones.

Exercise Give the reduced forms of the Reynolds equation in the zone $\theta < 1$ and $\theta = 1$?

2.10 *Discrete Starved Problem

Starting from the discrete equation for the HL problem and choosing $\Delta X = \Delta Y$:

$$\frac{\epsilon_{i+1/2,j}P_{i+1,j} + \epsilon_{i,j+1/2}P_{i,j+1}}{\Delta X^2} - \frac{(\epsilon_{i+1/2,j} + \epsilon_{i-1/2,j} + \epsilon_{i,j+1/2} + \epsilon_{i,j-1/2})P_{i,j}}{\Delta X^2} +$$

$$\frac{\epsilon_{i-1/2,j}P_{i-1,j} + \epsilon_{i,j-1/2}P_{i,j-1}}{\Delta X^2} - \frac{\bar{\rho}_{i+1/2,j}H_{i+1/2,j} - \bar{\rho}_{i-1/2,j}H_{i-1/2,j}}{\Delta X} = 0$$

the starved discrete problem is a trivial extension of the fully flooded problem:

$$\frac{\epsilon_{i+1/2,j}P_{i+1,j} + \epsilon_{i,j+1/2}P_{i,j+1}}{\Delta X^2} - \frac{(\epsilon_{i+1/2,j} + \epsilon_{i-1/2,j} + \epsilon_{i,j+1/2} + \epsilon_{i,j-1/2})P_{i,j}}{\Delta X^2} +$$

$$\frac{\epsilon_{i-1/2,j}P_{i-1,j} + \epsilon_{i,j-1/2}P_{i,j-1}}{\Delta X^2} - \frac{\bar{\rho}_{i+1/2,j}\theta_{i+1/2,j}H_{i+1/2,j} - \bar{\rho}_{i-1/2,j}\theta_{i-1/2,j}H_{i-1/2,j}}{\Delta X} = 0$$

Notice that this discretisation uses a so called *staggered* grid: the filling ratio θ and the film thickness H are defined in intermediate points: $(i + 1/2, j)$ or $(i, j + 1/2)$. The Reynolds equation and the pressure P are defined in the central points (i, j). The discretized Reynolds equation in the point (i, j) can be interpreted as a flow Φ continuity equation over a square with sides ΔX and ΔY, centered around the point (i, j):

$$\frac{\partial \Phi}{\partial X} + \frac{\partial \Phi}{\partial Y} = 0$$

discretising in the point (i, j) and again assuming $\Delta X = \Delta Y$ one finds:

$$\frac{\Phi_{i+1/2,j} - \Phi_{i-1/2,j} + \Phi_{i,j+1/2} - \Phi_{i,j-1/2}}{\Delta X} = 0$$

where the flow terms are:

$$\Phi_{i+1/2,j} = -\epsilon_{i+1/2,j}\frac{P_{i+1,j} - P_{i,j}}{\Delta X} + \theta_{i+1/2,j}H_{i+1/2,j}$$

$$\Phi_{i-1/2,j} = -\epsilon_{i-1/2,j}\frac{P_{i,j} - P_{i-1,j}}{\Delta X} + \theta_{i-1/2,j}H_{i-1/2,j}$$

$$\Phi_{i,j+1/2} = -\epsilon_{i,j+1/2}\frac{P_{i,j+1} - P_{i,j}}{\Delta X}$$

$$\Phi_{i,j-1/2} = -\epsilon_{i,j-1/2}\frac{P_{i,j} - P_{i,j-1}}{\Delta X}$$

Where the flow Φ has a positive sign in the direction of the increasing i and j (X and Y).

Exercise Derive the Reynolds equation from the mass flow continuity equation over a rectangle, comments with respect to the discrete equation?

Chapter 3

Solutions

This chapter gives an overview of the analytical and numerical solutions that approximate the pressure distribution and the film thickness in an EHL contact, with increasing sophistication.
• The dry contact solution neglects the film thickness, but gives a good approximation of the pressure distribution (1d and 2d).
• The Ertel-Grubin approach predicts an accurate central film thickness using an inlet analysis and a Hertzian geometry (1d).
• The Dowson and Higginson solutions are numerical line contact solutions, curve fitted to give relations predicting central and minimum film thickness as a function of the dimensionless parameters W_1, U and G.
• The Hamrock and Dowson solutions are numerical point contact solutions, curve fitted to give relations predicting central and minimum film thickness as a function of the dimensionless parameters W_2, U and G.
• The 1d Moes and Venner solutions are accurate numerical line contact solutions, curve fitted to give relations predicting central and minimum film thickness as a function of the dimensionless parameters M_1, and L. These parameters allow a graphical representation of the EHL analysis, with analytical asymptotes describing the physical limiting solutions bounding the P.E. regime.
• The 2d Moes and Venner solutions are accurate numerical point contact solutions, curve fitted to give relations predicting central and minimum film thickness as a function of the dimensionless parameters M_2, and L. This representation allows the addition to the EHL analysis of other analytical asymptotes and a graphical representation.
Many other curve fitted film thickness solutions exist in the literature. Unfortunately, none of them clearly describe where the equation is valid. In order to reduce confusion to a minimum, the first (and most widely used) relations are given, to-

gether with the most general and precise equations available at the moment.

3.1 Dry Contact

As was indicated in the definition of EHL in the introduction, the elastic deformation in an EHL contact is generally much larger than the lubricant film thickness. Since the pressure necessary for the elastic deformation is linearly proportional to the deformation δ, neglecting this small lubricant film thickness hardly alters the pressure distribution.
The dry contact approximation becomes even better for the limits of high load and low speeds, since $h/\delta \to 0$. Thus for $w \to \infty$ and/or $u_m \to 0$, the dry contact pressure distribution accurately approximates the lubricated one.

3.1.1 Line contact

If the reduced radii of curvature of the contacting bodies are very different in x and y direction for instance $R_x << R_y$, one can neglect the curvature in the y direction and approximate the problem by an infinitely long line contact problem, depending only on the coordinate x. The reduced radius of curvature in the x direction will be denoted R. The deformed geometry is given by:

$$h(x) = h_0 + \frac{x^2}{2R} - \frac{2}{\pi E'} \int_{-\infty}^{+\infty} p(x') \ln \left(\frac{x - x'}{x_0} \right)^2 dx'$$

where h_0 is the rigid body displacement, or the undeformed minimum film thickness (which can be negative). E' is the reduced elastic modulus, defined by:

$$\frac{2}{E'} = \frac{1 - \nu_1^2}{E_1} + \frac{1 - \nu_2^2}{E_2}$$

NB, please note that a second definition E of the reduced elastic modulus is used in the literature, which simplifies the dimensionless deformation integral even more: $\pi/E = (1 - \nu_1^2)/E_1 + (1 - \nu_2^2)/E_2$.

In this work we will use the definition of E' since it is used in the dimensionless numbers, introduced later in this chapter.
Because the two bodies are in contact, for $x \in [-b, +b]$ or $X = x/b \in [-1, +1]$, the gap height $H(X) = h(x/b)R/b^2 = 0$ for $X \in [-1, +1]$. The analysis by Hertz, Boussinesq, Cerutti shows that a semi-elliptical pressure distribution gives the required deformation, see Johnson [23]:

$$p(x) = \begin{cases} p_h\sqrt{1-(x/b)^2}, & \text{if } |x| \le b; \\ 0, & \text{otherwise.} \end{cases}$$

or using dimensionless variables $P = p/p_h$ and $X = x/b$:

$$P(X) = \begin{cases} \sqrt{1-X^2}, & \text{if } |X| \le 1; \\ 0, & \text{otherwise.} \end{cases}$$

The dimensionless pressure distribution, and the dimensionless gap height are plotted in Figure 3.1, together with the undeformed geometry, with the same rigid body displacement (h_0).

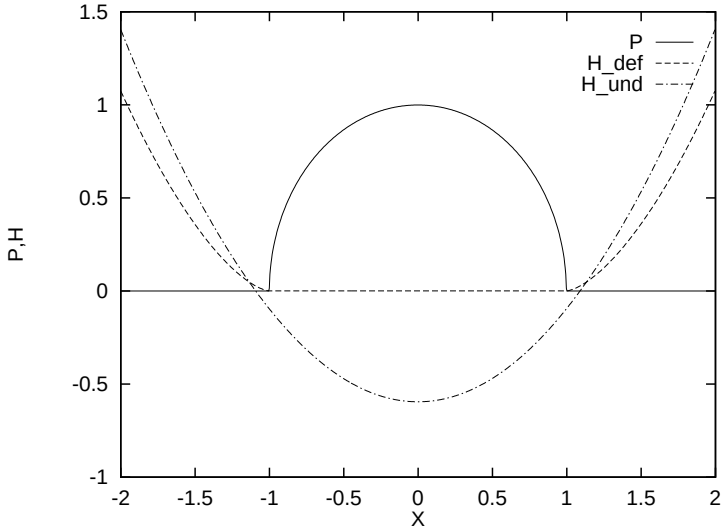

Figure 3.1 *Dimensionless Hertzian contact pressure, dimensionless deformed and undeformed geometry, for the line contact case.*

It is now possible to compute relations between:

b the half-width of the contact
p_h the maximum pressure
w_1 the load per unit width
R the (reduced) radius of contact
E' the reduced elastic modulus.

Starting with the force balance equation, and remembering that the surface of half an ellipse is $\pi/2$ times the product of the two semi-axes, one finds:

$$w_1 = \int_{-\infty}^{+\infty} p(x')\,dx' = \int_{-b}^{+b} p_h\,\sqrt{1-(x'/b)^2}\,dx' = \frac{\pi p_h b}{2}$$

or

$$p_h = \frac{2w_1}{\pi b}$$

The contact half-width b is proportional to the square root of the contact radius R and to the square root of the load per unit length w_1, and inversely proportional to square root of the reduced elastic modulus E'. One obtains:

$$b = \sqrt{\frac{8\,w_1\,R}{\pi\,E'}}$$

Finally the maximum deformation δ is found in the centre of the contact for $x = 0$, it is:

$$\delta = \delta(x=0) = (\frac{1}{4} + \frac{1}{2}\ln 2)\frac{b^2}{R} \approx 0.596\ldots\frac{b^2}{R} \approx 1.52\frac{w_1}{E'}$$

when x_0 is chosen as b.
NB: δ is also the approach of the centres of the two bodies under load, when the two bodies were just contacting at zero load.

Exercise Express the Hertzian pressure p_h in terms of w_1, E' and R only. In order to double the pressure, p_h, how much should the load w_1 change, how much the contact radius R, and how much the reduced Elastic modulus E'?

Exercise Compute δ for a contact with $b = 0.001$ m and $R = 0.05$ m. If the reduced elastic modulus $E' = 2 \cdot 10^{11}$ Pa what is the load per unit length w_1, what is p_h?

Exercise Figure 3.1 shows the deformed and the undeformed geometry for a line contact. From the difference the maximum deformation can be estimated as 0.6. Deduce which dimensionless film thickness relation has been used to obtain H.

3.1.2 Circular contact

If the reduced radii of curvature of the contacting bodies are identical in x and y direction $R_x = R_y$, the contact area is a circle of radius a, and the deformed geometry is given by, see Johnson [23]:

$$h(x,y) = h_0 + \frac{x^2}{2R_x} + \frac{y^2}{2R_x} + \frac{2}{\pi E'} \int_{-\infty}^{+\infty} \int_{-\infty}^{+\infty} \frac{p(x',y')\,dx'\,dy'}{\sqrt{(x-x')^2 + (y-y')^2}}$$

Contact occurs for $x^2 + y^2 < a^2$ so $h(x,y) = 0$ for $x^2 + y^2 < a^2$. A semi-elliptical pressure distribution gives the required deformation:

$$p(x,y) = \begin{cases} p_h\sqrt{1-(x/a)^2-(y/a)^2}, & \text{if } x^2+y^2 \le a^2; \\ 0, & \text{otherwise.} \end{cases}$$

or using the dimensionless variables $P = p/p_h$, $X = x/a$ and $Y = y/a$:

$$P(X,Y) = \begin{cases} \sqrt{1-X^2-Y^2}, & \text{if } X^2+Y^2 \le 1; \\ 0, & \text{otherwise.} \end{cases}$$

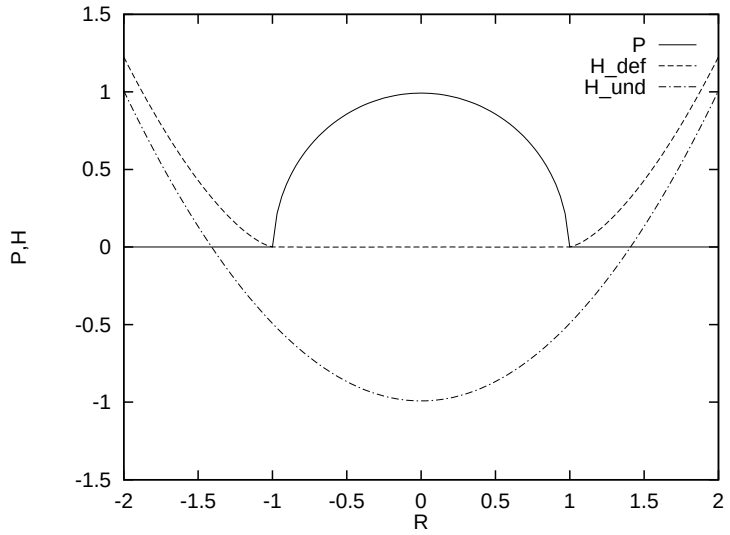

Figure 3.2 *Dimensionless Hertzian contact pressure, dimensionless deformed and undeformed geometry, for the circular contact case.*

It is now possible to compute relations between:
a the radius of the contact area
p_h the maximum pressure
w the load
R_x the (reduced) radius of contact
E' the reduced elastic modulus.

from the force balance equation we find that:

$$w = \int_{-\infty}^{+\infty} \int_{-\infty}^{+\infty} p(x', y')\, dx'\, dy'$$

which is the volume of a semi-ellipsoid with axes p_h, a and a, thus:

$$w = \frac{2\pi a^2 p_h}{3} \qquad or \qquad p_h = \frac{3w}{2\pi a^2}$$

the radius of the contact area a is found to be:

$$a = \sqrt[3]{\frac{3wR_x}{2E'}}$$

the maximum deformation is obtained in $x = y = 0$ is

$$\delta = \delta(x = 0, y = 0) = \frac{a^2}{R_x} = \sqrt[3]{\frac{9w^2}{4E'^2 R_x}}$$

Once again the approach of the centres of the two bodies is given by this value of δ.

Exercise Express the Hertzian pressure p_h in terms of w, E' and R_x only. In order to double the pressure, p_h, how much should the load w change, how much the contact radius R_x, and how much the reduced Elastic modulus E'?

Exercise Compute δ for a contact with $a = 0.001$ m and $R_x = 0.05$ m. If the reduced elastic modulus $E' = 2 \cdot 10^{11}$ Pa, what is the load w, what is the value of p_h?

Exercise Figure 3.2 shows the deformed and the undeformed geometry for a circular contact. From the difference the maximum deformation can be estimated as 1. Deduce which dimensionless film thickness relation has been used for H.

3.1.3 Elliptical contact

If the reduced radii of curvature have similar but not identical values, the contact area cannot be approximated by a line contact, nor is it a circular area. In that case the contact area is elliptical, and the deformed geometry is given by a similar equation as in the previous section:

$$h(x,y) = h_0 + \frac{x^2}{2R_x} + \frac{y^2}{2R_y} + \frac{2}{\pi E'} \int_{-\infty}^{+\infty} \int_{-\infty}^{+\infty} \frac{p(x',y')\,dx'\,dy'}{\sqrt{(x-x')^2 + (y-y')^2}}$$

Introducing the elliptical integrals $\mathcal{E}$ and $\mathcal{F}$, see Hamrock and Brewe [16]:

$$\mathcal{E} = \int_0^{+\pi/2} \left[1 - (1 - \frac{1}{k^2}) \sin^2\phi\right]^{1/2} d\phi$$

$$\mathcal{F} = \int_0^{+\pi/2} \left[1 - (1 - \frac{1}{k^2}) \sin^2\phi\right]^{-1/2} d\phi$$

one can define the semi-axes of the contact ellipse by:

$$b = \sqrt[3]{\frac{6k^2\mathcal{E}w\bar{R}}{\pi E'}}$$

$$a = \frac{b}{k} = \sqrt[3]{\frac{6\mathcal{E}w\bar{R}}{\pi k E'}}$$

where k is the ratio of the contact semi-axes: $k = b/a$, and $1/\bar{R} = 1/R_x + 1/R_y$. The maximum deformation $\delta(x = 0, y = 0) = \delta$ is given by:

$$\delta(x=0,y=0) = \delta = \mathcal{F}\sqrt[3]{\frac{9}{2\mathcal{E}\bar{R}}\left(\frac{w}{\pi k E'}\right)^2}$$

the pressure distribution $p(x, y)$ is given by:

$$p(x,y) = \begin{cases} p_h\sqrt{1-(x/a)^2-(y/b)^2}, & \text{if } (x/a)^2 + (y/b)^2 \le 1; \\ 0, & \text{otherwise.} \end{cases}$$

where the maximum Hertzian pressure p_h is given by:

$$p_h = \frac{3w}{2\pi ab}$$

Approximate solutions for the elliptical integrals are given in [16]:

$$k \simeq \beta^{2/\pi}$$

$$\mathcal{E} \simeq 1 + \frac{s}{\beta}$$

$$\mathcal{F} \simeq \frac{\pi}{2} + s \ln \beta$$

with $\beta = R_y/R_x$ and $s = \pi/2 - 1$

Exercise Check that for the case of a circular contact $k = 1$, the equations for a, b and δ reduce to the ones found in the previous section.

Exercise Compute a, b, p_h and δ for a contact with $R_x = 0.005$ m, $R_y = 0.05$ m, $E' = 2 \cdot 10^{11}$ Pa and $w = 10^4$ N?

3.2 *Adhesive contacts

The contact problem including adhesion was addressed by Johnson, Kendall and Roberts [22]. In order to understand the phenomenon of adhesion it is important to understand the origin of attraction and repulsion between two neighbouring atoms. The following equation describes the relation between force f and distance r:

$$f(r) = \frac{A}{r^m} - \frac{B}{r^n} \quad \text{and} \quad n > m$$

Figure 3.3 depicts this relation. Please note that at distance r_0 the net force is zero and attraction and repulsion cancel. Generalising this type of behaviour to perfectly smooth and clean surfaces, one can define the surface energy 2γ as the work necessary to separate two surfaces starting at the equilibrium point r_0 up to $r = \infty$.

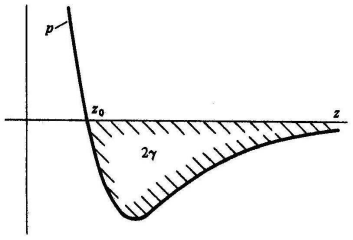

Figure 3.3 *Force between atoms as a function of distance (positive is repulsion) [22].*

Figure 3.4 shows the contact radius predicted by the JKR theory versus measured points. Note the good correlation between theoretical prediction and experimental result and the big difference with the Hertzian contact for small loads.

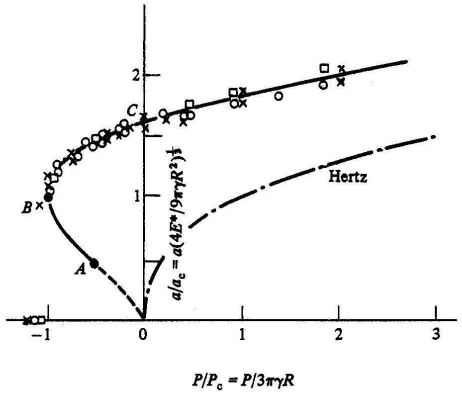

Figure 3.4 *Variation of the contact radius with load [22].*

3.3 Ertel Grubin

The approximation of the central film thickness of Ertel [11] and Grubin [12] is valid for a stationary line contact, with an incompressible fluid. It is obtained through an inlet analysis, using a displaced Hertzian geometry, and the Barus viscosity-pressure relation $\eta(p) = \eta_0 \exp(\alpha p)$.
The Reynolds equation

$$\frac{\partial}{\partial x}(\frac{h^3}{12\eta}\frac{\partial p}{\partial x}) - u_m\frac{\partial h}{\partial x} = 0$$

is simplified using the reduced pressure q:

$$q = \frac{1}{\alpha}(1 - e^{-\alpha p})$$

the derivative of the reduced pressure with respect to x is:

$$\frac{\partial q}{\partial x} = \frac{1}{\alpha}\alpha e^{-\alpha p}\frac{\partial p}{\partial x} = e^{-\alpha p}\frac{\partial p}{\partial x} = \frac{\eta_0}{\eta}\frac{\partial p}{\partial x}$$

substitution in the above Reynolds equation gives:

$$\frac{\partial}{\partial x}(h^3\frac{\partial q}{\partial x}) = 6\eta_0(u_1+u_2)\frac{\partial h}{\partial x}$$

integrating once gives:

$$h^3\frac{\partial q}{\partial x} = 6\eta_0(u_1+u_2)(h-h^*) \qquad \text{with} \qquad h^* = h|_{\partial q/\partial x=0}$$

with the boundary conditions:
$p(x\to-\infty)=0 \quad : \quad q(x\to-\infty)=0$
$p(x=x_s)=0 \quad : \quad q(x=x_s)=0$
$\partial p/\partial x(x=x_s)=0 \quad : \quad \partial q/\partial x(x=x_s)=0$
$p\to 0 \quad : \quad q\to p\to 0$
$p\to\infty \quad : \quad q\to 1/\alpha$

rearranging the terms gives:

$$\frac{\partial q}{\partial x} = 6\eta_0(u_1+u_2)\frac{h-h^*}{h^3}$$

some numerical values are given in table 3.1, using $\alpha = 2.0\cdot 10^{-8}$.

p [Pa]	q [Pa]
$1.0\cdot 10^4$	$0.9999\cdot 10^4$
$1.0\cdot 10^5$	$0.999\cdot 10^5$
$1.0\cdot 10^6$	$0.990\cdot 10^6$
$1.0\cdot 10^7$	$0.906\cdot 10^7$
$1.0\cdot 10^8$	$0.432\cdot 10^8$
$2.0\cdot 10^8$	$0.491\cdot 10^8$
$5.0\cdot 10^8$	$0.49998\cdot 10^8$
$1.0\cdot 10^9$	$0.5\cdot 10^8$

Table 3.1 *Reduced pressure q as a function of the pressure p for $\alpha = 2.0\cdot 10^{-8}$.*

Exercise Check the two asymptotes of q for $p\to 0$ and for $p\to\infty$?

3.3.1 Hypotheses

The hypotheses used in deriving the Ertel Grubin film thickness equation are:
• The contact geometry is that of a Hertzian contact $h_h(x)$ with a translation h^*, where h^* is the thickness of the oil film: $h(x) = h^* + h_h(x)$. It reads:

$$h_h(x) = -(\frac{b^2}{R})(\frac{1}{4} + \frac{1}{2}\ln 2) + \frac{x^2}{2R} - \frac{2p_h}{\pi E'}\int_{-b}^{+b}\sqrt{1-(x'/b)^2}\,\ln\left(\frac{x-x'}{x_0}\right)^2 dx'$$

• The reduced pressure q reaches the value $1/\alpha$ for $x = -b$: $q(x = -b) = 1/\alpha$.
These two hypotheses are very accurate for the slow speed highly loaded conditions, where the Hertzian assumption is accurate: $\delta >> h$. In other words for $w_1 \to \infty$ and/or $(u_1 + u_2) \to 0$.

3.3.2 Results

Substituting the second hypothesis in the reduced and integrated Reynolds equation one finds, through a second integration from $-\infty$ to $-b$:

$$q(-b) = \frac{1}{\alpha} = 6\eta_0(u_1 + u_2)\int_{-\infty}^{-b}\frac{h - h^*}{h^3}\,dx$$

and using the displaced Hertzian geometry one finds that:

$$\int_{-\infty}^{-b}\frac{h_h(x)}{(h_h(x) + h^*)^3}\,dx = \frac{1}{6\alpha\eta_0(u_1 + u_2)}$$

Since $h_h(x)$ is a function of w_1, E' and R, this equation gives h^* as a function of w_1, $u_1 + u_2$, η_0, α, E' and R.
The Hertzian geometry is approximated by:

$$h_h(x) = \frac{2\sqrt{2b}(-x-b)^{3/2}}{3R} \qquad \text{for} \qquad -\infty < x < -b$$

NB: note that $h_h(x = -b) = 0$.
Integration gives the following relation:

$$\boxed{\frac{h^*}{R} = 1.31\left(\frac{(\alpha E')\eta_0(u_1 + u_2)}{E'R}\right)^{3/4}\left(\frac{w_1}{E'R}\right)^{-1/8}}$$

where h^* is an approximation of the central or mean film thickness. h^* is very sensitive to changes in viscosity η_0 and speed $(u_1 + u_2)$, whereas the film thickness is hardly affected by variations in the load per unit length w_1. The parameters α and E' can only be varied very little, at least when using steel bodies and mineral oils.

Exercise Compute h^* for $R = 0.01$ m, $\eta_0 = 0.1$ Pas, $\alpha = 2 \cdot 10^{-8}$ Pa^{-1}, $u_1 + u_2 = 1$ m/s, $E' = 2 \cdot 10^{11}$ Pa, $w_1 = 10^4$ kg/m.

Exercise* Calculate the integral to find h^* using Mathematica/Maple and by hand. In both cases the integral should be simplified (introduce dimensionless variables, shift the origin etc).

3.4 Dimensionless Groups

The film thickness obtained by the Ertel Grubin analysis in the previous section is a function of seven parameters: $h^* = f(\eta_0, \alpha, R, E', u_1, u_2, w_1)$, which makes it difficult to understand its behaviour. In order to simplify the study of h^*, it is possible to introduce a relation between four dimensionless parameters [9], which can already be seen from the way the previous equation is written.

$$W_1 = \frac{w_1}{E'R}$$
$$U = \frac{\eta_0(u_1 + u_2)}{E'R}$$
$$G = \alpha E'$$
$$H^* = h^*/R$$

where W_1 is called the load parameter, U is called the speed parameter, G is called the materials parameter and H is the dimensionless film thickness parameter.

NB: a second definition of U using the mean surface velocity is also commonly used in the literature: $U = \eta_0(u_1 + u_2)/(2E'R_x)$, the coefficients of the equations change, so be careful. In this work we use the first definition with the sum velocity.

Using these four parameters the Ertel Grubin equation can be rewritten as:

$$H^* = 1.31\,(GU)^{3/4}(W_1)^{-1/8}$$

NB, the index 1 in W_1 is used to distinguish the dimensionless load parameter in the one and two dimensional case, see later sections.
Common values for steel-steel contacts lubricated with a mineral oil are: $W_1 = 10^{-7} - 10^{-5}$, $U = 10^{-12} - 10^{-10}$, $G \simeq 4000$.

Exercise Compute h^* for $R = 0.01$ m, $\eta_0 = 0.1$ Pas, $\alpha = 2 \cdot 10^{-8}$ Pa^{-1}, $u_1 + u_2 = 1$ m/s, $E' = 2 \cdot 10^{11}$ Pa, $w_1 = 10^4$ kg/m, using the parameters W_1, U and G. Same question using Figure 3.3.

Exercise Using Figure 3.3 find h^* for $R = 0.01$ m, $\eta_0 = 0.1$ Pas, $\alpha = 2 \cdot 10^{-8}$ Pa^{-1}, $u_1 + u_2 = 1$ m/s, $E' = 2 \cdot 10^{11}$ Pa, $w_1 = 10^4$ kg/m.

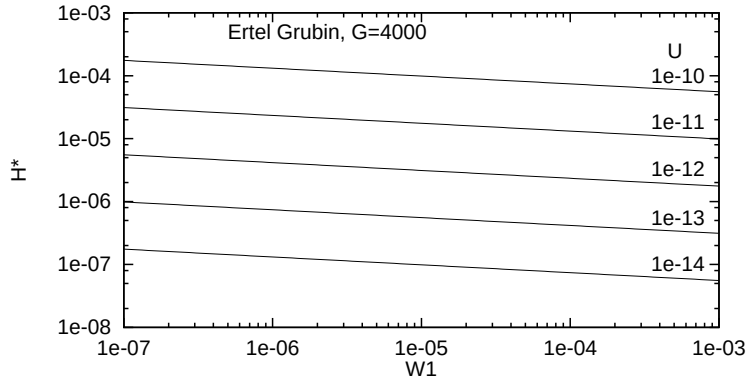

Figure 3.3 *Dimensionless film thickness H^* as a function of W_1 and U for G=4000.*

Exercise How much does the film thickness h change if the atmospheric viscosity η_0 is doubled? How much if the speed $u_1 + u_2$ is doubled? How much if the load per unit length w_1 is doubled? How much if the reduced elasticity E' is doubled (careful)? How much if the reduced contact radius R is doubled (careful)?

Exercise The aim of this exercise is to keep the film thickness constant. How much does one have to change the speed $u_1 + u_2$ when the viscosity η_0 is halved? How much does the load have to change when the viscosity is doubled?

Exercise Express the Hertzian contact half width b in terms of W_1 and R.

3.5 Dowson Higginson

The numerical line contact results of Dowson and Higginson, were published in the 1960's, [9] and form the basis of film thickness equations derived by curve-fitting of the numerical results. The general shape of the pressure and film thickness distributions are given in Figure 3.4. Three distinct zones can be identified:
• the inlet, $x < -b$, $p(x) << p_h$, $h(x) >> h_c$, is the zone where the pressure is built up due to the converging gap.
• the high pressure zone, $-b < x < b$, $p(x) \simeq p_h$, $h(x) \simeq h_c$, is the zone where the film thickness is nearly parallel, and the pressure close to the dry contact pressure.
• the outlet, $x > b$, $p(x) << p_h$, $h(x) >> h_c$, is the zone where the gap increases and the pressure drops rapidly and cavitation occurs.
The Reynolds equation has a very different character in these three zones, and

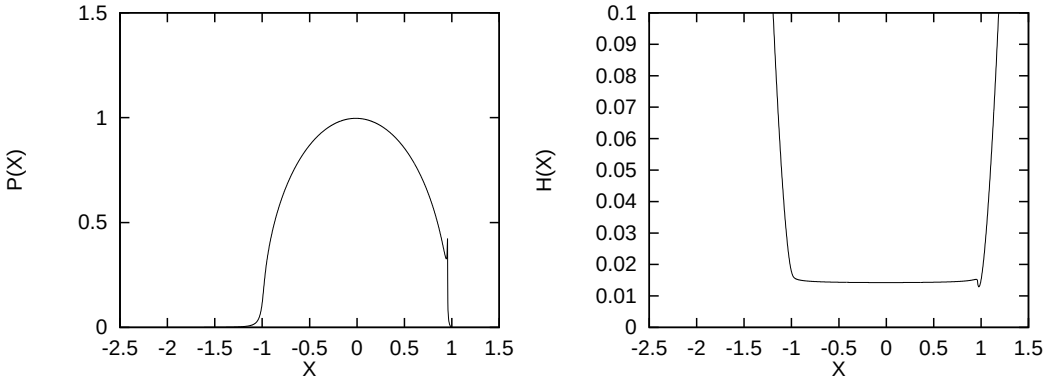

Figure 3.4 *Dimensionless pressure $P(X)$ and film thickness $H(X)$ distribution.*

Dowson and Higginson used different solution techniques in these different zones. These techniques are outlined in a later section.

On the boundary between the high pressure zone and the outlet a pressure spike appears, which is accompanied by a local film thickness reduction. The film thickness reaches a global minimum h_m. The deformations in the inlet and outlet region are relatively small, in the high pressure zone, on the contrary, they are important.

3.5.1 Numerical results: varying U

This section presents a series of pressure and film thickness results for increasing contact speed. All other parameters, including load, are kept constant.

Note that for increasing speed, the film thickness increases, and the pressure distribution and the film thickness distribution become less Hertzian. Increasing speed produces a similar effect as decreasing load (see next section). This is an indication that the parameter set W_1, U and G can be reduced to a two parameter set such as the one proposed by Moes with: $M_1 = W_1/\sqrt{U}$ and $L = G\sqrt[4]{U}$.

Exercise What is the dimensionless film thickness $H(X = 0)$ in the Figures 3.5 to 3.7? What is the relative evolution of $h(x = 0)$? Compare the evolution with the one predicted by Ertel-Grubin?

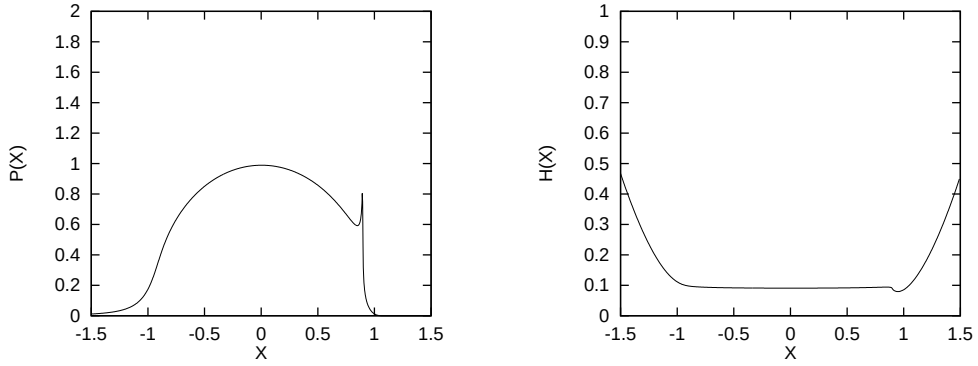

Figure 3.5 *Dimensionless pressure and film thickness distribution* $W_1 = 1.53 \cdot 10^{-4}$, $U = 5.89 \cdot 10^{-11}$, $G = 4000$.

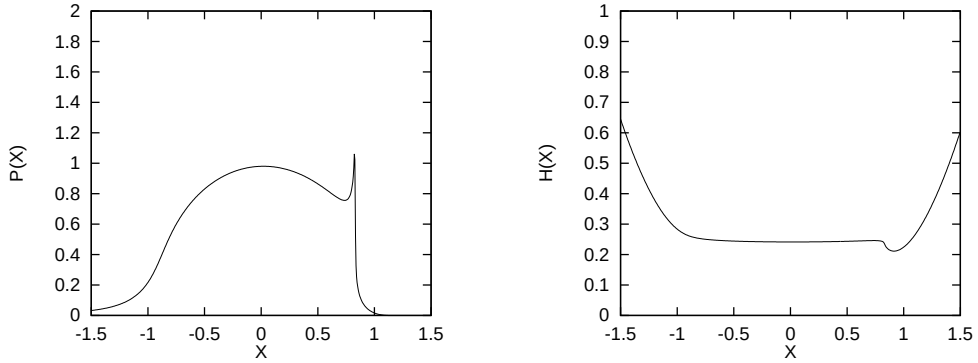

Figure 3.6 *Dimensionless pressure and film thickness distribution* $W_1 = 1.53 \cdot 10^{-4}$, $U = 2.36 \cdot 10^{-10}$, $G = 4000$.

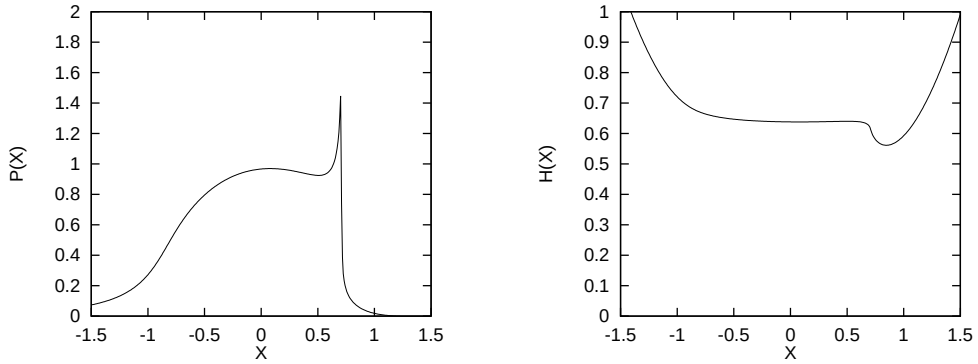

Figure 3.7 *Dimensionless pressure and film thickness distribution* $W_1 = 1.53 \cdot 10^{-4}$, $U = 9.42 \cdot 10^{-10}$, $G = 4000$.

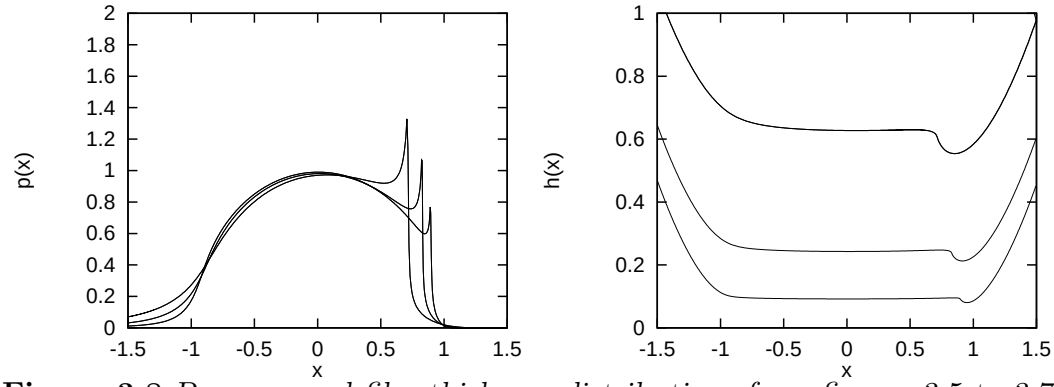

Figure 3.8 *Pressure and film thickness distributions from figures 3.5 to 3.7, (arbitrary units).*

3.5.2 Numerical results: varying W_1

This section presents a series of pressure and film thickness results for increasing contact load. All other parameters, including speed, are kept constant.

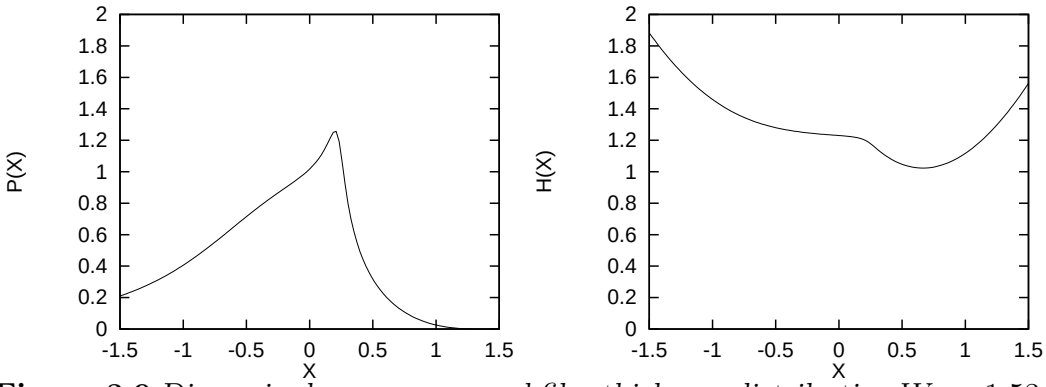

Figure 3.9 *Dimensionless pressure and film thickness distribution* $W_1 = 1.53 \cdot 10^{-5}$, $U = 5.89 \cdot 10^{-11}$, $G = 4000$.

From these figures it can be observed that with increasing load the pressures in the inlet region become of less importance (relatively). The film thickness in the high pressure zone becomes more and more parallel, and the pressure spike moves towards the exit of the high pressure zone. With increasing load a reduction in the central and minimum film thickness takes place as well.
NB1: please note the changing scale on the film thickness axis $H = hR/b^2$ in the figures.
NB2: please note that when the load per unit length w_1 increases, the contact width

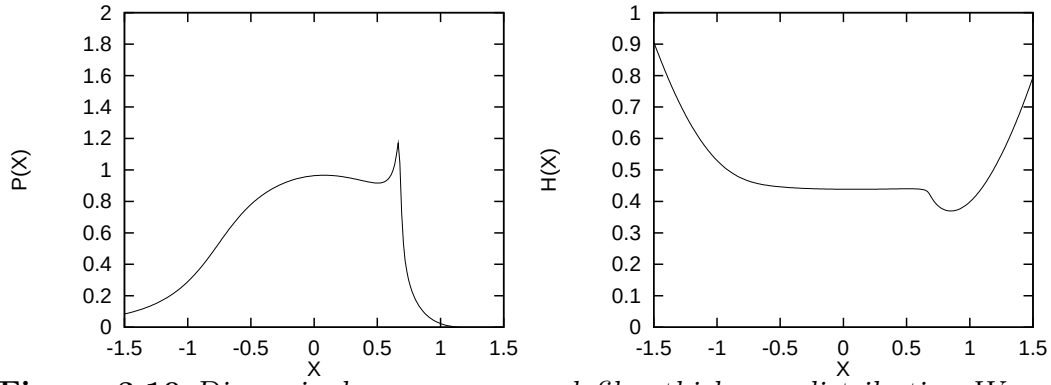

Figure 3.10 *Dimensionless pressure and film thickness distribution* $W_1 = 3.84 \cdot 10^{-5}$, $U = 5.89 \cdot 10^{-11}$, $G = 4000$.

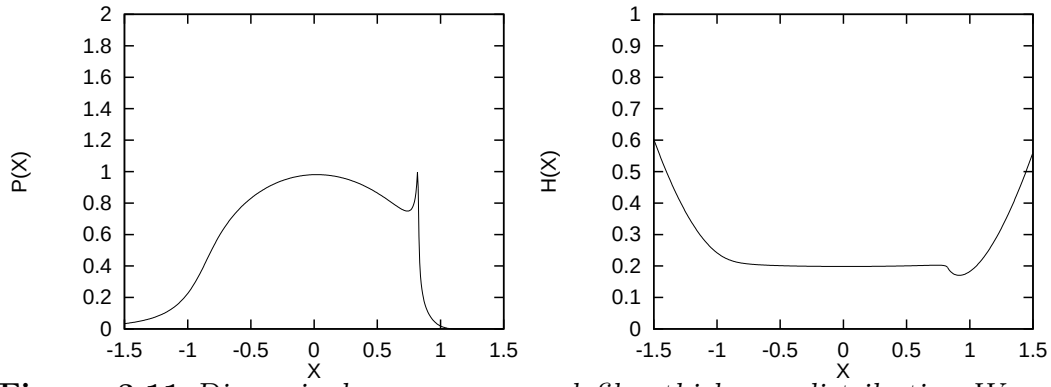

Figure 3.11 *Dimensionless pressure and film thickness distribution* $W_1 = 7.67 \cdot 10^{-5}$, $U = 5.89 \cdot 10^{-11}$, $G = 4000$.

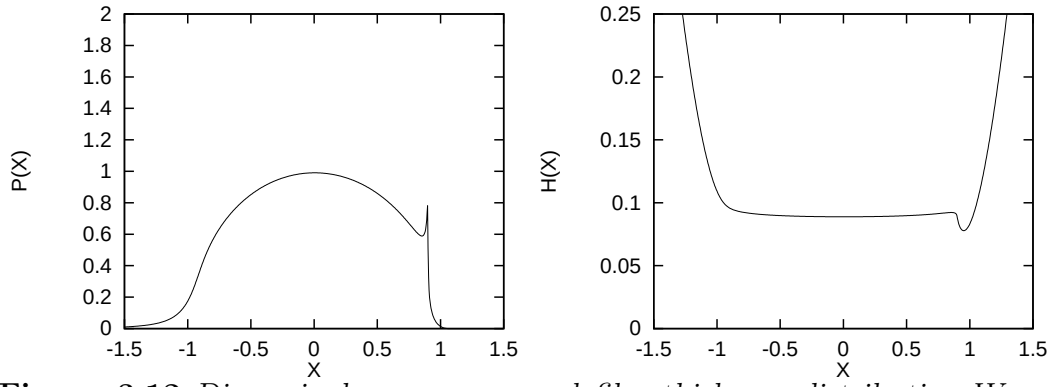

Figure 3.12 *Dimensionless pressure and film thickness distribution* $W_1 = 1.53 \cdot 10^{-4}$, $U = 5.89 \cdot 10^{-11}$, $G = 4000$.

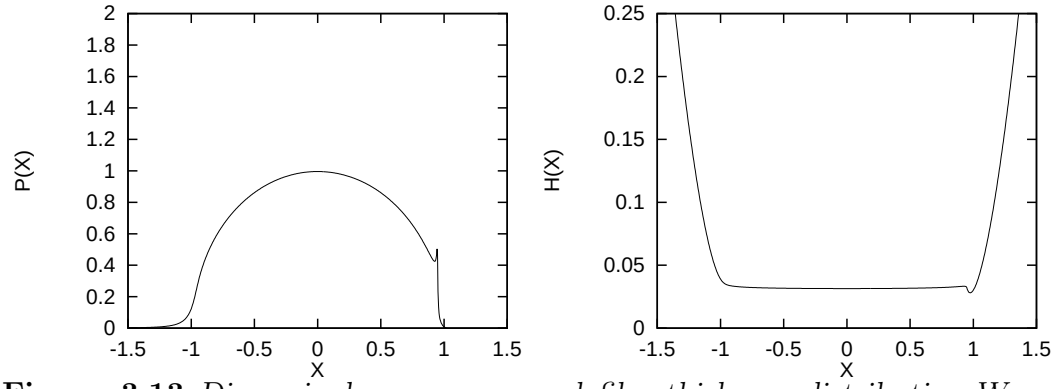

Figure 3.13 *Dimensionless pressure and film thickness distribution* $W_1 = 3.84 \cdot 10^{-4}$, $U = 5.89 \cdot 10^{-11}$, $G = 4000$.

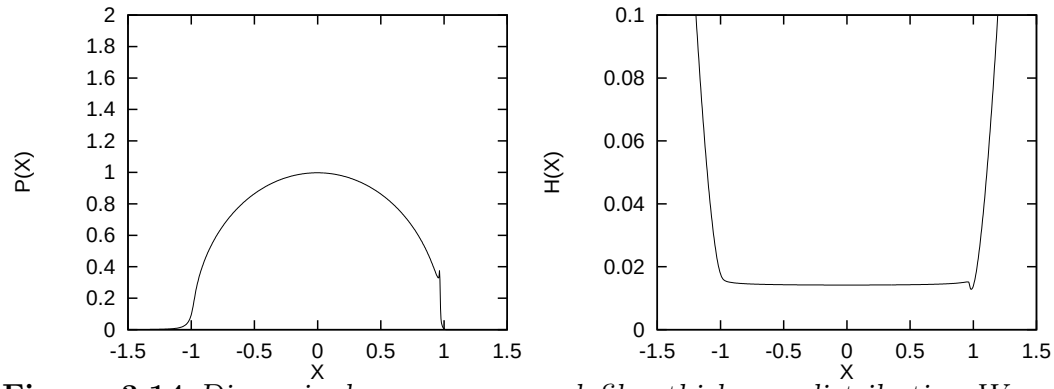

Figure 3.14 *Dimensionless pressure and film thickness distribution* $W_1 = 7.67 \cdot 10^{-4}$, $U = 5.89 \cdot 10^{-11}$, $G = 4000$.

b and the maximum Hertzian pressure p_h also increase. In the dimensionless graphs presented in this section, this change does not appear, due to the use of dimensionless pressure $P = p/p_h$ and dimensionless coordinate $X = x/b$. The evolution of the dimensional pressure and film thickness is shown in figure 3.15

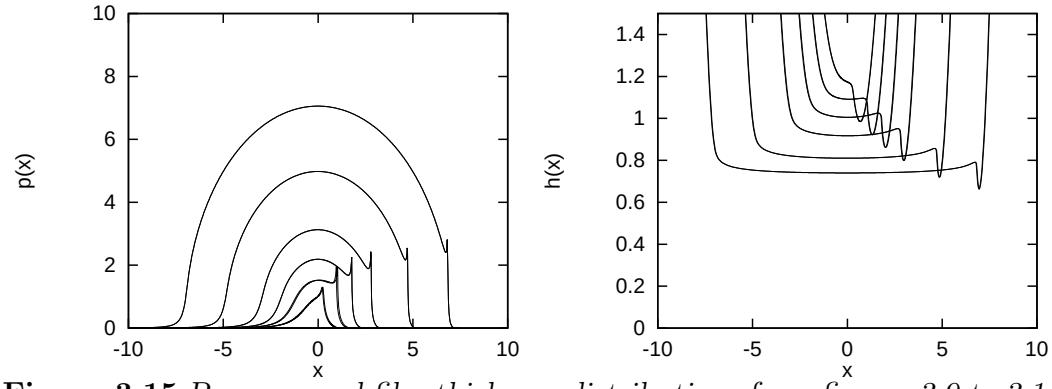

Figure 3.15 *Pressure and film thickness distributions from figures 3.9 to 3.14 (arbitrary units).*

NB3: please note how for increasing load the pressure and the film thickness distribution tend to the Hertzian distributions.

Exercise What is the dimensionless central film thickness $H(X = 0)$ in the Figures 3.9 to 3.14? What is the relative evolution of $h(x = 0)$, careful?

Exercise What is the dimensionless central pressure $P(X = 0)$ in the Figures 3.9 to 3.14? What is the relative evolution of $p(x = 0)$?

Exercise Compare the answers on $h(x = 0)$ and $p(x = 0)$ from the two previous exercises with the Figure 3.15.

3.5.3 Film thickness equation

Dowson and Higginson have computed a large number of minimum film thickness values, for different sets of operating conditions. They then curve fitted these results to obtain a film thickness equation. In order to reduce the number of parameters, they used the dimensionless parameters introduced in a previous section:

$$W_1 = \frac{w_1}{E'R}$$

$$U = \frac{\eta_0(u_1 + u_2)}{E'R}$$

$$G = \alpha E'$$
$$H_m^D = h_m/R$$

where h_m is the minimum film thickness. They obtained the following equation as a best curve fit of their results:

$$H_m^D = 0.985\, G^{0.6} U^{0.7} W_1^{-0.13}$$

a comparison of the powers found by Dowson and Higginson with those of the Ertel Grubin formula

$$H^* = 1.31\, (GU)^{3/4} (W_1)^{-1/8}$$

gives:

	E.G.	D.H.
G	0.75	0.60
U	0.75	0.70
W_1	-0.125	-0.13

Table 3.2 *Comparison of the powers obtained in the Ertel Grubin and the Dowson Higginson film thickness equations.*

One sees that all powers are comparable, thus both equations will predict similar film thickness values and similar trends. However, when comparing these results one has to keep in mind that both equations approximate different properties: H^* is a kind of mean or averaged film thickness, while H_m^D represents a minimum film thickness.
Even though the numerical techniques have vastly improved over the last four decades, the Dowson and Higginson equation has only undergone slight modifications. It remains a reference equation for film thickness in EHL line contacts.

Exercise Compute h_m for $R = 0.01$ m, $\eta_0 = 0.1$ Pas, $u_1 + u_2 = 1$ m/s, $\alpha = 2 \cdot 10^{-8}$ Pa^{-1}, $E' = 2 \cdot 10^{11}$ Pa, $w_1 = 10^4$ kg/m. Compare with the Ertel Grubin value, comments?

3.5.4 *Pressure spike

In the previous section two distinct phenomena have been observed in the EHL film thickness and pressure distributions. First of all a local film thickness reduction

is obtained at the end of the high pressure zone (near $X = 1$). Just before this restriction a local second pressure maximum: the pressure spike, is observed.
The local film thickness reduction can be explained by studying the Reynolds equation. In this region the Couette flow and the Poiseuille flow act in the same direction. Because the pressure gradient is very large and because the viscosity is close to its ambient value, the flow would be too large. To maintain flow continuity, a local film thickness reduction is required.
In order to understand the pressure spike it is necessary to study the elastic deformation equation. This equation shows that a pressure distribution with a logarithmic singularity (the spike) is required to produce a nearly constant film thickness followed by a sudden restriction [13]. Physically, this abrupt film thickness reduction is required to ensure mass flow continuity, when the reduction in pressure causes the viscosity to decrease very rapidly, and increases the flow. For a compressible fluid the logarithmic singularity is softened, and the maximum peak pressure remains finite.

3.5.5 *Numerical technique

The solution method of Dowson and Higginson for the EHL line contact problem consists of solving the Reynolds equation and the film thickness equation one after the other, and iterating between the two solutions until convergence is obtained. Then the third equation of force balance is adjusted, and one returns to the first two. This is repeated until all equations have converged to within a certain accuracy. The way the Reynolds and film thickness equation are solved however, is different in the high pressure zone and in the low pressure zone.

In the low pressure zones a so called direct method is applied: given an initial film thickness profile $h(x)$, the Reynolds equation is solved for the pressure distribution $p(x)$. Then this new pressure distribution is used to compute the new elastic deformations, thus resulting in a new film thickness distribution etc. etc, until convergence.

In the high pressure zones a so called inverse method is applied: given an initial pressure profile $p(x)$, the Reynolds equation and the film thickness equation are solved to give two film thickness profiles: $h(x)$. These two are compared and the pressure distribution is altered to reduce the difference between the two film thickness profiles. This process is repeated until convergence.

The two pressure distributions in the inlet and the high pressure zone are matched in such a way that a continuous pressure and film thickness profile occurs over the entire domain of calculation. In an outer loop, the force balance equation is adjusted to obtain the required load.

The reason why the inverse method is introduced in the solution process, is that the straightforward direct method fails to converge in the high load zone, whenever the applied load becomes important. The reason for this divergence has only been discovered recently, and will be outlined in a later section.

3.6 Moes Venner, 1d

There exist other sets of dimensionless parameters, the best known set of two parameters are named after Moes, and are called M_1 and L. Moes himself prefers to call them the Delft parameters, since they were originally developed at the University of Delft. This set has the advantage of being even smaller, and it allows a graphical representation which includes other (non-EHL) solutions, which act as asymptotic solutions to the EHL solution. In this section the line contact parameters are presented. The parameters M_1 and L are formed by regrouping the parameters W_1, U and G. One has to be careful when using these parameters since the minimum film thickness parameter H_m^M incorporates the speed parameter U.

$$M_1 = \frac{W_1}{\sqrt{U}}$$

$$L = G\sqrt[4]{U}$$

$$H_m^M = \frac{h_m}{R\sqrt{U}}$$

$$H_m^M = 1.56\, L^{0.55} M_1^{-0.125}$$

NB: be careful not to mix up $H_m^D = h_m/R$ and $H_m^M = h_m/(R\sqrt{U})$!

Exercise What are the advantages of the set M_1, L over the set W_1, U, G? What are its disadvantages?

Exercise What is the order of magnitude of H_m^D and of H_m^M? Use typical values given before for oil/steel contacts.

Exercise Compute h_m for $R = 0.01$ m, $\eta_0 = 0.1$ Pas, $u_1 + u_2 = 1$ m/s, $\alpha = 2 \cdot 10^{-8}$ Pa^{-1}, $E' = 2 \cdot 10^{11}$ Pa, $w_1 = 10^4$ kg/m. Compare with the Dowson and Higginson value and the Ertel Grubin value, comments?

Exercise Express the Ertel Grubin formula in terms of H_{min}, M_1 and L.

3.6.1 Comparison

In this section the powers of the three film thickness formulae are compared. The Ertel Grubin equation can be expressed in terms of M_1 and L, see the last exercise of the previous section. The Dowson and Higginson equation cannot be expressed in terms of M_1 and L, consequently the Moes Venner equation is expressed in terms of W_1, U and G, and the three equations are compared. In terms of these parameters this equation reads:

$$H_m^D = 1.56\, G^{0.55} U^{0.7} W_1^{-0.125}$$

NB: $H_m^D = h_m/R$ whereas $H_m^M = h_m/(R\sqrt{U})$!

	E.G.	D.H.	M.V.
G	0.75	0.60	0.55
U	0.75	0.70	0.70
W_1	-0.125	-0.13	-0.125

Table 3.3 *Comparison of the powers obtained in the Ertel Grubin, Dowson Higginson and Moes Venner film thickness equations.*

Exercise Check the expression of the Moes Venner formula in terms of H_m^D, W_1, U and G.

3.6.2 Graphical representation

Using the Moes dimensionless parameters two additional asymptotes can be represented. These are the rigid isoviscous asymptote, when no elastic deformations occur, and the viscosity is constant and equal to the ambient pressure value η_0. The parameter L is zero since $\alpha = 0$ (isoviscous assumption).

$$H_m^M = \frac{2.45}{M_1}$$

A second asymptote is called the elastic isoviscous asymptote. The elastic deformations can no longer be neglected, but the viscosity remains at its ambient pressure value η_0, in other words α remains zero.

$$H_m^M = \frac{2.05}{\sqrt[5]{M_1}}$$

The following figure represents these three asymptotes together with numerical film thickness values computed by Venner [37].

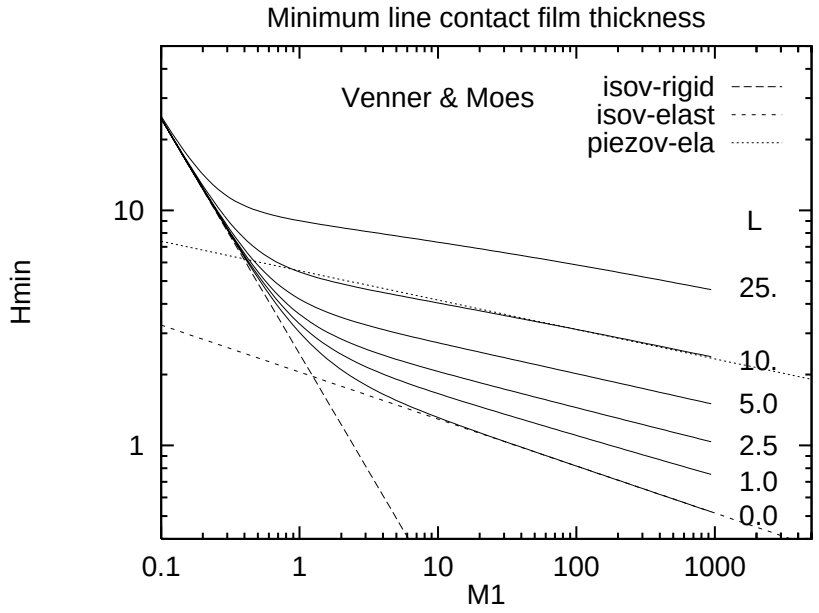

Figure 3.16 *Moes-Venner film thickness prediction together with the three asymptotes, the piezo viscous-elastic asymptote given for* $L = 10$.

This Figure shows that the three asymptotes describe the film thickness behaviour accurately in a wide range of operating conditions.

NB Note that the Ertel Grubin formula, presented in section 3.3.2 and 3.4, the Dowson and Higginson formula presented in section 3.5.3, and the Moes-Venner equation from this section are only valid under **Piezoviscous Elastic** conditions, which can be approximated by the Moes parameters: $M_1 > 5$, $L > 2.5$.

Exercise Which of the three regimes is the appropriate regime for $M_1 = 1$, $L = 0$? and for $M_1 = 100$, $L = 0$? and for $M_1 = 100$, $L = 10$? and for $M_1 = 10$, $L = 1$ (careful)? Compute for each of the cases the film thickness H_m^M.

Exercise Draw the EHL domain in Figure 3.3, where the Ertel Grubin formula is valid. Use $M_1 > 5$ and $L > 2.5$ as criteria. What happens if one uses the EG equation beyond these limits?

3.7 *I.R. Friction

In this section the friction is calculated in the Isoviscous Rigid regime. The friction force F_t is equal to the mean shear stress times the contact area. The shear stress is approximated by the Couette term in a pure sliding situation: $u_1 = u$, $u_2 = 0$. The shear stress is equal to $\eta_0 \partial u(z)/\partial z|_{z=0}$ (for the lower surface). Using the Couette approximation one writes the shear rate as

$$\frac{\partial u(z)}{\partial z} = \frac{u}{h}$$

Thus one needs to compute the dimensional film thickness and we take the minimum film thickness h_m obtained in the previous section. The dimensionless film thickness for the Isoviscous Rigid regime is given by:

$$H_m^M = \frac{2.45}{M_1}$$

Using the definition of H_m^M and M_1 one obtains:

$$\frac{h_m}{R\sqrt{U}} = 2.45\frac{\sqrt{U}}{W_1}$$

Using the definition of U and W_1 one finds:

$$h_m = 2.45\frac{R\eta_0 u E' R}{E' R w_1} = 2.45\frac{R\eta_0 u}{w_1}$$

Assuming that the friction force F_t is proportional to the area A times the shear stress and that the area is proportional to R (remember this is area per unit length!) one finds:

$$F_t \propto A\eta_0 \frac{u}{h_m} \propto \frac{Ru\eta_0 w_1}{\eta_0 Ru} \propto w_1$$

As a result the friction force F_t per unit length is proportional to the load per unit length. Consequently, the friction coefficient $f = F_t/w_1$ is constant, that is independent of load, speed and viscosity!

Exercise Calculate the dimension of the term $\eta_0 u/w_1$. What is the consequence for the minimum film thickness h_m?

Exercise Explain why the film thickness h_m is independent of E' in the I.R. regime. What about the dependence on α?

Exercise Show that for the I.E. regime $h_m \propto \eta_0^{0.4}$ and $h_m \propto w_1^{0.2}$. Show that as a consequence the friction coefficient $f \propto w_1^{-0.8}$. Derive the complete equation

showing the dependence of F_t with respect to all parameters η_0, R, w_1 and E'. Show through a dimensional analysis that indeed $[F_t] = N/m$.

3.8 Hamrock Dowson

In the mid seventies, Hamrock and Dowson [15] published a series of four papers, describing the film thickness in circular ($R_x = R_y$) and elliptical ($R_x \neq R_y$) EHL contacts. Their film thickness equation was based on numerous numerical calculations of the film thickness for different sets of operating conditions. In order to reduce the number of parameters they extended the Dowson and Higginson dimensionless parameters to the circular contact case:

$$W_2 = \frac{w}{E' R_x^2}$$

$$U = \frac{\eta_0 (u_1 + u_2)}{E' R_x}$$

$$G = \alpha E'$$

$$H_c^D = h_c / R_x$$

notice that the index 2 in W_2 corresponds to the two dimensional case, and the load is divided by the square of the reduced radius. All these results were curve fitted to obtain the following equations:

$$H_c^D = 1.69\, G^{0.53} U^{0.67} W_2^{-0.067} \left(1 - 0.61 \exp(-0.73k)\right)$$

$$H_m^D = 2.27\, G^{0.49} U^{0.68} W_2^{-0.073} \left(1 - \exp(-0.68k)\right)$$

where $k = 1.03 (R_y / R_x)^{0.64}$.
These equations have been derived for the condition that $k \geq 1$, they are not valid when $R_y < R_x$.

Exercise Compare the exponents of U and W_2 in H_c^D and H_m^D. What do you conclude. Will the difference between H_m^D and H_c^D increase or decrease with increasing values of W_2 and U?

3.9 Moes Venner 2d

Once again it is possible to simplify the film thickness relation, and to eliminate one parameter. The best known set of two parameters are named after Moes, and are called M_2 and L. It is an extension of the one dimensional set. This choice allows a graphical representation which includes other (non-EHL) solutions, which act as asymptotic solutions to the EHL solution. In this section the circular contact parameters are presented.

$$M_2 = \frac{W_2}{U^{3/4}}$$

$$L = G\sqrt[4]{U}$$

$$H_c^M = \frac{h_c}{R_x\sqrt{U}}$$

Using these parameters it is possible to express the isoviscous-rigid asymptote, it reads:

$$H_c^M = 47.3\, M_2^{-2}$$

whereas the isoviscous-elastic asymptote reads:

$$H_c^M = 1.96\, M_2^{-1/9}$$

The Figure 3.17 shows the two asymptotes together with the full EHL solution. It shows once again the regions where each of the solutions is valid. This solution was obtained using the following (rather complex) formula.

$$H_c^M = \left[\left\{(1.70\, t\, M_2^{-1/9} L^{3/4})^r + (1.96\, M_2^{-1/9})^r\right\}^{s/r} + (47.3\, M_2^{-2})^s\right]^{1/s}$$

where $r = \exp\{1 - 6/(L+8)\}$
$s = 12 - 10\exp(-M_2^{-2})$
$t = 1 - \exp(-0.9 M_2^{1/6}/L^{1/6})$

NB1 No piezo-viscous elastic asymptote can easily be extracted from this equation, it has to be used as a whole.

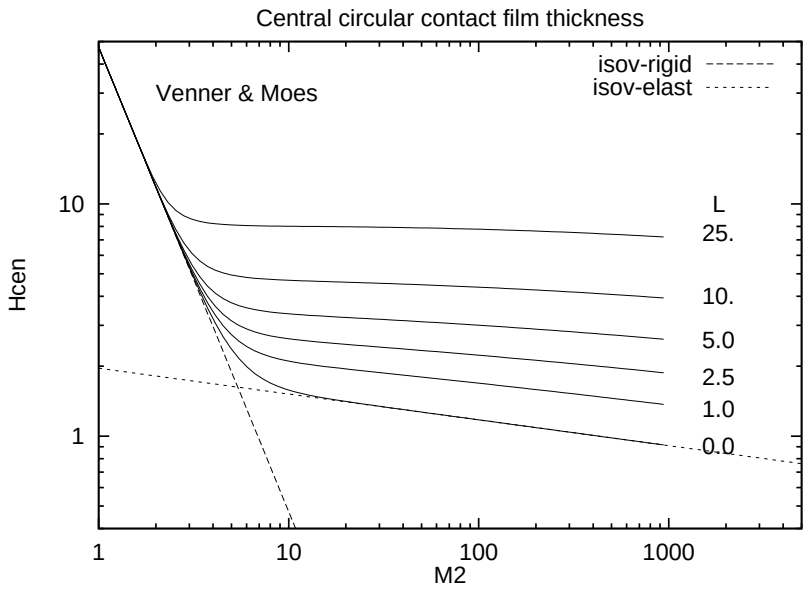

Figure 3.17 *Moes-Venner film thickness prediction together with two of the three asymptotes.*

NB2 Note that the Hamrock and Dowson formula presented in section 3.7 is only valid under EHL conditions, which can be approximated by the Moes parameters: $M_2 > 10$, $L > 2.5$.

Exercise Which of the three regimes is the appropriate regime for $M_2 = 3$, $L = 0$? and for $M_2 = 100$, $L = 0$? and for $M_2 = 100$, $L = 10$? and for $M_2 = 10$, $L = 1$ (careful)? Compute for each of the cases the film thickness H_c^M.

Exercise Calculate the film thickness assuming $R_x = R_y = 30$ mm, $w = 90$ kg, $\eta_0 = 10^{-4}$ Pa s, $\alpha = 10^{-9}$ Pa^{-1}, $u_1 + u2 = 60$ m/s, $E' = 2\,10^{11}$ Pa, careful, which regime?

Exercise Derive the dimensional film thickness equation in the I.R. regime. Comment on the absence of E'. Check the dimension.

Exercise Derive the dimensional film thickness equation in the I.E. regime. Comment on the absence of α. Check the dimension.

Exercise Calculate the film thickness H_c^D and H_c^M for $W_2 = 10^{-5}$, $U = 10^{-11}$ and $G = 4000$. Compare the two values and list another advantage of the Moes parameter set.

3.9.1 Film thickness graphs

When studying the point contact problem, one finds that the film thickness in the central zone is roughly constant, as in the line contact case. This constant central zone is surrounded by a horse shoe shaped zone of minimum film thickness. The opening of the horse shoe is in the inlet region. The smallest film thickness is normally found away from the centre line of the contact, in the side lobe region. The precise shape of the film thickness distribution evolves with the operating conditions as is shown by the following graph.

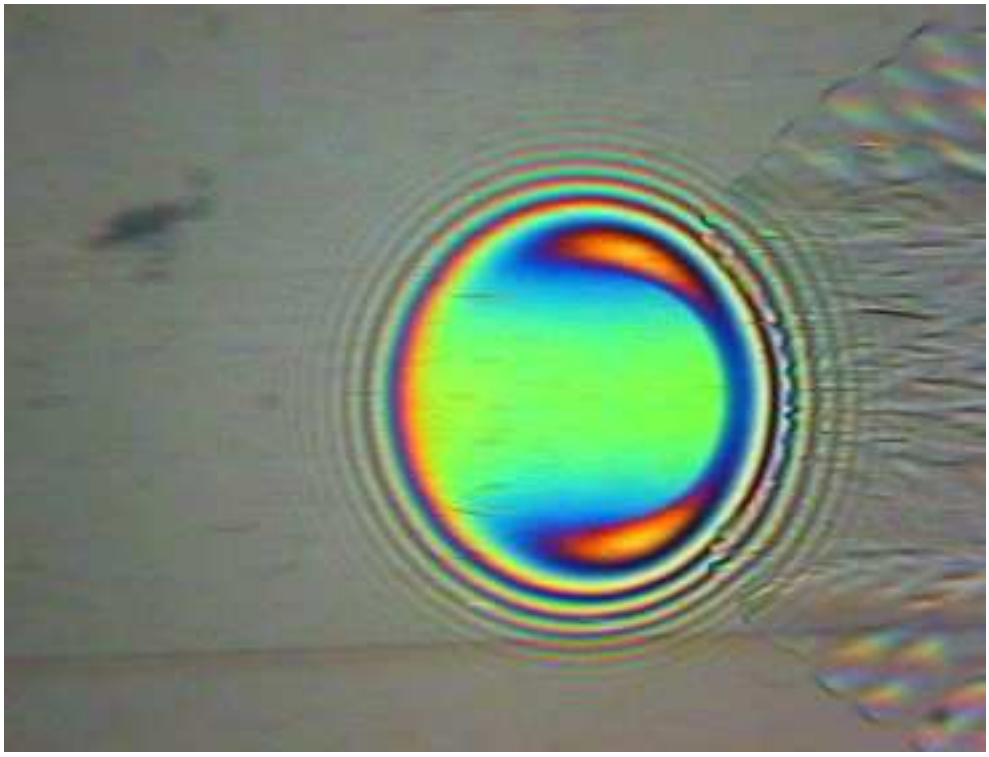

Figure 3.18 *Interferometric pictures showing the film thickness distribution by P.M.E. Cann.*

3.9.2 *Central and minimum film thickness

In the line contact section, only one equation for the central (Ertel Grubin) or minimum film thickness was given, in the line contact case, the central and minimum film thickness are connected through the flow continuity equation, because the same

flux has to pass the central and the minimum film thickness.
In a circular or an elliptical contact, this is no longer true, the minimum film thickness occurs in the side lobes, and no continuity equation connects the two. As a consequence, the minimum film thickness and the central film thickness vary in an independent way. In general, one can say that for increasing loads, the minimum film thickness has the tendency to decrease **faster** than the central film thickness.

Chapter 4

*Advanced Topics

In this chapter an overview of more recent developments is given. Due to its very nature, there is not yet a scientific consensus on some of these topics.

4.1 Friction

Friction in thin films is generally simple to predict under normal atmospheric conditions. Whenever slip is important, the fluid flow in the contact can be approximated by a Couette shear flow. The shear stress obtained in such a contact is simply the product of the fluid viscosity η_0 and the shear rate $\partial u/\partial z$. The shear stress is simple to measure in standard laboratory equipment such as a concentric viscometer.

In EHL contacts, however, the viscosity depends on the pressure and can be very high. Furthermore, because of the small film thicknesses, and the large velocity differences between the two surfaces, the shear stresses can be enormous. This results in general in two different phenomena: thermal dissipation and rheological effects. Due to the thermal dissipation, the temperature in the contact will increase, thereby changing the fluid properties such as the density and the viscosity. Rheological effects cause the shear stress - shear rate relation to deviate from the Newtonian law used above. Finally, when the film thicknesses in EHL contacts are approximating molecular values, such thin fluid films can show behaviour that deviates from that of the bulk fluid.

The extreme conditions inside an EHL contact make a direct and detailed study of these effects difficult or impossible. As a result, the majority of the studies have resulted from average traction measurements, without a detailed study of what really happens inside an EHL contact under sliding conditions. Such average measures are

used in traction curves, where the friction coefficient in a contact is plotted against the sliding speed $(u_2 - u_1)/(u_2 + u_1)$.

Three different regimes can be observed:
a linear regime, where the friction increases linearly with the slip.
a nonlinear regime, where the friction increases less than linearly with the slip.
a thermal regime where the friction coefficient decreases with increasing slip.
These three regimes can be observed in Figure 4.1. It should be noted that a general friction curve consists of all these three regimes.

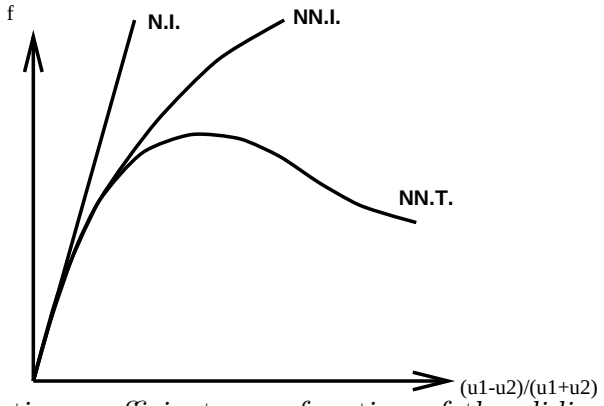

Figure 4.1 *Friction coefficient as a function of the sliding speed, for three different regimes: Newtonian Isothermal, Non-Newtonian Isothermal, Non-Newtonian Thermal.*

4.2 Rheology

Whenever the shear stress - shear rate behaviour deviates from the linear behaviour called Newtonian, one calls this behaviour non-Newtonian. General rheological behaviour can show both an increase as well as a decrease in the effective viscosity. Another possibility is that the film shows other than pure viscous behaviour such as elastic or plastic behaviour or time dependent behaviour. In general the behaviour of the fluid film in an EHL contact, is a combination of these individual ones: visco-elastic, visco-plastic etc. Such behaviour reflects phenomena taking place on a molecular scale: fluid molecules might align in a shear flow, resulting in a shear stress that is lower than that predicted by the Newtonian laws. The first fluid layers adhering to the boundary may impose on the film a character different from the bulk character. Due to the high pressures, the fluid molecules are pressed together, and start to interact in a way which resembles that of solids. In this last

case, the fluid is called solidified (glassy-state) and for numerous fluids this solidification pressure has been studied as a function of temperature, see Jacobson and Vinet [20]. An overview of this rheological behaviour with a tribological background is given by Jacobson [21].

4.3 Additives

So far we have only discussed the base oil viscosity of the lubricant (and its density to a lesser extent), but additives are generally added to all commercial oils to improve certain characteristics of the lubricant. In this section we will rapidly discuss a number of different additives and their use.

VI improvers: the Viscosity Index is a measure of the variation of viscosity with temperature. In order to build up a sufficiently thick film, oils with a high viscosity are to be preferred. However, these high viscosity oils lead to high viscous losses due to churning (oil bath). Consequently, a compromise between losses and film thickness has to be found. Now the operating temperatures, for instance in cars (summer & winter) can vary significantly, and perturb this balance. Thus VI improvers are used to reduce the viscosity variation with temperature. VI improvers are generally high molecular weight polymers.

EP (Extreme Pressure) additives: mathematically smooth surfaces are easily separated by an oil film, however, engineering surfaces are generally rough and especially during running-in, metal to metal contact can occur. The local conditions when metal to metal contact occurs can be extreme, and the protective oxide layer can be damaged. Under these extreme conditions, the EP additives will react quickly with the surfaces, creating low friction protective films. They are organic compounds with a reactive non-metal as S or Cl which reacts with hot metal surfaces.

Anti-Wear additives are S or P containing organic compounds, reducing wear by forming a protective layer, (ZDDP).

Anti-oxidants: lubricating oils are generally very stable against oxidation at ambient temperature, but the operating temperature in an internal combustion engine is substantially higher. However, even under those conditions, a good chemical stability of the lubricant is required. Anti-oxidants are used to limit the chemical aging of the oil. The metal surfaces, present in the system, (or the wear particles) can act as oxidation catalysts.

Dispersant additives: diesel engines produce relatively high amounts of carbon rich particles (soot), that accumulate in the lubricants. The high soot concentration can diminish lubricant performance. Consequently dispersant additives are used to keep the soot particles in suspension.

Other additives that are found in lubricants include pour point additives, anti-foam

additives, corrosion inhibitors, etc, etc.
It should be kept in mind that whereas the base oil ages during operation, some of the additives are actually consumed. After a certain period, the concentration of this additive will become too low and lubricant performance will degrade very rapidly.

4.4 Thermal Effects

When studying thermal effects, one has to distinguish between the effect on the film thickness and the effect on the friction. Shear heating in an EHL contact has little influence on the film thickness once the fluid has entered the high pressure zone. Due to the high pressures and the very high viscosity, the Poiseuille term in the Reynolds equation will be close to zero. Hence the fluid will have no other choice than to continue its path through the contact. Thus film thickness variations are excluded because of flow continuity. Whenever the thermal effects inside the high pressure zone start to influence the inlet zone, through conduction for instance, a serious reduction in film thickness can arise. In high speed applications, the thermal generation in the *inlet* itself can become important and induce a film thickness reduction. As the film thickness in the high pressure zone is determined in the inlet zone, a temperature increase in the inlet, which results in a viscosity decrease, will lead to a reduction in the film thickness. This smaller film thickness might in its turn give rise to a larger thermal production, due to a higher shear rate, or due to asperity interaction. This will then reduce the film thickness even more, etc, until rapid failure occurs (scuffing).

If the thermal dissipation in the high pressure zone gives rise to a local temperature increase confined to the high pressure zone only, the film thickness will remain unaffected, but due to a local viscosity decrease, the total shear stress may be reduced considerably. As a result the overall traction, as measured in a traction curve can decrease with increasing slip. The contact operates in the thermal regime of the traction curve. From these observations it is important to retain the following conclusion: the film thickness is governed by the conditions in the inlet, the shear stress, or traction, is governed by the conditions in the high pressure region. In a nutshell this observation explains the success of film thickness predictions, and the difficulties of the traction prediction. The low pressure lubricant behaviour is much easier to study and much better understood than the high pressure behaviour.

4.5 Fatigue Life

Whenever the fluid film completely separates the two surfaces, the stresses endured by the two surfaces will be made up of the normal pressure distribution cycle, together with a shear stress component. Even in the absence of any other stress contribution, these stress cycles will lead to a deterioration of the surfaces (spalling) after many cycles (high cycle fatigue). For a given contact load and material parameters, this represents the ultimate number of stress cycles a contact can endure (expressed in the number of cycles). This endurance life is inversely proportional to the load. A classical relation for bearings is given by the Lundberg-Palmgren equation. However, this life is submitted to statistical variations. Consequently, one speaks of L_{10} the '$L-ten$' life or the number of stress cycles 90% of a population of identical bearings, submitted to an identical load and under identical lubricating conditions will surpass. The life of every individual bearing in a test is normally plotted on a logarithmic scale in a Weibull plot, which allows the determination of L_{10}

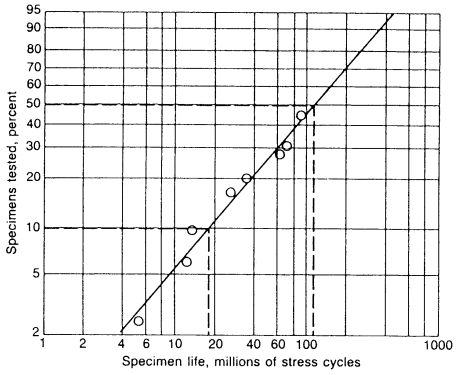

Figure 4.2 *Weibull plot: individual life in a test.*

The Lundberg-Palmgren relation [31, 32] assumes a Hertzian pressure and stress distribution, it reads:

$$\frac{1}{L_{10}} = A\frac{\sigma^c}{z^h}$$

Where A is a constant depending on the material, σ is the maximum shear stress, and z is the depth at which the maximum shear stress occurs. The exponents c and h have been established empirically for different types of bearings: $c \simeq 10$, $h \simeq 2$.

Factors that reduce the life with respect to these ideal conditions are: local stress raisers such as indentations and surface roughness (non-smoothness of the surfaces) or contaminants (small foreign particles present in the oil). Obviously, the quality of the steel, and its capacity to resist to these stress cycles without the formation of micro cracks which grow to form macro cracks and then spalls, is an essential factor in this L_{10} life. The steel quality determines the value of the constant A and A'. Since the Lundberg-Palmgren equation can only account for a Hertzian pressure distribution, the previous equation was extended into an integral formulation by Ioannides and Harris [19]. Furthermore, a fatigue limit σ_u was introduced. Whenever the stresses remain below this fatigue limit, no material damage occurs, and the predicted life is infinite.

$$\frac{1}{L_{10}} = A' \int_V \frac{(\sigma - \sigma_u)^c}{z^h}\, dv$$

where the volume V is taken to be the volume where the shear stress exceeds the fatigue limit σ_u.
This equation permits the study of the influence of roughness, and indentations stemming from contaminant particles, in terms of life. If the surface roughness is accounted for explicitly, the term z^h can be omitted.

Bearing manufacturers give the L_{10} life of their products as a function of the load, the lubrication type and level, the cleanliness of the lubricant, etc, etc.

4.6 Contamination

The previous sections have demonstrated that real surfaces are not mathematically smooth, and that the roughness can significantly influence contact performance. In this section we will show that lubricants are never perfectly clean and that the contaminant particles present in the oil can seriously diminish contact performance (mainly precision, noise and life).

On a macroscopic level new lubricants are reasonably free from particles, however, one has to keep in mind that lubricant film thicknesses in EHL contacts, have heights that are of the order of less than one micrometer. Consequently, particles that are say of the order of ten micrometers can do serious damage to the contacting surfaces, by plastically deforming them whilst passing through the contact. Thus one needs to study the cleanliness level of oils at this scale. An ISO standard is in use giving the number of particles, in a logarithmic way, exceeding the size of 15, 5 and 2 micrometers.

The type of contaminant particle will also largely influence the type and amount of damage inflicted on the bearing. Four particle types are distinguished:

• Soft ductile particles: such as PVC or copper particles leave relatively small and shallow indents when they are overrolled. They cause only minor damage to the raceway without affecting the performance of the contact.

• Hard ductile particles: such as steel or M50 particles leave relatively large and deep indents when they are overrolled. These indentations can act as stress raisers that increase the risk of surface initiated spalling. When the indents are relatively large and deep, the operating life of the bearing can be greatly reduced.

• Hard brittle particles: such as $Si\,O_2$ (sand) and glass, fracture very early in the inlet, creating large amounts of small fragments. These fragments can cause very rapid wear, when the number of particles is high. This wear can lead to loss of precision of the components, resulting in a loss of performance.

• Hard tough particles: such as ceramic particles B_6C, SiC and diamond, fracture very late in the contact, creating large defects with steep edges and fragments are also embedded into the surface. A complicated damage mechanism occurs with either spalling or wear damage.

Of course, the damage inflicted depends both on the amount of particles, their size and their type (hardness).

A very different type of contamination is formed by water. A very small amount of water in a classical lubricant (such as oil) can reduce the lubricant performance dramatically. The effect is widely recognized, but remains for the moment largely unexplained.

4.7 Transient Effects

In real life all processes are transient in nature, consequently the stationary Reynolds equation, neglecting the $\partial(\rho h)/\partial t$ term, is always an approximation of reality. When the changes are very slow, the stationary equation can correctly approximate the transient results, in a quasi static way. A simple criterion says that as long as the speed variation during the contact passage is small, the lubrication regime is quasi-stationary. Defining a as the contact acceleration, u the entrainment velocity and b the contact half-width this relation becomes $a/u \ll u/(2b)$.

However, when the variations are too important, or too fast, true transient behaviour occurs, requiring the solution of the transient Reynolds equation. The transient process can be generated in several different ways: transient load $w(t)$, transient speed $u(t)$, transient geometry $h(t)$. The last case occurs for instance in

Figure 4.3 *Picture of disk raceway tested with M50 particles (magnification 40x), picture by F.Ville.*

Figure 4.4 *Picture of disk raceway tested with ACFTD (sand) (magnification 40x), picture by F.Ville.*

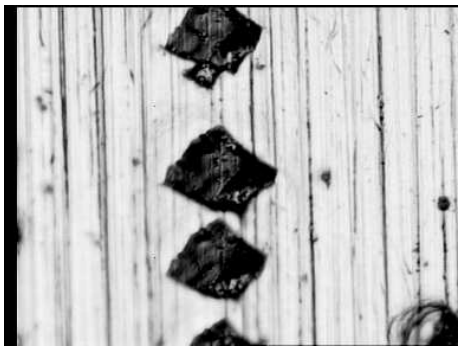

Figure 4.5 *Picture of disk raceway tested with B_6C particles (magnification 40x), picture by F.Ville.*

the cam tappet contact, where the contact radius varies throughout the rotation of the cam. An example showing the pressure distribution and film thickness in such a cam-tappet contact is given in Figure 4.6.

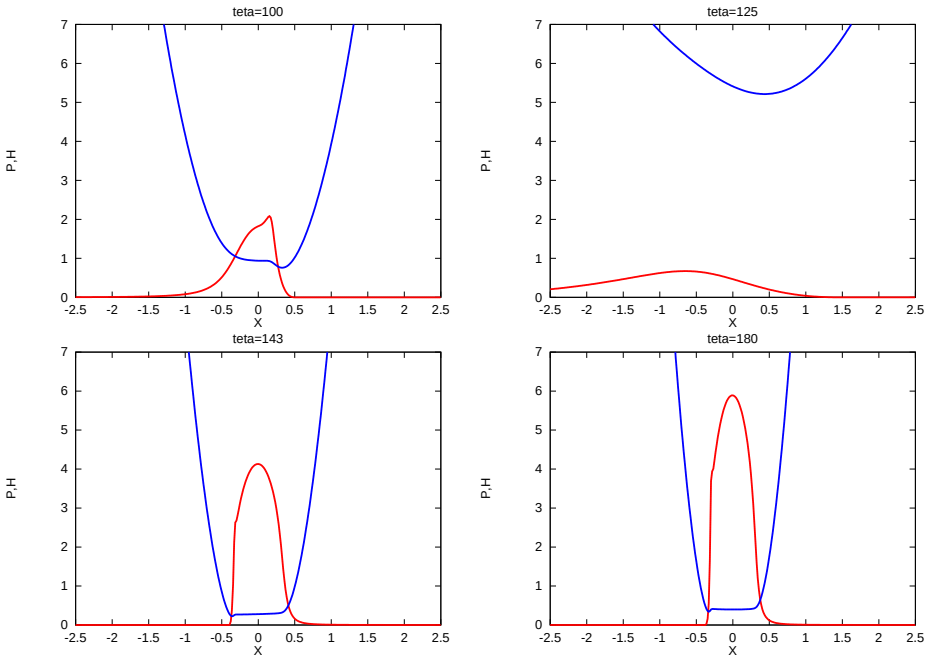

Figure 4.6 *Pressure and film thickness distribution for a rotating cam, note the variation of the radius of curvature (undeformed geometry) (S. Messé).*

Another example of a transient geometry occurs when roughness is present on the surfaces. Since the surfaces move through the contact, a varying gap height will result from it, as is explained in the next section. Generally, several variables will change in time: load, speed, temperature, etc, and the user has to make a choice to study a certain aspect that he suspects to be dominant.

4.8 Approximating Transient Effects

Full numerical predictions of the film thickness in transient EHL contacts are rather time consuming. As an example: the film thickness calculations of the cam-tappet contact presented in the previous section required many hours of calculation [34]. Such times are acceptable in a research environment, but in a development environment many different geometries need to be calculated, and a calculation time of the

order of a second is required. Aiming for such short times requires a major simplification of the Reynolds equation. In Section 2.4.5 it was shown that the Reynolds equation reduces in the high pressure zone to a propagation equation:

$$\frac{\partial(\rho h)}{\partial x} + \frac{\partial(\rho h)}{\partial t} = 0$$

Assuming that the film thickness $h(x)$ was defined by the velocity u when the point passed the inlet, one can compute the film thickness profiles, see Messé [33]. As an example the film thickness profile for a linear accelerating contact is computed:

$$u_e(t) = at \quad t \geq 0$$

The film profile at $t = \sigma$ will be computed with $u_e(\sigma) = u_0 = a\sigma$, or $\sigma = u_0/a$

$$x(\sigma) = -b + \int_t^\sigma u_e(t')\ dt' \quad t \geq 0$$

where t is the time the particular fluid element now at position $x(\sigma)$ entered the contact. This yields:

$$x(\sigma) = -b + \frac{a(\sigma^2 - t^2)}{2} \quad t \geq 0$$

Using $X = x/b$, $\tau = 2b/u_0$ and $\sigma = u_0/a$ one obtains:

$$\sigma\tau(X+1) = \sigma^2 - t^2$$

Taking the positive root for t one finds

$$t = \sqrt{\sigma^2 - \sigma\tau(X+1)}$$

Consequently:

$$u_e(t) = at = a\sqrt{\sigma^2 - \sigma\tau(X+1)}$$

The classical film thickness equation predicts that

$$h(u_e) = k_1 u_e^{0.7}$$

defining $h_0 = k_1 u_0^{0.7} = k_1(a\sigma)^{0.7}$ and $H(X) = h(x/b)/h_0$ we find

$$H(X,\sigma) = \left(\frac{at}{a\sigma}\right)^{0.7} = (1 - \frac{\tau}{\sigma}(X+1))^{0.35}$$

Thus $H(X = -1, \sigma) = 1$, and the film has obtained a positive value $H(X,\sigma) > 0$ for $-1 \leq X \leq \sigma/\tau - 1$. If $\sigma/\tau > 2$ the film thickness is positive in the entire 'contact

zone'. Please note that calculated film thickness values outside the domain $-1 \leq X \leq 1$ are physically meaningless. Furthermore, the predictions around $|X| = 1$ are not very accurate as viscous effects are important (due to lower pressures) see Figure 4.7.

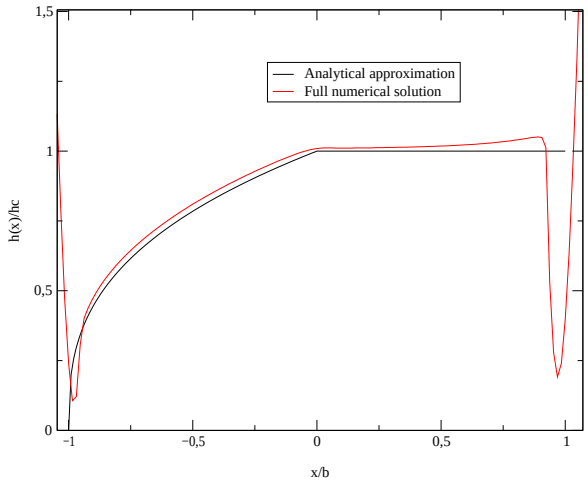

Figure 4.7 *Comparison full numerical model and transport approximation, decelerating contact* ($a < 0$).

However, away from the contact edges, the film thickness prediction is rather accurate. Finally, for more complicated velocity variations $u_e(t)$, the film thickness can best be computed through numerical integration of $u_e(t)$.

4.9 Roughness

As explained above, whenever the surfaces are rough, the Reynolds equation becomes a transient equation. As was outlined in the introduction, the roughness to film thickness ratio, can be used to predict contact performance. However, it was found numerically and experimentally that sub contact size features deform inside the EHL contact. Hence their amplitude is less (sometimes much less) than when measured under atmospheric conditions. Experimental evidence of the deformation of a ridge in an EHL contact was published by Kaneta [24, 25].
In this paper it is also shown that for a given set of operating conditions (M, L or W, U, G), the deformation depends on the amount of slip in the contact. The

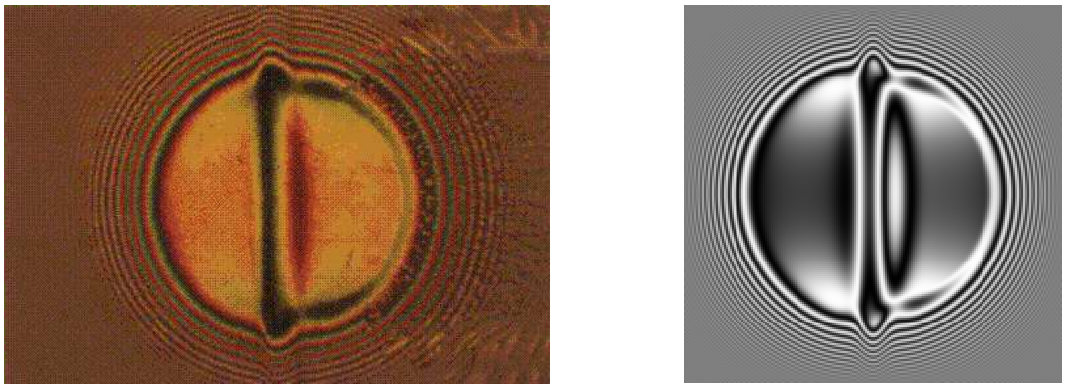

Figure 4.8 *Comparison of experimental and numerical results of a transverse ridge under pure rolling, experimental results by M. Kaneta.*

experimental results have been compared to numerical ones, and excellent agreement between the two was found [28], see Figure 4.8.

For low load situations the deformations of the roughness features will obviously be small, in high load cases they might be large, but in general, the deformation depends on the operating conditions. In order to study this deformation, the deformation of waviness in an EHL contact was studied first [30]. This study shows that for a line contact the deformation of waviness can be described by a single parameter:

$$\frac{A_d}{A_i} = \frac{1}{1 + 0.125\nabla_1 + 0.04\nabla_1^2}$$

where A_d is the amplitude of the deformed waviness, A_i is the amplitude of the initial waviness and $\nabla_1 = (\lambda/b)(M_1^{3/4}/L^{1/2})$ where λ is the waviness wavelength, b is the half width of the Hertzian contact, and M_1 and L are the dimensionless Moes parameters.

When sliding occurs ($u_1 \neq u_2$) the equation of the amplitude reduction can be generated, including the slide to roll ratio [29].
For a point contact a similar parameter and a similar equation have been found. However, in this case the problem becomes more complicated, since the wavelength in x and y direction both play a role.

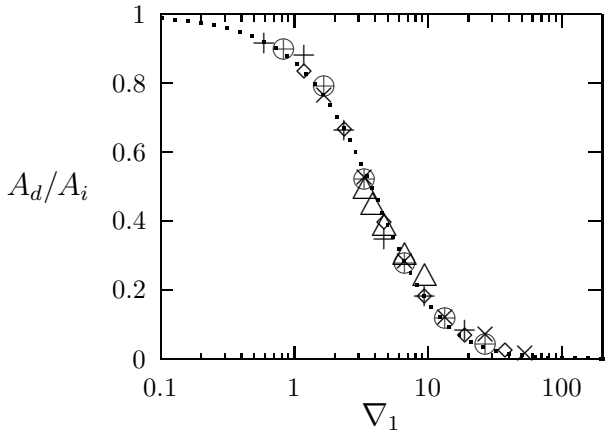

Figure 4.9 *Relative amplitude as a function of* ∇_1*, under pure rolling.*

4.10 Lubricated Wear

Wear forms a vast research area, on which very much work is being done. For an initiation and an overview the reader is referred to Williams [42]. In this section we will discuss two wear types. The first type of wear is termed running in. It concerns the operation of new machine components. The initial surface topography (roughness) will normally be too rough to avoid contact and asperity-asperity interaction will take place. Generally this type of interaction is very mild, the asperities will quickly wear away and contact stops. In the case of run in surfaces a complete fluid film is once again established and the wear rate will remain very low for the rest of the component life. In order to enable successful running in, it is generally recommended to use rather mild operating conditions for the first hours of operation. A second and very dramatic type of lubricated wear is called scuffing. If the operating conditions (load, slip, temperature) are continuously increased, a point is reached above which the contact will fail catastrophically. First indications are increased noise and vibration levels followed by a thermal runaway. When analyzing the contacting surfaces afterwards, material transfer from one surface to the other is obvious, together with the destruction of the original surface finish. Local lubricant failure has led to such dramatic conditions that local welding has taken place. In general after scuffing has happened, the intended function of the machine element is completely lost.

4.11 Starved Lubrication

Until now the lubricant film thickness has been calculated assuming that sufficient oil was present in the inlet, to allow this film to be built up. Whenever insufficient oil is available, the generated oil film thickness will be less than for the fully flooded case, see Figure 4.10.

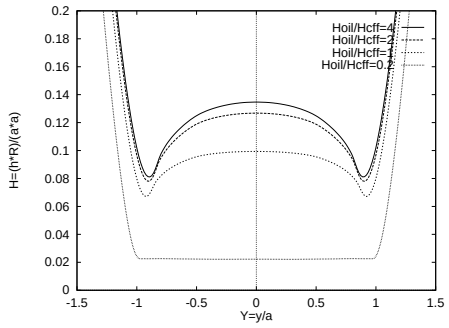

Figure 4.10 *Numerical calculations of the transverse film thickness* $H(X = 0, Y)$ *as a function of* H_{oil}.

In a study by Chevalier et al. [6] it was shown that it is advantageous to express the problem in terms of amount of lubricant present on the surfaces, in front of the contact H_{oil}. Furthermore, the film thickness was made dimensionless by dividing it by the fully flooded central film thickness H_{cff}.

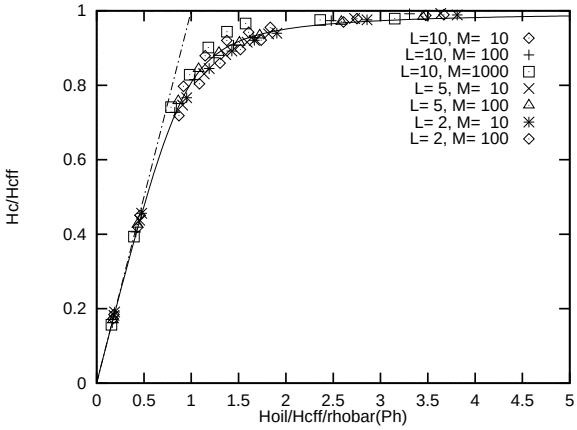

Figure 4.11 *Numerical calculations of the central film thickness* H_c *as a function of* H_{oil} *for various sets of operating conditions, and a circular contact.*

Figure 4.10 and the following equation give the film thickness ratio $\mathcal{R} = H_c/H_{cff}$, as a function of the dimensionless amount of oil available on the surfaces $r = H_{oil}/H_{cff}$.

$$\mathcal{R} = \frac{r}{\sqrt[\gamma]{1 + r^\gamma}}$$

The value of γ for EHL contacts lies between 2 and 5. In this equation and in the figure, two asymptotes are important: $r \to 0$ and $r \to \infty$ which give $\mathcal{R} \to r$ and $\mathcal{R} \to 1$ respectively. Of these two, the asymptote for thin films is the most interesting, since it shows that for very thin oil films, the EHL film thickness is the same as the film in front of the contact. In other words: the contact becomes very efficient in building up an oil film when very little oil is available in the inlet. Thus for $r \to 0$, $H_c \to H_{oil}$ (neglecting the compressibility effects).

NB1: In such severely starved cases the complex film thickness equations of chapter 3 can be replaced by the trivial equation $h_c = h_{oil}$. However, predicting or measuring h_{oil} in a realistic application is far from trivial, see Figure 4.12.

NB2: The relation for severely starved contacts $h_c = h_{oil}$ neglects the lubricant compressibility. As the maximum compressibility is of the order of 30%, the relation still gives a fair approximation. A much better approximation is given by $\rho(p_h)h_c = \rho_0 h_{oil}$!

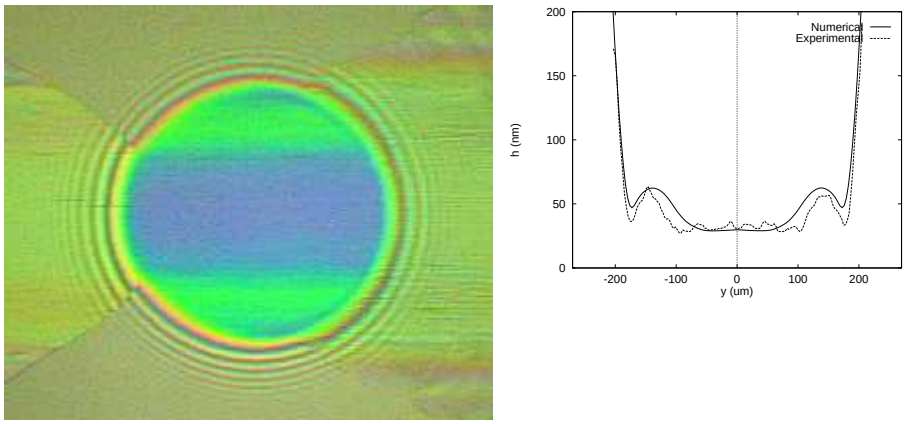

Figure 4.12 *Comparison of experimental and numerical results (heavily starved), experimental results by P.M.E. Cann.*

Exercise Derive the solution of the starved 1d EHL problem, i.e. obtain $h_c(h_{oil})$ for the line contact problem. NB consider flow continuity.

4.12 Grease Lubrication

A very common example of starved lubrication is given by a grease lubricated contact. One could even say that a fully flooded contact is the exception to the rule, since the majority of the contacts are grease lubricated.

A grease consists of a base oil mixed with a thickener agent, in such a way that a semi-solid material is obtained, which has a shear strength. The material behaves in an elastic way if the shear stress applied remains below this limit. Greases are applied generally because of this quality: one can put it in/around a contact, and it will stay in place, without requiring retainer (oil bath) or lubrication system (including pump, tank, etc.). Furthermore, the bulk grease can act as an efficient seal, which hinders dirt and dust to contaminate and thus to damage the contact zone.

Grease lubrication works by a slow release of base oil from the grease matrix, a release that can be increased by a temperature increase. However, due to its structure, once the grease is removed from the contact track, it will not flow back into the track. Consequently, the contact will operate with very little lubricant available: it operates under starved conditions. During the first few overrollings the contact is lubricated with a thick grease film, and during these overrollings, a deposited layer is sometimes observed. Such a layer can later on play a protective role, separating the surfaces, whenever the film thickness has become to small.

The fact that the film thickness is governed by track replenishment and not by classical fully flooded parameters as speed and viscosity, leads to surprising behaviour, in which the film thickness in the starved regime *decreases* with increasing speed and with increasing viscosity, see Cann et al. [5] and Damiens et al. [8].

4.13 Hydrodynamic Impact Analysis

The problem of a cylinder impacting a lubricated plane (or sphere in two dimensions) is an interesting problem for more than one reason. In this section the dimensionless equations that describe this problem will be studied. Assuming no entrainment velocity $u = 0$, the Reynolds equation reduces to:

$$\frac{\partial}{\partial x}\left(\frac{\rho h^3}{12\eta}\frac{\partial p}{\partial x}\right) - \frac{\partial(\rho h)}{\partial t} = 0$$

Deciding that the Hertzian parameters are the most appropriate, we introduce $P = p/p_h$, $X = x/b$, and $H = hR/b^2$, based on Hertz and $T = t/t_0$, $\bar{\eta} = \eta/\eta_0$ and $\bar{\rho} = \rho/\rho_0$.

Using these parameters the dimensionless Reynolds equation reads:

$$\frac{\rho_0 b^6 p_h}{12\eta_0 R^3 b^2}\frac{\partial}{\partial X}(\frac{\bar{\rho}H^3}{\bar{\eta}}\frac{\partial P}{\partial X}) - \frac{\rho_0 b^2}{t_0 R}\frac{\partial(\bar{\rho}H)}{\partial T} = 0$$

Introducing $t_0 = (12\eta_0 R^2)/(p_h b^2)$ results in:

$$\frac{\partial}{\partial X}(\frac{\bar{\rho}H^3}{\bar{\eta}}\frac{\partial P}{\partial X}) - \frac{\partial(\bar{\rho}H)}{\partial T} = 0$$

each individual term is now dimensionless and it seems as if no single parameter would influence the dimensionless cylinder falling down. This is incorrect as the parameter αp_h is hidden in $\bar{\eta}$. As such the result depends on the product αp_h.

In order to solve the Reynolds equation, the film thickness as a function of the pressure distribution $p(x)$ is required:

$$h(x) = h_0 + \frac{x^2}{2R} - \frac{2}{\pi E'}\int_{-\infty}^{+\infty} p(x')\ln\left(\frac{x-x'}{x_0}\right)^2 dx'$$

using the same parameters this equation can be written in a dimensionless way as:

$$H(X) = H_0 + \frac{X^2}{2} - \frac{1}{2\pi}\int_{-\infty}^{+\infty} P(X')\ln\left(\frac{X-X'}{X_0}\right)^2 dX'$$

the force balance equation determining H_0 is replaced by the kinematic equations describing the problem:

$$\frac{\partial v}{\partial t} = \frac{\sum p\Delta x - w}{i}$$

$$\frac{\partial h_0}{\partial t} = v$$

where i is the inertia of the cylinder (per meter), v is the vertical velocity of the cylinder and h_0 is the position of the cylinder.
Starting with the last equation it can be made dimensionless introducing $V = v/v_0$:

$$\frac{b^2}{Rt_0}\frac{\partial H_0}{\partial T} = v_0 V$$

defining $v_0 = b^2/(Rt_0)$ results in the equation:

$$\frac{\partial H_0}{\partial T} = V$$

now using this on the first equation and remembering that $w = \pi p_h b/2$ gives:

$$\frac{v_0}{t_0}\frac{\partial V}{\partial T} = \frac{p_h b}{i_0}\frac{\sum P\Delta X - \pi/2}{I}$$

using $i = i_0 I$, $i_0 = p_h b t_0/v_0$ can be defined, yielding maximum simplification:

$$\frac{\partial V}{\partial T} = \frac{\sum P\Delta X - \pi/2}{I}$$

as can be observed from these four dimensionless equations only two parameters influence the dimensionless solution $\bar{\alpha} = \alpha p_h$ and I.
N.B.: note that $\bar{\alpha}$ is a dimensionless parameter.

4.14 Hertzian Impact Analysis

The following study is a Hertzian impact analysis of a cylinder falling onto a lubricated plane using a modification of the analysis given by Johnson [23]. Assume its initial velocity is v_0. From the Hertzian problem analysis (Section 3.1.1) we know that the deformation in $x = 0$ called δ is given by:

$$\delta \approx 0.596\frac{b^2}{R} \approx 1.52\frac{w_1}{E'}$$

since

$$b = \sqrt{\frac{8w_1 R}{\pi E'}}$$

as the force per unit length w_1 decelerates the cylinder of mass per unit length i

$$w_1 = i\frac{\partial v}{\partial t} = i\frac{\partial^2 \delta}{\partial t^2} = -\frac{E'}{1.52}\delta$$

thus

$$\frac{\partial^2 \delta}{\partial t^2} = -\frac{E'}{1.52i}\delta$$

integrating once, introduces the initial velocity v_0, and gives (the same result can be found using the characteristic equation)

$$v_0^2 - (\frac{\partial \delta}{\partial t})^2 = \frac{E'}{1.52i}\delta^2$$

the maximum deformation δ^* occurs when $\partial\delta/\partial t = 0$ thus

$$\delta^* = \sqrt{\frac{1.52i}{E'}} v_0$$

from δ^* we can compute w_1^* the maximum load, p_h^* the maximum Hertzian pressure and b^* the maximum half-width. Using these parameters we can derive a dimensionless Reynolds equation.

$$\frac{\partial}{\partial x}(\frac{\rho h^3}{12\eta}\frac{\partial p}{\partial x}) - \frac{\partial(\rho h)}{\partial t} = 0$$

we introduce $P = p/p_h^*$, $X = x/b^*$, $H = hR/b^{*2}$, $T = t/t^*$, $\bar{\eta} = \eta/\eta_0$ and $\bar{\rho} = \rho/\rho_0$. Using these parameters the dimensionless Reynolds equation reads:

$$\frac{\rho_0 b^{*6} p_h^*}{12\eta_0 R^3 b^{*2}}\frac{\partial}{\partial X}(\frac{\bar{\rho}H^3}{\bar{\eta}}\frac{\partial P}{\partial X}) - \frac{\rho_0 b^{*2}}{t^* R}\frac{\partial(\bar{\rho}H)}{\partial T} = 0$$

Introducing $t^* = \delta^*/v_0$ results in:

$$\frac{\partial}{\partial X}(\frac{\bar{\rho}H^3}{\lambda^*\bar{\eta}}\frac{\partial P}{\partial X}) - \frac{\partial(\bar{\rho}H)}{\partial T} = 0$$

with $\lambda^* = (12\eta_0 R^2)/(b^{*2} p_h^* t^*)$.

In order to solve the Reynolds equation, the film thickness as a function of the pressure distribution $p(x)$ is required:

$$h(x) = h_0 + \frac{x^2}{2R} - \frac{2}{\pi E'}\int_{-\infty}^{+\infty} p(x') \ln\left(\frac{x - x'}{x_0}\right)^2 dx'$$

using the same variables this equation can be written in a dimensionless way as:

$$H(X) = H_0 + \frac{X^2}{2} - \frac{1}{2\pi}\int_{-\infty}^{+\infty} P(X') \ln\left(\frac{X - X'}{X_0}\right)^2 dX'$$

the force balance equation determining H_0 is replaced by the kinematic equations describing the problem:

$$\frac{\partial v}{\partial t} = \frac{\sum p\Delta x}{i}$$

and

$$\frac{\partial h_0}{\partial t} = v(t)$$

where i is the inertia of the cylinder (per meter), v is the vertical velocity of the cylinder and h_0 is the position of the cylinder.
Starting with the last equation it can be made dimensionless introducing $V = v/v^*$:

$$\frac{b^{*2}}{Rt^*}\frac{\partial H_0}{\partial T} = v^* V$$

defining $v^* = b^{*2}/(Rt^*)$ results in the equation:

$$\frac{\partial H_0}{\partial T} = V$$

introducing the dimensionless velocity $V = v/v^*$ in the first equation gives:

$$\frac{v^*}{t^*}\frac{\partial V}{\partial T} = \frac{p_h^* b^*}{i^*}\frac{\sum P\Delta X}{I}$$

using $i = i^* I$, $i^* = p_h^* b^* t^*/v^*$ can be defined, yielding maximum simplification:

$$\frac{\partial V}{\partial T} = \frac{\sum P\Delta X}{I}$$

Not all the variables introduced previously are independent. It can easily be shown (see exercise) that for instance $I = i/i^* = 2.633\ldots$ and $V_0 = v_0/v^* = 0.596\ldots$.

An example of the evolution of the maximum pressure and the minimum film thickness with time is given in Figure 4.13. This figure shows that the 'contact time' lasts from $T = 3$ to little over $T = 6$ and is indeed of order 2 as predicted by t^* and P_m is of order 1, so the Hertzian approximation is valid. During this period important pressures and elastic deformations occur, and the minimum film thickness is small compared to the elastic deformation ($O(1)$).
There remains a last aspect to this problem which is not yet analysed: the velocities at which the fluid is expulsed.

For this an extension of the previous analysis is needed. Consider a descending body over a length Δx. The amount of liquid displaced is Δq.

$$\Delta q(x,t) = \frac{\partial h(x,t)}{\partial t}\,\Delta x$$

or written in a differential form:

$$\frac{\partial q(x,t)}{\partial x} = \frac{\partial h(x,t)}{\partial t}$$

to obtain $q(x,t)$ one integrates:

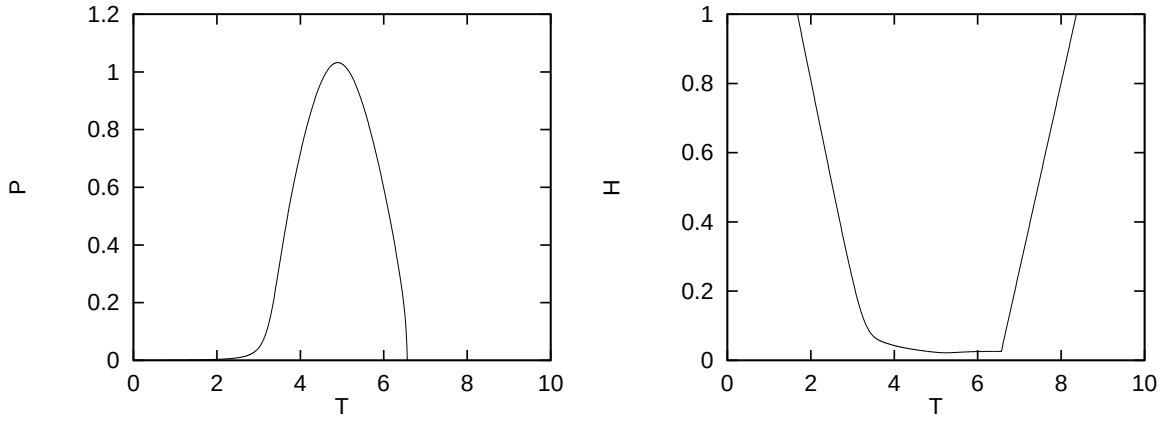

Figure 4.13 *Evolution of maximum pressure and minimum film thickness with time.*

$$q(x,t) = \int_0^x \frac{\partial h(x',t)}{\partial t}\, dx'$$

assuming a plug-flow one obtains the following relation between fluid velocity u and fluid displaced q:

$$u(x,t) = \frac{q(x,t)}{h(x,t)}$$

if one assumes a triangular flow profile u is multiplied by 2, for a parabolic profile it is multiplied by 1.5.
Combining the two equations one obtains:

$$u(x,t) = \frac{1}{h(x,t)} \int_0^x \frac{\partial h(x',t)}{\partial t}\, dx'$$

The dimensionless velocity $U(X,T)$ is introduced, using $u = u^* U$.
Using the previous equation one finds for u^*:

$$u^* U(X,T) = \frac{1}{(b^{*2}/R) H(X,T)} \int_0^X \frac{(b^{*2}/R)\, \partial H(X',T)}{\partial (t^* T)}\, d(b^* X')$$

$$= \frac{b^*}{t^*} \frac{1}{H(X,T)} \int_0^X \frac{\partial H(X',T)}{\partial T}\, dX'$$

As a consequence, the reference velocity u^* is chosen as $u^* = b^*/t^*$ yielding:

$$U(X,T) = \frac{1}{H(X,T)} \int_0^X \frac{\partial H(X',T)}{\partial T}\, dX'$$

In Figure 4.14 the evolution of the maximum velocity U_m as a function of time T is given, as well as the location X_m where the maximum velocity is taken on.

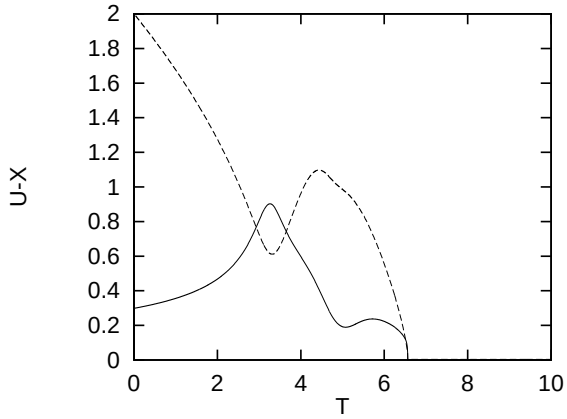

Figure 4.14 *Evolution of maximum velocity and its position with time.*

During the first three time units the maximum velocity $U_m(T)$ increases as $1/\sqrt{T_c - T}$, where T_c is the time the two (undeformed) bodies would touch. From $T = 4$ onwards the elastic deformation becomes important, limiting the descent of the body and the reduction of the gap height H, see Figure 4.14, and thus limiting U_m. As the cylinder starts to rebound ($T > 5$), the maximum velocity rapidly tends to zero, as zero pressure (cavitation) spreads over the domain.

Exercise Show that the maximum velocity $U_m(T) = \max_X U(X,T)$ during the initial period when deformations can be neglected is of the form $1/\sqrt{1 - aT}$. Use the parabolic geometry and a constant vertical velocity.

Exercise Using the previous exercise compute the position $X_m(T)$ of maximum velocity U_m.

Exercise From a certain point in time the analysis obtained in the previous exercise is no longer valid for two reasons, which? Correlate the different events in Figures 4.12 and 4.13.

Exercise Show that $V_0 = v_0/v^* = (1 + 2\ln(2))/4 = 0.596\ldots$ and $I = i/i^* = (2\pi)/(1 + 2\ln(2)) = 2.633\ldots$.

4.15 Boundary layers

When closely studying the EHL pressure distribution from figure 3.8, it can be observed that the size of the inlet pressure sweep domain decreases with increasing load parameter M. This inlet zone separates two distinct zones. The first zone is the inlet where pressures are low, the deformation small and the flow iso-viscous. The second zone is the high pressure Hertzian zone, the deformation is important and the flow Couette dominated because of the piezo-viscosity. When analysing the film thickness profiles, it can also be concluded that the transition zone from inlet to Hertz zone, diminishes with increasing M value.

For medium to high M values, this transition zone becomes significantly smaller than the Hertzian zone and as such can be regarded as a boundary layer [41]. The remaining question is then if a set of local coordinates exists that allows a local description of this boundary layer. The analysis will first focus on the inlet boundary layer around $r = -1$.

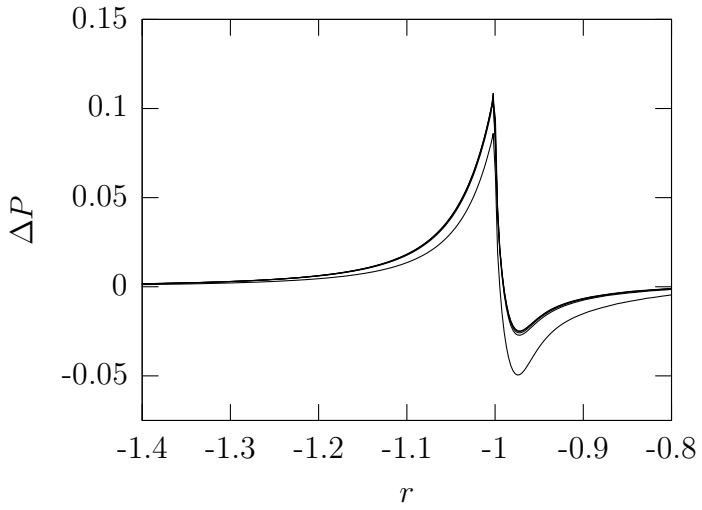

Figure 4.15 *Pressure difference ΔP as a function of r for $\phi = 0, 5, 10, 15, 20$ and 45 degrees. $M = 1000$, $L = 10$.*

Figure 4.15 shows the pressure difference distribution $P(r) - P_h(r)$. The dimensionless coordinate r is defined as $r = \text{sign}(X)\ \sqrt{X^2 + Y^2}$, which allows a study of the inlet as well as the outlet zone. The physical reason that r is used, is that the pressure (and film thickness distribution) is largely independent of the angle ϕ with the X-axis.

It can be observed that, apart from 45 degrees, all pressure difference profiles

are superimposed, proving the radial symmetry.

The second striking feature is the discontinuity in the pressure difference, however, as this is the difference between the EHL pressure (continuous) and the Hertz pressure (discontinuous in $r = -1$) the resulting discontinuity makes sense. Because the origin of the discontinuity stems from the Hertz pressure, it will always be located at $r = -1$. As such the inlet boundary layer will be studied relative to $r = -1$.

The pressure difference is positive in the inlet (which is logical, when one thinks about it) and negative in the Hertz zone. Overall, the integral of the pressure difference is positive.

One can now study the width of the inlet layer and the maximum pressure, as a function of the operating conditions M. This gives rise to the following inlet boundary layer parameters:

$$\bar{X} = -1 + (X + 1)\sqrt[2]{M} \tag{4.1}$$

$$\overline{\Delta P} = \Delta P \sqrt[3]{M} \tag{4.2}$$

$$\bar{H} = H \sqrt[16]{M} \tag{4.3}$$

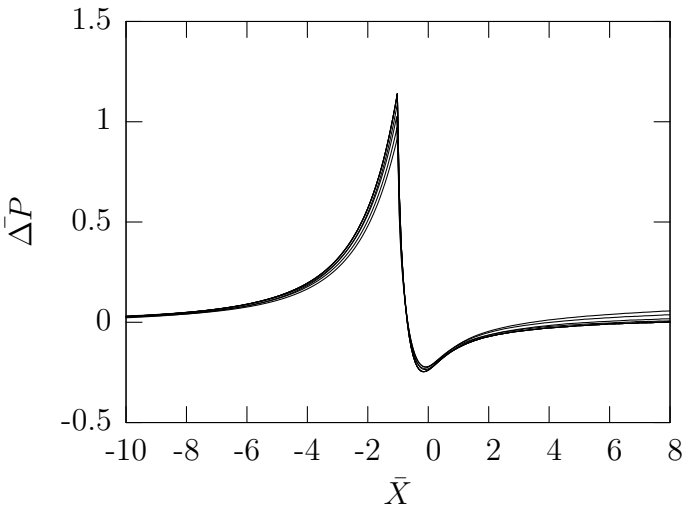

Figure 4.16 *Pressure difference* $\overline{\Delta P}$ *as a function of local coordinate* $\overline{X}$ *for* $M = 200, 500 \ldots 10000$ *and* 20000 *and* $L = 10$.

Figure 4.16 shows the pressure difference in the inlet boundary layer as a function of the new coordinates, for a wide range of M values. As can be seen all curves are superimposed.

A similar study on the film thickness shows that $\bar{H}(\bar{X})$ gives superimposed curves for various M values. It means that the inlet boundary layer is self-similar when using the boundary layer parameters $\bar{X}$, $\overline{\Delta P}$ iand $barH$.

We can now study the outlet boundary layer around $r = 1$. Figure 4.17 shows the pressure difference around $r = 1$. One can observe that the pressure difference is qualitatively similar to the one in the inlet boundary layer. A positive difference and a spike is followed by a rounded negative zone.

Contrary to the inlet zone, the overall pressure difference integral is negative (force balance requires this!). Furthermore, the discontinuity is not located at $r = 1$, but before. As such the discontinuity generates a discontinuity in the pressure distribution: the pressure spike. A second (minor) discontinuity occurs for $r = 1$, canceling the Hertzian discontinuity and satisfying flow balance in the outlet.

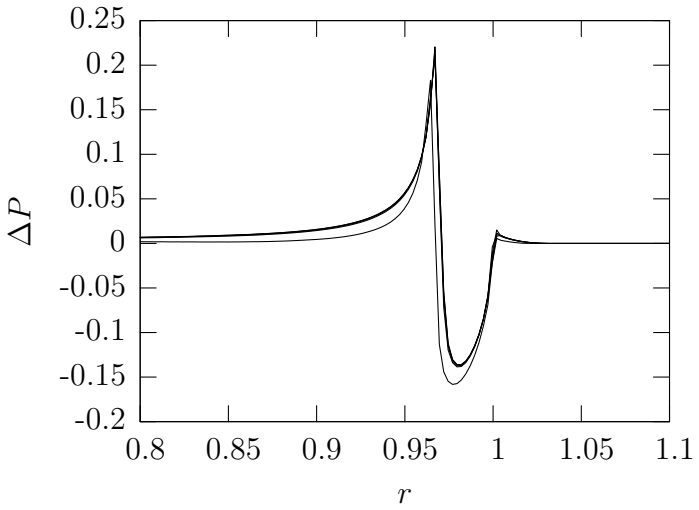

Figure 4.17 *Pressure difference ΔP as a function of r for $M = 1000$, $L = 10$ and $\phi = 0, 5, 10, 15, 20$ and 45 degrees.*

The maximum pressure difference and the width of the outlet layer, show identical trends with respect to M, up to a multiplicative constant. However, the position of the discontinuity changes as a function of M, making the definition of the $\bar{X}$ parameter in the outlet more difficult.

Overall one can conclude that inlet and outlet are indeed boundary layers, that they are self-similar and are gouverned by the same three local dimensionless pa-

rameters $\bar{X}$, $\bar{H}$ and $\overline{\Delta P}$. Finally, the inlet and outlet boundary layers show a qualitatively very similar behaviour in ΔP and H.

Exercise Give a detailed explanation why the pressure difference in the inlet and in the exit boundary layers have integrals of opposing signs.

Exercise$*$ Infer how the pressure difference in inlet and outlet will shape the film thickness difference in these two zones. Make a link with the actual film geometry in these two zones.

Exercise$**$ Explain why the main pressure discontinuity occurs for $r < 1$.

Exercise Explain why a minor main pressure discontinuity occurs at $r = 1$.

Exercise$**$ Explain why the pressure difference is positive and then i negative in inlet and outlet, and NOT $+-$ in inlet and $-+$ in outlet.

Chapter 5

*Basic Techniques

This chapter regroups some of the basic techniques frequently used when dealing with lubrication. They combine experimental and numerical techniques which were developed to deal with some of the specific problems encountered in Elasto Hydrodynamic Lubrication.

5.1 Interferometry

The experimental technique of interferometry has contributed a lot to the detailed understanding of the way an EHL contact works. It allows the precise and detailed measurement of the film thickness in an EHL contact. As such it merits a brief description. We will first outline how the basic interferometric technique works, then we will discuss its resolution, and finally a recent improvement of the technique which allows the precise measurement of very thin film thicknesses.

The classical interferometric technique measures the film thickness between a metal surface (normally a steel ball) and a semi-transparent one (generally a glass disk with a semi-transparent coating). Light which is shined through the disk has two different path lengths: one beam will be transmitted by the coating and reflected on the steel ball, another beam will be reflected by the semi-transparent coating. The different distance traveled by the two beams $2h$ will result in a phase difference of the two beams. Whenever this phase difference is $(2k+1)\pi$ negative interference will occur, the two beams will 'cancel', resulting in a dark spot. Whenever the phase difference is a multiple of 2π, positive interference occurs, and a bright spot appears. The film thickness distribution is represented by an intensity distribution. When one knows the wavelength of the light used, this interference distribution can be translated back into a height map (film thickness map), using some calibration

procedures, and incorporating the phase shift at the interfaces.

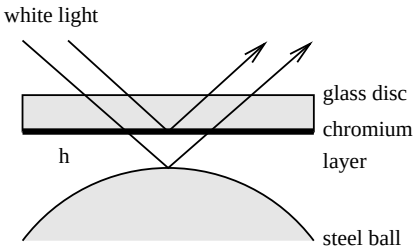

Figure 5.1 *Principle of optical interferometry.*

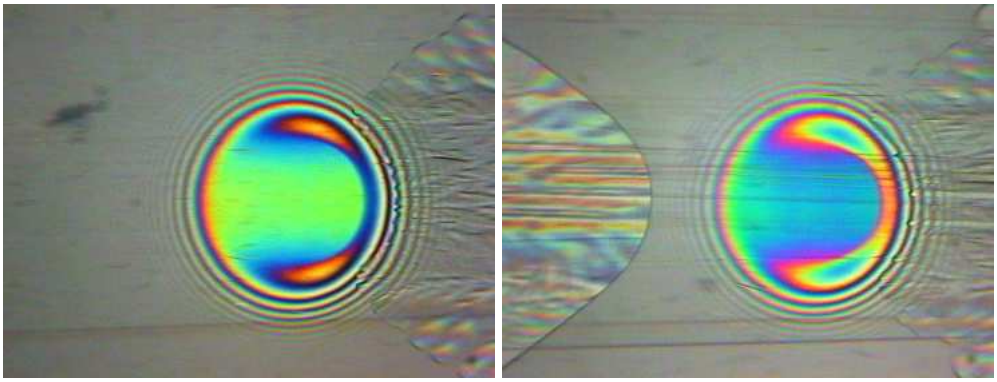

Figure 5.2 *Interferometry pictures of a fully flooded and a classically starved contact by P.M.E. Cann.*

This means that the classical interferometric technique can measure film thicknesses up to half a wavelength. Using a spacer layer (offset) and more precise ways to determine the exact maximum of the combined beam, film thicknesses down to several nanometers can be measured.

5.2 Disc Machines

In order to measure traction in EHL contacts, two disc and four disc machines have been developed [7]. The simplest machine is the two disc machine, sketched in Figure 5.3. It is composed of two crowned discs, independently driven by two motors and loaded together by a dead-weight. One of the motors is suspended (in air bearings) so that it is free to rotate. This motor is then connected by an arm to a load cell, and the rotational speeds of both motors are accurately measured. The two discs are generally supported by two sets of roller bearings.

By varying the rotational speed of both motors, while keeping the sum speed constant, a traction curve is measured, for the load imposed, and the lubricant used.

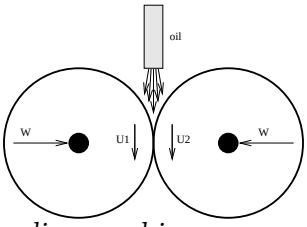

Figure 5.3 *Principle of two disc machine.*

The main disadvantage of the 2 disc machine resides in the roller bearing pair supporting the discs. This disadvantage can be overcome using specially designed test rigs. The friction force measured will consist of the friction force in the disc-disc contact, and the friction force in the bearings. In general this additional force is small, but around pure rolling it tends to dominate the measurements.
For very small sliding speeds the four disc machine was conceived, which has no bearing set supporting the central disc. A sketch of this machine is given in Figure 5.4.

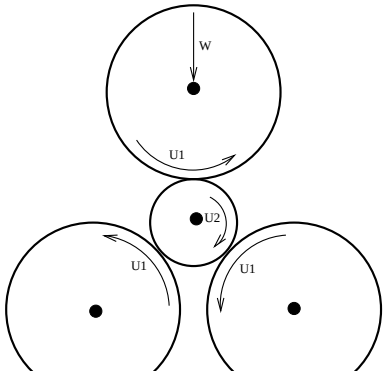

Figure 5.4 *Principle of four disc machine.*

The central disc is the disc on the motor suspended in air bearings. This disc is only supported by the three identical discs surrounding it. These three surrounding discs are driven by a single motor through a gear set. The upper disc is loaded. By changing the sliding speed, the frictional moment on the central disc can now be measured accurately around the pure rolling point. Because of the unsupported central disc the load, speed and slip range of the four disc machine is generally smaller than that of the two disc machine.

5.3 Rolling Element Bearings

Rolling element bearings (REB) allow a degree of rotational freedom to a shaft, with small frictional losses, capable of transmitting large loads, at a reasonable cost and within a small envelope. For an in depth analysis the reader is referred to Harris [17]. Different types of REB's exist, each with its special characteristics and applications.
A REB consists generally of four different components: the inner ring, the outer ring, the rolling element set and the cage, see Figure 5.5.

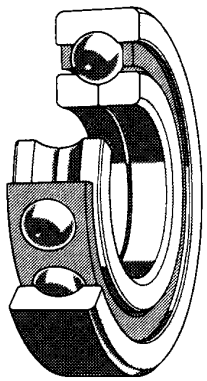

Figure 5.5 *Figure showing the different bearing components.*

The inner ring is generally mounted on a shaft using thermal expansion. The outer ring is connected to the environment using some kind of housing. The rolling elements are either spheres, cylinders, cones, or barrel-shaped. Ordinary bearings have a dozen rolling elements. However, some special bearings have many more rolling elements. These rolling elements enable the shaft to rotate with respect to the environment. They are generally manufactured with great precision, and have extremely smooth operating surfaces. They run against parts of the inner ring and the outer ring, which have a specially shaped and finished surface.
Inner and outer ring and rolling element set are normally made from hardened steel (52100). For special bearing applications other steels are used and sometimes even ceramic components. The cage serves as a separator of the rolling elements, and is generally made of steel, brass or plastic. Rolling element bearings are generally lubricated with oil or grease.

First we will discuss the most common types of REB's and their applications,

then we will address the question of how to choose a bearing of the correct size. It should be noted that most bearing types exist as well as thrust bearings.

5.3.1 Bearing types

Deep Groove Ball Bearings (DGBB) have spherical rolling elements (balls) rolling in deep grooves of the inner and outer ring. These deep grooves create a large contact area between ball and ring, and thus allow the bearing to support important radial loads, and moderate axial loads. Furthermore, these bearing are suitable for high speed applications, they generate low friction and little noise. However, they cannot support important moment loading or misalignment.
A cross section through inner ring, ball and outer ring is shown in Figure 5.6.

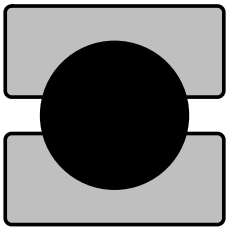

Figure 5.6 *Sketch of a DGBB, half cross section.*

Self Aligning Ball Bearings (SABB) are a modified type of DGBB's with two parallel rows of balls running in deep grooves in the inner ring against a spherical outer ring. This configuration reduces the load carrying capacity of the bearing, but allows it to adjust itself to angular misalignment.

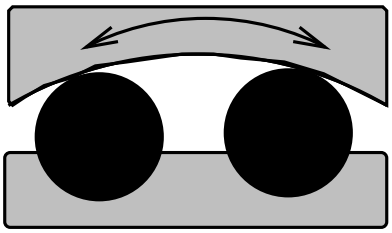

Figure 5.7 *Sketch of a SABB cross section.*

Angular Contact Ball Bearings (ACBB) have spherical rolling elements (balls) rolling in deep grooves in the inner ring and the outer ring. The grooves are positioned at a certain angle, which allows the bearing to transmit forces in the radial and the axial direction. Used in pairs (back-to-back) they can also support moment

loading.

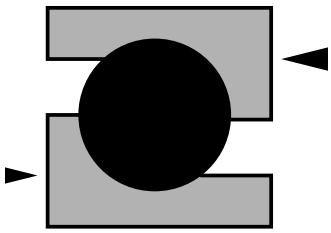

Figure 5.8 *Sketch of an ACBB cross section.*

Cylindrical Roller Bearings (CRB) have cylindrical rolling elements (cylinders) rolling on a cylindrical inner and outer ring. The large contact area results in a bearing which can take up very high radial loads. When flanges are used on the inner and outer ring, the bearing can also support moderate axial loads. Without flanges the CRB can accommodate small axial displacement. These bearings can operate under high speed conditions.
Needle Roller Bearings (NRB) have very thin cylindrical rolling elements (needles), and therefore they give most of the CRB performance in a very small (low) envelope. Sometimes the inner ring is absent and the needles roll directly on the shaft, to save space.

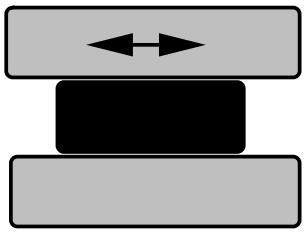

Figure 5.8 *Sketch of a CRB cross section.*

Tapered Roller Bearings (TRB) have conical rolling elements rolling on conical inner and outer rings. The large contact area results in a bearing which can transmit very high radial and tangential loads. These bearings can operate under relatively high speed conditions, and are capable of taking up moment loads.

Spherical Roller Bearings (SRB) have barrel shaped rolling elements rolling on spherical parts of the inner and outer ring. The large contact area results in a bearing which can transmit very high radial and moderate tangential loads. This bearing can take up angular misalignment, just as the SABB.

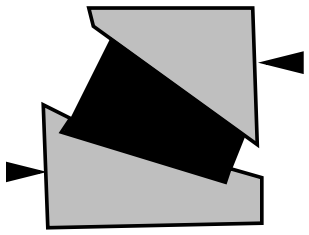

Figure 5.9 *Sketch of a TRB.*

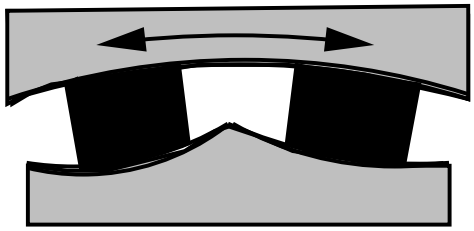

Figure 5.10 *Sketch of a SRB.*

5.3.2 Bearing rating

The size of a bearing for a certain application is determined by two different parameters: the static load rating C_0 and the dynamic load rating C. The static load rating C_0 is used to indicate the maximum load for very slowly rotating applications, or for shock load applications.
The dynamic load rating C is an indicator of the fatigue life of the bearing. Since the fatigue life is subject to statistical variations, the L_{10} life is introduced as the number of million revolutions 90% of a population of bearings will survive, under the same operating conditions. The other 10% of the population will have failed at this point.
The L_{10} life is given by:

$$L_{10} = \left(\frac{C}{P}\right)^p$$

Where L_{10} is the given in million revolutions, C is the dynamic load rating in [N], P is the applied load in [N] and $p = 3$ for ball bearings and $p = 10/3$ for roller bearings. The values of C and C_0 are given by each bearing manufacturer for each type/size bearing. More advanced equations to calculate the fatigue life are used by many manufacturers. These include amongst others information on lubrication conditions, lubricant contamination levels etc.

Exercise An ACBB front wheel bearing in a passenger car has an average load

of $P = 4000\,N$. Compute the required C of the bearing such that the L_{10} life is superior to 100.000 km, assume that 1 revolution is equivalent to 1 m. In reality will one choose a bearing with smaller or larger C? Why?

5.4 Numerical Techniques

The stable and precise numerical solutions of the line and the point contact EHL problem have been made possible by three different application of Multilevel (Multigrid) techniques. These techniques have been pioneered by Prof. A. Brandt.
•1 Application of MultiLevel (multigrid) techniques to the solution of the Reynolds equation.
•2 Application of MultiLevel Multi Integration to the calculation of the elastic deformation equation.
•3 Detailed understanding of the different characteristics of the Reynolds equation in the inlet and high pressure zone.

ad 1: When solving the Reynolds equation using an iterative technique like Gauss Seidel relaxation, one encounters generally two problems. The first problem concerns the convergence speed, and is addressed in this point. The second problem concerns stability and is addressed in the third point.
For the low load EHL problem as well as for Hydrodynamic Lubrication, the Reynolds equation resembles an elliptical equation in p with varying coefficients. The film geometry is close to that given by the rigid geometry, i.e. the elastic deformations are small. Thus the coupling of the Reynolds equation through the elastic deformation is nearly absent, which causes the Gauss Seidel relaxation to be stable. However, the number of iterations (relaxation sweeps) needed to obtain convergence, is large, and increases when the number of points increases. This is a general problem, and the application of multigrid techniques [3] results in a solution in less than 10 relaxation sweeps, leading to a reduction in computing times of several orders of magnitude. In order to achieve this, multigrid uses coarser grids, to accelerate the convergence on the finest grid. These coarser grids are also used to obtain an accurate initial solution on a finer grid as a starting solution. Multigrid techniques also allow the solution of the force balance in the same time as the Reynolds equation is obtained, with little or no additional work required. Finally Multigrid techniques allow an estimation of the discretisation error in the solution, through the comparison of solutions on different grids.
ad 2: The elastic deformation integrals are very time consuming to solve. When the discrete grid consists of n points, the calculation of the integral in a single point requires $O(n)$ operations. Computing the integrals in all n thus requires $O(n^2)$ op-

erations. Since we are interested in accurate and detailed solution, we want n to be very large, hence the time required by the calculation of these integrals becomes very large.
This problem was remedied by the application of multilevel multi-integration techniques [4]. Using this technique, one exploits the smoothness properties of the deformation kernel in order to perform part of the integrals on a coarser grid. This technique results in a reduction of the computing time from $O(n^2)$ to $O(n\ln(n))$, without the loss of accuracy.
ad 3: As was already indicated in the first point, the low load EHL problem has elliptical character in p. Even the high load EHL problem conserves this character in its inlet (low pressure) zone. In the high pressure zone, the viscosity rises enormously, and the Reynolds equation changes to the equation $\partial(\rho h)/\partial x = 0$. This is an integral equation in p, and its correct solution is not trivial. Applying a simple Gauss Seidel relaxation scheme results in stability problems, as the integral character accumulates all the changes of a point by point relaxation. To solve this problem, a distributed relaxation scheme was introduced, in which the value of p in different points is changed simultaneously (dipole). The combination of these two relaxation schemes in the inlet and in the high pressure zone, leads to an efficient and very robust solution method, see Venner [37, 40].

Bibliography

[1] **Bair, S.,** 2001, "Measurement of Non-Newtonian Response for Liquid Lubricants under Moderate Pressure", IMecE. J.o.E., **215**, pp. 223-233.

[2] **Barus, C.,** 1893, "Isothermals, Isopiestics and Isometrics relative to Viscosity", Am. J. of Science, **45**, pp. 87-96.

[3] **Brandt, A.,**. "MultiGrid Techniques: 1984 Guide with Applications to Fluid Dynamics", GMD Bonn, ISBN 3884570811.

[4] **Brandt, A. and Lubrecht, A.A.,** 1990, "Multilevel Matrix Multiplication and Fast Solution of Integral Equations", Journal of Computational Physics, **90**, No. 2, pp. 348-370.

[5] **Cann, P.M.E. and Lubrecht, A.A.**, 1999, "An Analysis of the Mechanisms of Grease Lubrication in Rolling Element Bearings," *Lubrication Science*, **11**, pp. 227-245.

[6] **Chevalier, F., Lubrecht A.A., Cann, P.M.E., Colin, F. and Dalmaz, G.**, 1998, "Film Thickness in Starved EHL Point Contacts," *ASME J. o. Tribology.*, **120**, pp. 126-133.

[7] **Crook, A.W.**, 1963, "The Lubrication of Rollers - IV - Measurement of Friction and Effective Viscosity," *Phil. Trans.*, **A225**, pp. 281.

[8] **Damiens, B., Lubrecht, A.A. and Cann, P.M.E.,** 2000, "Lubrication Regimes in Rolling Element Bearings", Proceedings of the Leeds-Lyon Symposium on Tribology, pp. 295-301.

[9] **Dowson, D. and Higginson, G.R.**, 1966, "Elastohydrodynamic Lubrication, The Fundamentals of Roller and Gear Lubrication," Pergamon Press, Oxford, Great Britain.

[10] **Dowson, D.**, 1979, "History of Tribology," Longman, London, New York.

[11] **Ertel, A.M.**, 1939, "Hydrodynamic Lubrication based on New Principles", Akad. Nauk SSSR Prikadnaya Mathematica i Mekhanika, 3, 2, pp. 41-52.

[12] **Grubin, A.N.**, 1949, "Fundamentals of the Hydrodynamic Theory of Lubrication of Heavily Loaded Cylindrical Surfaces", Central Scientific Research Institute for Technology and Mechanical Engineering, Book no 30, Moscow, D.S.I.R. translations pp. 115-166.

[13] **Greenwood, J.A.**, 1972, "An Extension of the Grubin Theory of Elastohydrodynamic Lubrication," *J. Phys. D: Appl. Phys.,* **5**, pp. 2195-2211.

[14] **Greenwood, J.A. and Johnson, K.L.**, 1992, "The Behaviour of Transverse Roughness in Sliding Elastohydrodynamically Lubricated Contacts," *WEAR*, **153**, pp. 107-117.

[15] **Hamrock, B.J. and Dowson D.,** 1976, "Isothermal Elastohydrodynamic Lubrication of Point Contacts, part I, Theoretical Formulation," *ASME J. Lub. Tech.*, **98**, pp. 223-229.

[16] **Hamrock, B.J. and Brewe D.,** 1983, "Simplified Solution for Stresses and Deformations," *ASME J. Lub. Tech.*, **105**, pp. 171-177.

[17] **Harris, T.A.,** "Rolling Bearing Analysis", 2000, Whiley and Sons.

[18] **Hertz, H.,** 1881, "Über die Berührung fester elastischer Körper," *J. reine und angew. Math.*, **92**, pp. 156-171.

[19] **Ioannides, E. and Harris, T.A.,** 1985, "A New Fatigue Life Model for Rolling Bearings", ASME JOLT, **107**, pp. 367-378.

[20] **Jacobson, B.O. and Vinet, P.**, 1987, "A Model for the Influence of Pressure on the Bulk Modulus and the Influence of the Temperature on the Solidification Pressure of Liquid Lubricants", ASME JOT, **109**, pp. 709-713.

[21] **Jacobson, B.O.**, 1991, "Rheology and ElastoHydrodynamic Lubrication," Elsevier, ISBN 0 444 88146 8.

[22] **Johnson, K.L., Kendall, K. and Roberts A.D.**, 1971, "Surface energy and the contact of elastic solids," Proc. Roy. Soc., **A324**, pp. 301.

[23] **Johnson, K.L.**, 1985, "Contact Mechanics," Cambridge University Press, ISBN 0 521 34796.

[24] **Kaneta, M.**, 1992, "Effects of Surface Roughness in Elastohydrodynamic Lubrication," *JSME*, III, **35**, 4, pp. 535-546.

[25] **Kaneta, M., Sakai, T. and Nishikawa, H.**, 1992, "Optical Interferometric Observations of the Effects of a Bump on Point Contact EHL," *ASME JOT*, **114**, pp. 779-784.

[26] **Lubrecht, A.A.,** 1987, "Numerical Solution of the EHL Line and Point Contact Problem Using Multigrid Techniques," Ph.D. Thesis, University of Twente, Enschede, The Netherlands, ISBN 90-9001583-3.

[27] **Lubrecht, A.A. and Ioannides, E.,** 1991, "A Fast Solution to the Dry Contact Problem and the Associated Sub-surface Stress Field, Using Multilevel Techniques", ASME JOT, **113**, pp. 128-133.

[28] **Lubrecht, A.A.,** 1996, "Influence of Local and Global Features in EHL Contacts", Proceedings of the Leeds-Lyon Symposium on Tribology, pp. 17-25.

[29] **Lubrecht, A.A., Graille, D., Venner C.H. and Greenwood, J.A.** 1997, "Waviness Deformation in EHL Line Contacts, under Rolling/Sliding", ASME JoT, **120**, pp. 705-709.

[30] **Lubrecht, A.A. and Venner C.H.,** 1999, "ElastoHydrodynamic Lubrication of Rough Surfaces", Proceedings of the IMechE part J, J5, pp. 397-404.

[31] **Lundberg, G. and Palmgren A.,** 1947, "Dynamic Capacity of Rolling Bearings", Acta Polytech. Mech. Eng. Ser. 1. R.S.A.E.E. No. 3.

[32] **Lundberg, G. and Palmgren A.,** 1952, "Dynamic Capacity of Rolling Bearings", Acta Polytech. Mech. Eng. Ser. 2. R.S.A.E.E. No. 4.

[33] **Messé, S., and Lubrecht, A.A,** 2002, "Approximating EHL Film Thickness during Acceleration", ASME JoT, **124**, pp. 443-447.

[34] **Messé, S.,** 2001, "Analyse Transitoire de la Lubrification et du Frottement dans un Système de Distribution Automobile", Thèse INSA-LYON.

[35] **Reynolds, O.**, 1886, "On the theory of Lubrication and its Application to Mr. Beauchamps Tower's Experiments, including an Experimental Determination of the Viscosity of Olive Oil", Phil. Trans., **177**, pp. 157-234.

[36] **Roelands, C.J.A.**, 1966, "Correlational Aspects of the ViscosityTemperature-Pressure Relationship of Lubricating Oils" Ph.D. Thesis, Technical University Delft, Delft, The Netherlands, (V.R.B., Groningen, The Netherlands).

[37] **Venner, C.H.**, 1991, "Multilevel Solution of the EHL Line and Point Contact Problems," Ph.D. Thesis, University of Twente, Enschede, The Netherlands. ISBN 90-9003974-0.

[38] **Venner, C.H. and Lubrecht, A.A.**, 1994, "Transient Analysis of Surface Features in an EHL Line Contact in the case of Sliding," ASME JOT, **116**, pp. 186-193.

[39] **Venner, C.H. and Lubrecht, A.A.**, 1996, "Numerical Analysis of the influence of Waviness on the Film Thickness of a Circular EHL Contact", ASME JOT, **118**, pp. 153-161.

[40] **Venner, C.H. and Lubrecht, A.A.**, 2000, "Multilevel Methods in Lubrication", Elsevier, ISBN 0-444-50503-2.

[41] **Venner, C.H., Biboulet, N. and Lubrecht, A.A.**, 2014, "Boundary Layer Behaviour in Circular EHL Contacts in the Elastic-Piezoviscous Regime", submitted to Tribology Letters.

[42] **Williams, J.A.**, 1994, "Engineering Tribology", Oxford University Press, ISBN 0198563434.

Appendix A

Hertzian parameters

A.1 Line Contact

The dimensionless equations are the same as those used in Section 3.1.1. The important parameters are repeated:

b half-width of the contact area
x coordinate, (infinitely long in y direction)
p_h the maximum pressure
R the (reduced) radius of contact

$$p(x) = \begin{cases} p_h \sqrt{1-(x/b)^2}, & \text{if } |x| \leq b; \\ 0, & \text{otherwise.} \end{cases}$$

the deformation δ as a function of the coordinate x is given by:

$$\delta(x) = \begin{cases} b^2/(2R)\,(x/b)^2, & \text{if } |x| \leq b; \\ b^2/(2R)\left[(x/b)^2 + \ln\left(|x/b| + \sqrt{(x/b)^2-1}\right)\right. & \\ \qquad \left. -|x/b|\sqrt{(x/b)^2-1}\right] & \text{otherwise.} \end{cases}$$

in terms of the dimensionless deformation $\Delta = \delta R/b^2$ and the dimensionless coordinate $X = x/b$ this gives:

$$\Delta(X) = \begin{cases} (X^2/2, & \text{if } |X| \leq 1; \\ \left[X^2 + \ln\left(|X| + \sqrt{X^2-1}\right) - |X|\sqrt{X^2-1}\right]/2 & \text{otherwise.} \end{cases}$$

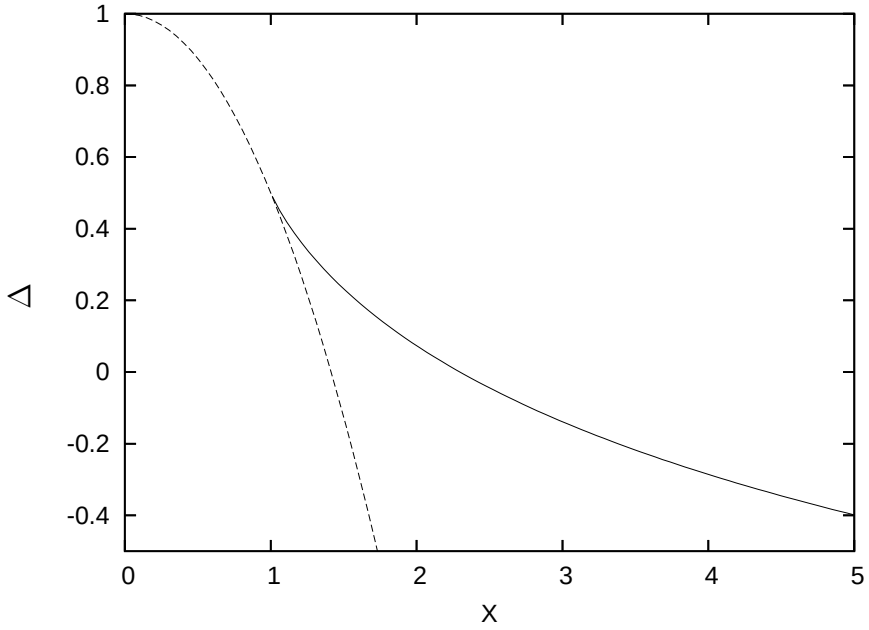

Figure A1.1 *Dimensionless one dimensional contact deformation* Δ *as a function of* $X = x/b$.

Note1: the deformation is determined up to a constant, hence the arbitrarily positive and negative values. In general the boundary conditions determine this constant.
Note2: the deformation tends to infinity for $X \to \infty$, this is physically coherent as the (line) load acts over an infinite length, and the integral is therefore infinite.

A.2 Point Contact

The dimensionless equations are the same as those used in Section 3.1.2. The important parameters are repeated:

a the radius of the contact area
r the radius $r = \sqrt{x^2 + y^2}$, as the problem depends only on r
p_h the maximum pressure
R_x the (reduced) radius of contact

$$p(r) = \begin{cases} p_h \sqrt{1 - (r/a)^2}, & \text{if } r \leq a; \\ 0, & \text{otherwise.} \end{cases}$$

the deformation δ as a function of the radius r is given by ([23] pg. 61):

$$\delta(r) = \begin{cases} (2a^2 - r^2)/(2R_x), & \text{if } r \leq a; \\ \left[(2a^2 - r^2)\arcsin(a/r) + a\sqrt{r^2 - a^2}\right]/(\pi R_x), & \text{otherwise.} \end{cases}$$

the dimensionless deformation $\Delta = \delta R_x/a^2$ as a function of the dimensionless radius $\rho = r/a$ is given by:

$$\Delta(\rho) = \begin{cases} (2 - \rho^2)/2, & \text{if } \rho \leq 1; \\ \left[(2 - \rho^2)\arcsin(1/\rho) + \sqrt{\rho^2 - 1}\right]/\pi, & \text{otherwise.} \end{cases}$$

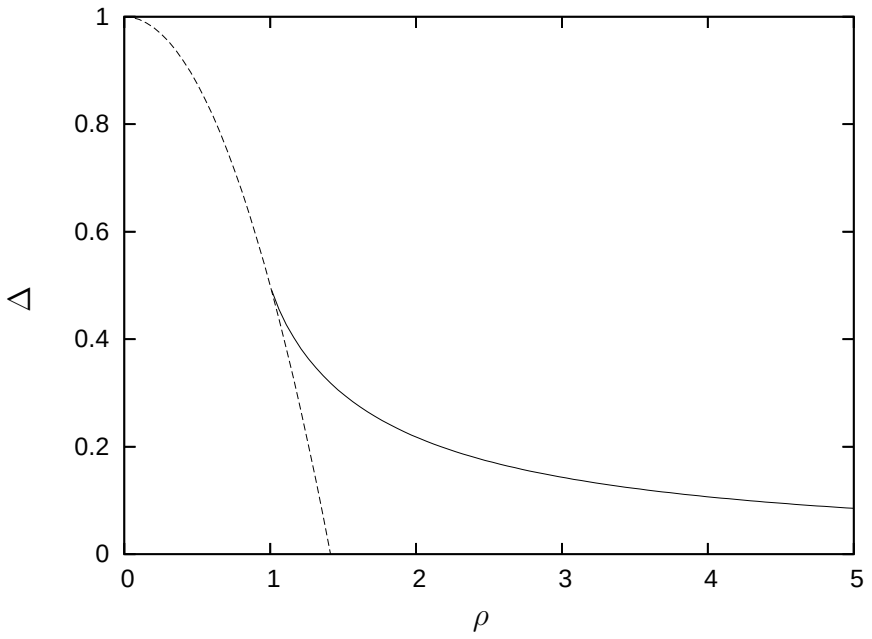

Figure A1.2 *Dimensionless two dimensional contact deformation Δ as a function of $\rho = r/a$.*

Appendix B

Reynolds Equation

Two different forms of the Reynolds equation are generally used in the literature. The equation given in the course notes (polycope Mecanique des Contacts 1, pg. 56) reads:

$$\frac{\partial}{\partial x}(\frac{\rho h^3}{\eta}\frac{\partial p}{\partial x}) + \frac{\partial}{\partial z}(\frac{\rho h^3}{\eta}\frac{\partial p}{\partial z}) = 6\rho(u_1 - u_2)\frac{\partial h}{\partial x} + 6\rho(w_1 - w_2)\frac{\partial h}{\partial z}$$

$$+6h\frac{\partial}{\partial x}\{\rho(u_1 + u_2)\} + 6h\frac{\partial}{\partial z}\{\rho(w_1 + w_2)\} + 12\rho v_2 + 12h\frac{\partial \rho}{\partial t}$$

This equation can be simplified since the three velocity components u, v and w are dependent. A material point on surface 2 remains always a point on surface 2! One can describe the surface S in its general form as an equation linking space and time: $S(x, y, z, t) = y - h(x, z, t) = 0$. As a point on the surface remains on the surface the total derivative of S with respect to time should be zero:

$$\frac{DS}{Dt} = 0$$

or using the chain-rule:

$$\frac{DS}{Dt} = \frac{\partial y}{\partial t} - \frac{\partial h}{\partial x}\frac{\partial x}{\partial t} - \frac{\partial h}{\partial z}\frac{\partial z}{\partial t} - \frac{\partial h}{\partial t} = 0$$

or:

$$v - u\frac{\partial h}{\partial x} - w\frac{\partial h}{\partial z} - \frac{\partial h}{\partial t} = 0$$

or:

$$v = u\frac{\partial h}{\partial x} + w\frac{\partial h}{\partial z} + \frac{\partial h}{\partial t}$$

for surface 2 the above equation, this becomes:

$$v_2 = u_2\frac{\partial h}{\partial x} + w_2\frac{\partial h}{\partial z} + \frac{\partial h}{\partial t}$$

substitution in the above equation gives:

$$\frac{\partial}{\partial x}(\frac{\rho h^3}{\eta}\frac{\partial p}{\partial x}) + \frac{\partial}{\partial z}(\frac{\rho h^3}{\eta}\frac{\partial p}{\partial z}) = 6\rho(u_1 - u_2)\frac{\partial h}{\partial x} + 6\rho(w_1 - w_2)\frac{\partial h}{\partial z} + 6h\frac{\partial}{\partial x}\{\rho(u_1 + u_2)\}$$
$$+6h\frac{\partial}{\partial z}\{\rho(w_1 + w_2)\} + 12\rho u_2\frac{\partial h}{\partial x} + 12\rho w_2\frac{\partial h}{\partial z} + 12\rho\frac{\partial h}{\partial t} + 12h\frac{\partial \rho}{\partial t}$$

simplifying:

$$\frac{\partial}{\partial x}(\frac{\rho h^3}{\eta}\frac{\partial p}{\partial x}) + \frac{\partial}{\partial z}(\frac{\rho h^3}{\eta}\frac{\partial p}{\partial z}) = 6\rho(u_1 + u_2)\frac{\partial h}{\partial x} + 6\rho(w_1 + w_2)\frac{\partial h}{\partial z}$$
$$+6h\frac{\partial}{\partial x}\{\rho(u_1 + u_2)\} + 6h\frac{\partial}{\partial z}\{\rho(w_1 + w_2)\} + 12\frac{\partial}{\partial t}(\rho h)$$

finally this gives:

$$\frac{\partial}{\partial x}(\frac{\rho h^3}{\eta}\frac{\partial p}{\partial x}) + \frac{\partial}{\partial z}(\frac{\rho h^3}{\eta}\frac{\partial p}{\partial z}) = 6\frac{\partial}{\partial x}\{\rho h(u_1 + u_2)\} + 6\frac{\partial}{\partial z}\{\rho h(w_1 + w_2)\} + 12\frac{\partial}{\partial t}(\rho h)$$

in the EHL course notes the coordinates x and y are used instead of x and z, hence, interchanging the z direction and the y direction

$$\frac{\partial}{\partial x}(\frac{\rho h^3}{\eta}\frac{\partial p}{\partial x}) + \frac{\partial}{\partial y}(\frac{\rho h^3}{\eta}\frac{\partial p}{\partial y}) = 6\frac{\partial}{\partial x}\{\rho h(u_1 + u_2)\} + 6\frac{\partial}{\partial y}\{\rho h(v_1 + v_2)\} + 12\frac{\partial}{\partial t}(\rho h)$$

When one now aligns the coordinate axis x with the direction of the main velocity, the velocity term v becomes zero, and the relation simplifies to

$$\frac{\partial}{\partial x}(\frac{\rho h^3}{\eta}\frac{\partial p}{\partial x}) + \frac{\partial}{\partial y}(\frac{\rho h^3}{\eta}\frac{\partial p}{\partial y}) = 6\frac{\partial}{\partial x}\{\rho h(u_1 + u_2)\} + 12\frac{\partial}{\partial t}(\rho h)$$

This last alignment is possible whenever the velocities are linear, this means that the transformation is not possible in case of spin.
This last form is the Reynolds equation used in the current set of course notes and in the majority of the lubrication handbooks and publications.

Appendix C

Rigid Circular Punch

For certain problems, a reference different from Hertz might be useful. One alternative is the rigid circular punch, as described by K. L. Johnson [23].

The relation between the different parameters follows from the elastic deformation equation, using the punch dimensions $p_0 = p(x = 0, y = 0)$, h_0 the punch depth and a the punch radius. One defines the following dimensionless parameters: $X = x/a$, $Y = y/a$, $H = h/h_0$ and $P = p/p_0$:
The punch (height) equation reads

$$h(x,y) = \begin{cases} -h_0, & \text{if } x^2 + y^2 \leq a^2; \\ \infty, & \text{otherwise.} \end{cases}$$

The punch pressure equation reads

$$p(x,y) = \begin{cases} a\ p_0/\sqrt{a^2 - x^2 - y^2}, & \text{if } x^2 + y^2 \leq a^2; \\ 0, & \text{otherwise.} \end{cases}$$

Please note that the a term in the numerator cancels and that the pressure has indeed a dimension of N/m^2.
The maximum deformation is known from [23] to be

$$h_0 = 2\pi \frac{p_0 a}{E'}$$

The punch generates an elastic deformation given by:

$$h(x,y) = -h_0 + \frac{2}{\pi E'} \int_{-\infty}^{+\infty} \int_{-\infty}^{+\infty} \frac{p(x',y')\ dx'\ dy'}{\sqrt{(x-x')^2 + (y-y')^2}}$$

The dimensionless elastic deformation equation is given by:

$$H(X,Y) = -1 + \frac{2}{\pi E'} p_0 a \frac{E'}{2\pi p_0 a} \int_{-\infty}^{+\infty} \int_{-\infty}^{+\infty} \frac{P(X',Y')\ dX'\ dY'}{\sqrt{(X-X')^2 + (Y-Y')^2}}$$

Results in:

$$H(X,Y) = -1 + \frac{1}{\pi^2} \int_{-\infty}^{+\infty} \int_{-\infty}^{+\infty} \frac{P(X',Y')\ dX'\ dY'}{\sqrt{(X-X')^2 + (Y-Y')^2}}$$

The load equation w is made dimensionless in the same way:

$$w = \int_{-\infty}^{+\infty} \int_{-\infty}^{+\infty} p(x',y')\ dx'\ dy'$$

$$w = p_0\ a^2 \int_{-\infty}^{+\infty} \int_{-\infty}^{+\infty} P(X',Y')\ dX'\ dY'$$

Defining $W = w/(p_0\ a^2)$ results in:

$$W = 2\pi$$

Please notice that compared to the Hertz equations some factors change in the deformation equation and in the force balance equation.

exercise An elastic punch of 1 cm radius is pressed 1 μm into the same material (E=2200 GPa). What is the central pressure p_0? What is the load w?

exercise* A (rigid) punch of 1 cm radius is pressed 1 μm into the above material (E=2200 GPa). What is the central pressure p_0? What is the load w?

Index